Evaluating Post-fire Vegetation Recovery in Canadian Mixed Prairie Using Remote Sensing Approaches

A Thesis Submitted to the

College of Graduate and Postdoctoral Studies

in Partial Fulfillment of the Requirements

for the degree of Master of Science

in the Department of Geography & Planning

University of Saskatchewan

Saskatoon

By

Meng Li

Permission to Use

In presenting this thesis in partial fulfilment of the requirements for a Postgraduate degree from the University of Saskatchewan, I agree that the Libraries of this University may make it freely available for inspection. I further agree that permission for copying of this thesis in any manner, in whole or in part, for scholarly purposes may be granted by the professor or professors who supervised my thesis work or, in their absence, by the Head of the Department or the Dean of the College in which my thesis work was done. It is understood that any copying or publication or use of this thesis or parts thereof for financial gain shall not be allowed without my written permission. It is also understood that due recognition shall be given to me and to the University of Saskatchewan in any scholarly use which may be made of any material in my thesis.

Requests for permission to copy or to make other use of material in this thesis in whole or part should be addressed to:

Dean of College of Graduate and Postdoctoral Studies

University of Saskatchewan

116 Thorvaldson Building, 110 Science Place

Saskatoon, SK S7N 5C9, Canada

Head of the Department of Geography & Planning

University of Saskatchewan

105 Kirk Hall, 117 Science Place

Saskatoon, SK S7N 5C8, Canada

Abstract

This study investigated a wildfire occurred in April 2013 at Grasslands National Park, aiming to quantify vegetation's post-fire recovery with both field and remote sensing approaches. Biophysical parameters and hyperspectral reflectances were collected through field surveys conducted one year prior to the fire as well as five continuous years post-fire at growing seasons. These data were processed into burned and unburned samples followed by significance test to reveal biophysical differences across samples. Results indicated an overall recovery of the grassland within 4-5 years, with different vegetation forms recovering at various post-fire growing seasons. Green grass was the most resilient component that fully recovered one year post-fire, followed by forbs at two years post-fire, with shrubs and soil organic crust taking longer than four years to recover compared to the adjacent unburned communities. Hyperspectral dataset was used to establish the utility of remote sensing approaches in grasslands fire-study. Results suggested the potential of satellite remote sensing data in such application. Furthermore, Landsat dataset were processed and significance test was repeated to further prove the sensitivity of Landsat product (especially NDVI) in distinguishing burned and unburned samples, as well as good agreement with conclusions established from field data analysis. Finally, major driving factors were analyzed with ANOVA and results indicated the significant role of meteorological variables and topography in vegetation's post-fire recovery. Findings from this research contribute to a better understanding of fire's effect on the under-studied Canadian northern mixed prairie. Also, the successful validation of RS based approaches can provide as the theoretical basis for potential future RS applications in modelling grassland post-fire recovery in the mixed prairie.

Acknowledgements

First, I would like to acknowledge my supervisor Dr. Xulin Guo for the enormous effort and dedication in the whole process of my program. I am also grateful to all my committee members: Dr. Winston Zeng, Dr. Paul Hackett and also previous members Dr. Scott Bell and Dr. Geoff Cunfer for their support and guidance in creating this thesis.

I owe a big thank-you to all my lab peers and visiting scholars during the course of my program for field data collection as well as our weekly seminar discussions. I will always cherish the fun memory of the field trips with Carmen Finnigan, Dandan Xu, Bingrong Zhou and Tengfei Cui.

Lastly, I would like to acknowledge my family, particularly my parents and girlfriend. Without their constant love, support and sometimes sacrifice, this work would have been impossible.

This work is dedicated to my loving parents and fondest Xiao Benben who support me and stay with me especially through my darkest hours, to my mentor Gerry Falk who understands me and shines light on the rugged path of my life, and last but not least, to the One who says "Ἀρκεῖ σοι ἡ χάρις μου ἡ γὰρ δύναμις μου ἐν ἀσθενείᾳ τελειοῦται".

Contents

List of Tables

List of Figures

List of Abbreviations

GIS	Geographic Information System
RS	Remote Sensing
ANCOVA	Analysis of Covariance
TSA	Time Series Analysis
BP	Before Present
nm	nanometer, 10^{-9}m
SRF	Spectral Response Function
ASD	Analytical Spectral Device, Inc.
NIR	Near Infrared
VI	Vegetation Index
LAI	Leaf Area Index
NDVI	Normalized Difference Vegetation Index
GEMI	Global Environmental Monitoring Index
EVI	Enhanced Vegetation Index
SAVI	Soil Adjusted Vegetation Index
MSAVI	Modified Soil Adjusted Vegetation
BAI	Burned Area Index
NBR	Normalized Burn Ratio
CSI	Char Soil Index
MIRBI	Mid-Infrared Burn Index
USDA	U.S. Department of Agriculture
USGS	U.S. Geological Survey

Chapter 1

Introduction

1.1 Ubiquitous and Vulnerable Grasslands

Grasslands are ubiquitous throughout all continents. As one of the major vegetation types, grasslands cover approximately 40% of the land surface (Shantz, 1954; Collins & Wallace, 1990), and are especially significant in the study of terrestrial ecosystems. Commonly referred to as the prairie, grasslands in North America cover about 15% of its continent (Anderson, 2006), and stretching from central Canada to southern U.S. on the Great Plains (Figure 1.1).

Despite its global coverage, grasslands are vulnerable ecosystems with an alarming rate of shrinkage in area and loss in biodiversity, most of time underrated, overlooked and ignored by us. The relationship between biodiversity and the healthy functioning of ecosystems is essential in ecology, which posits that status and rate of ecosystem processes, e.g. productivity and resilience, has strong positive connection with species richness (Vitousek & Hooper, 1993). Biodiversity loss in grassland ecosystems is remarkable, ranking as the third most threatened biome after rainforests and arctic ecosystems (Sala et al., 2000). A study (Sala et al., 2005) shows that by year 2050 another 10% of vascular plant species will be lost in terrestrial ecosystems. Identifying the underlying mechanisms of change in community structure is a pressing and significant task for understanding and predicting community responses to changes in disturbances or future climate with a level of certainty useful to management (Ford & McPherson, 1996). Composition and structure of grass-

land ecosystems are constantly subject to many biotic and abiotic factors (White, 1979; Gibson & Hulbert, 1987), including the biophysical environment, fire, grazing, and other human activities (e.g. historical and current land-use patterns).

Through the course of evolution, grasslands ecosystems are maintained in conditions appropriate for its productivity and biodiversity in nature through self-organizing its biotic and abiotic components (Collins & Wallace, 1990). However, most of these mechanisms were fundamentally disrupted and often destroyed by anthropogenic causes (e.g. cultivation and urbanization) before they have been fully understood; mainly because the utility of grasslands for farming and grazing: flat, treeless, and rich soil. In fact, North American grasslands are ranked as one of the most extensively disrupted ecosystems on Earth. In USA nearly all land of the Great Plains is cultivated to sustain one of the largest agricultural landscapes (Cunfer, 2005). In the northern mix-prairie grassland virtually no major areas of intact habitat remain, with more than 75% of natural habitat has been destroyed due to agriculture activities (Savage, 2011; Shay et al., 2013). More than half of the prairie had greater than 80% grass cover in 1880's before the agricultural settlement (Archibold & Wilson, 1980). However, current percentage of cultivated land in the same area is between 15% in areas with little precipitation and 99% in areas more suitable for growing crops (Savage, 2011). The Northern Great Plains ecoregion is listed as critical and endangered (Shay et al., 2013) and demands high priority for conservation (WWF Global, 2009).

1.2 Disturbances on Grasslands

Disturbances are integral and significant natural components of the grassland ecosystem. Dynamics of grassland ecosystem is tightly connected to disturbances. The reader is encouraged to access Li & Guo (2014) for a systematic review of major disturbances on the Canadian northern mixed-prairie.

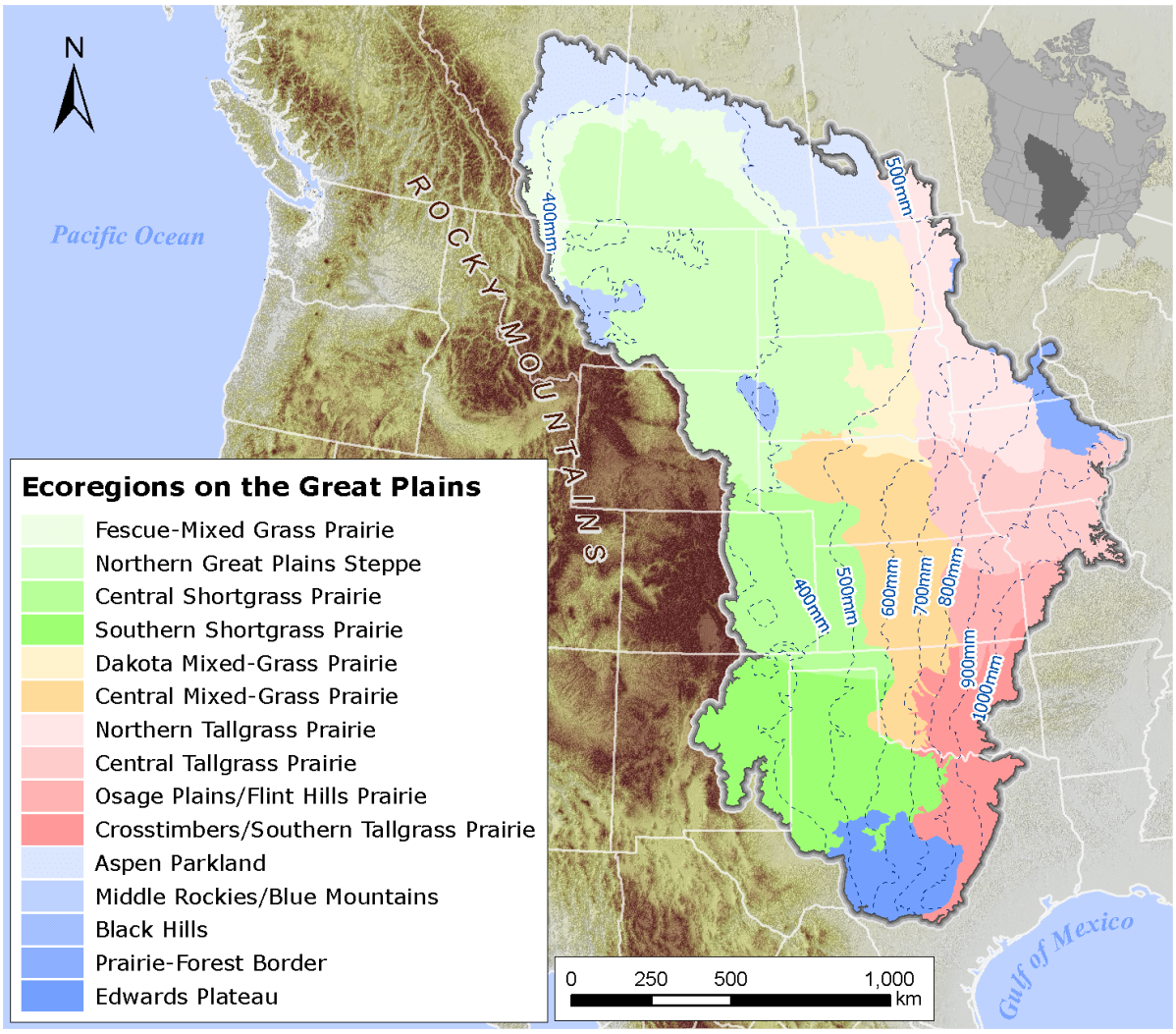

Figure 1.1: Location and ecoregions of the Great Plains in North America (ecoregion layer is from Nature Conservancy and Environmental Protection Agency; precipitation data is from WorldClim)

A widely accepted definition of disturbance is "any relatively discrete event in time that disrupts ecosystem, community, or population structure and changes resources, substrate availability, or the physical environment" (White & Pickett, 1985). Note that this definition refers to environmental fluctuations and destructive events, disregarding the normal equilibrium status of the system. The term "disturbance" possibly originated from people's early stage in comprehending the functioning and mechanism of the ecological processes and phenomena taking place on grasslands. Traditionally disturbance is defined in the context of major catastrophic events orig-

inated in the physical environment which abruptly affect the ecosystem (White, 1979). Later this idea was criticized because there is a gradient in disturbances and also disturbances can be cause by biotic factors. The term "disturbance" has been kept unchanged, still widely used in the literature today but the negative tone embedded in its concept has been ever challenged through our improved understanding in the mechanism of those ecological phenomena and processes in grassland ecosystems, which in fact are well documented to play significant roles in shaping and maintaining grasslands, especially in the case of checking the encroachment of woody vegetation.

Grasslands in North America were created and maintained through historical disturbance regimes that sustaining the structure, composition, and spatial-temporal dynamics of grassland communities by creating heterogeneity in abundance of individual plant species (Collins, 1987; Gibson, 1989). Disturbances alter various properties of an ecosystem at diverse spatial and temporal scales, most often causing "open space" and patchiness, hence resetting the succession trajectory of the ecosystem (Gibson, 2009), e.g. facilitating re-colonization by previous or other species. In the grassland ecosystem, disturbances such as fire, grazing, and other rangeland management (haying) can remove the accumulation of litter content, which in turn positively influence the productivity and plant diversity of the grassland ecosystem (Collins & Wallace, 1990; Kansas Natural Heritage Inventory, 2007). White & Pickett (1985) noted two types of disturbances: environmental fluctuation and destructive events. Disturbances can also be categorized as exogenous or endogenous depending on whether initiated within or outside the ecosystem. In the grassland ecosystem, there is a full spectrum of disturbances of different types and scales (Figure 1.2), of which fire, grazing and drought are regarded as major disturbances on the prairie.

Fire is one of the oldest natural phenomena on the prairie and functions as an inevitable and essential ecological force throughout the evolution history of the prairie. Fire occurrences are more accentuated in grasslands than other ecosystems due to its rolling topography, more combustible

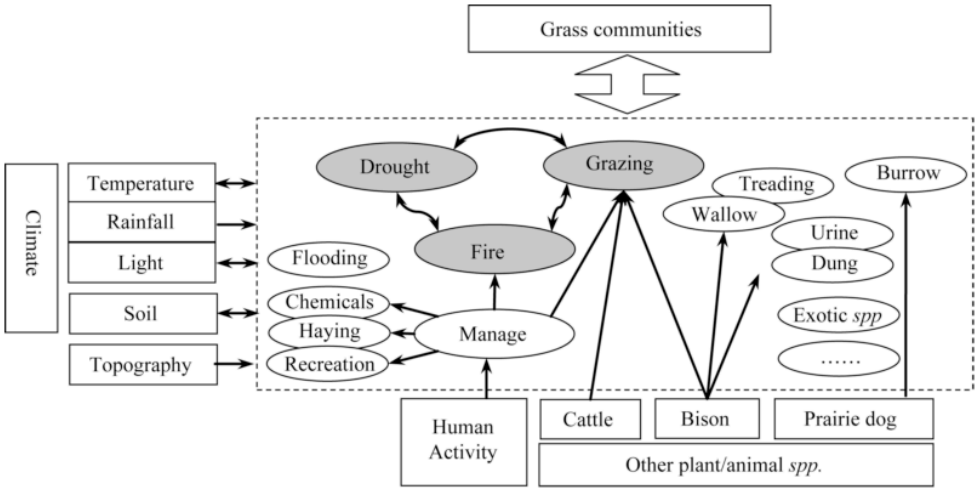

Figure 1.2: Major disturbances and their interactions in North American mixed-prairie grassland ecosystem (arrow indicates the direction of interactions; oval shapes within the dashed box are disturbances, with major disturbances highlighted with shade of gray)

materials, low humidity and frequent droughts, as well as high winds (Vogl, 1979). Grasslands are not only tolerant to fire, but often dependent on it to survive and thrive. Historically in the mixed prairie before European settlement, the ecosystem was maintained through fire events caused either by nature or aboriginal people (Pyne, 2001).Archaeological studies (Kucera, 1981) have proved fire to be significant in maintaining and expanding the northern mixed prairie, including both lightning-induced and human ignited fires.

Before early humans settled on the North American continent (<15,000 years BP), grasslands fires were solely caused by lightning storms in summer and fall, whereas only 1% of lightning fires occur during winter and early spring (Howe, 1994). Historic review and chronology studies from 1500 to early 1900 indicated that fires in the northern mixed prairie were regular events and were mainly set by first nation people (Wakimoto et al., 2005). Lightning strikes account for just 10% of fire occurrences here (Pyne, 1982), which makes humans its primary source of ignition. Meanwhile, mankind has been the primary vector of its propagation, as well as the most significant modifier of its regime. Historical journals noted that most first nation fires occurred in valley grasslands

and adjacent forests (Rannie, 2001; Barrett & Arno, 2010). Native Americans periodically burned grassland intentionally to modify local habitats and to aid in hunting activities by both driving and attracting wild game (Pyne, 2001; Barrett & Arno, 2010). Incidence of fire on the prairie has greatly declined since 1800s, when early Euro-Americans started to populate and cultivate the Great Plains. This post-settlement decline in fire was mainly caused by active fire suppression and reduction of fuel from grazing by domestic livestock. As a result, fire regimes were modified and vegetation cover was reshaped fundamentally on the Great Plains (Ford & McPerson, 1998). Absence of recurrent fire since the settlement of Euro-Americans significantly altered the grassland ecosystem of the Great Plains, resulting in declined productivity, sometimes accumulated litter and woody species invasion in this region. Over the past 125 years, decrease in fire frequency resulted in higher fire severity (Wakimoto et al., 2005). People once regarded fire suppression as equal to fire management (Courtwright, 2007). This misconception was carried on until 1930s, when prescribed fire as a management tool was introduced back to North America (south-eastern USA), supported by extensive scientific researches such as Chapman (1936); Heyward (1937). Nowadays we are well aware of fire as a vital component in shaping the structure of grassland ecosystems. It is employed as a management tool throughout all areas of North America in grassland ecosystems (Wright & Bailey, 1982).

As a management tool in grasslands, fire's significance often is not well regarded as other disturbances such as grazing and drought. Use of fire was largely an art (Vogl, 1979) and its use is still not well understood. National and provincial parks are active in implementing fire management programs. However, fire is often either excluded or misused by rangers. Fire plays indispensable role in initiating, terminating and maintaining many ecological processes in grasslands. It is inherent and inseparable from the ecosystem and cannot be replaced by any other disturbances or management activities, even some of those treatments may generate similar effects as fire (Vogl,

1979). Research indicates that the most effective way of managing natural resources is to return the environment to pre-disturbance conditions as much as possible (Vogl, 1979).

1.3 Grassland Fire and the Physical Geography

The Great Plains have different major grassland types (see Figure 1.1 on Page 3): shortgrass prairie, northern mixed-grass prairie, tallgrass prairie, and southern mixed-grass prairie, which is mainly influenced by physical environment such as climate, topography, and soil type. Precipitation is mainly from the Gulf and the Pacific (Bailey, 1980). Pacific airmass is usually dry after passing over several mountain ranges; thus the grasslands to the immediate east of the Rocky Mountains receive less precipitation. This forms grass communities with shorter stature, forming northern mixed grassland. Meanwhile, the Gulf airmass comes from tropical region producing higher humidity and greater precipitation, shortening the periods of drought in the mixed and tallgrass prairie (Collins & Wallace, 1990). Also, the polar airmass has impact on the northern part of the grassland which brings snow cover and in turn shortens the period of flammability (Knapp et al., 2009).

The Great Plains' susceptibility to fire can be mechanistically explained by its natural environment of fuels, weather and topography. The alternating wet-dry landscape of the Great Plains makes itself susceptible to fire. The limiting factor for ecosystem's productivity is moisture on the Great Plains, especially northern mixed prairie, where drought is a common phenomenon following short periods of precipitation. Moreover, precipitation is often in forms of lightning storms, concentrated in June and July. Plentiful and extra precipitation received in a wet season makes grasses grow rapidly and abundantly. Then the following dry year and sometimes droughts are able to dry the grasses, making them easily flammable. Because the prairie features flat or rolling landscape, when a fire has started it can be carried away by dry winds and spread swiftly, with

few obstacles to slow down or stop its progress (Sauer, 1950).

1.4 Research Scope

Composition and structure of grasslands can be modified in response to various biotic and abiotic factors present in the ecosystem (White, 1979). Of all those factors, impact of fire had been ignored and least investigated due to its complex nature. Study area for this research is part of the mixed prairie called the Grasslands National Park (GNP) of Canada, significant for its functioning as the abundant pool of CO_2, wildlife and vegetation (Parton et al., 1995). The park has the largest area of remaining pristine grasslands being preserved, where the importance of fire has long been recognized. However, its preservation and management strategy is in question as to its fire management, due to its unknown pre-settlement historical fire regime when burning was an essential ecological process in the ecosystem. This research aims to answer a series of questions in order to understand fire's role in the mixed-grassland ecosystem.

How does grassland ecosystem respond to fire across time? And how to quantify fire's effect with field surveys and RS based approaches? There exists a large body of literature studying fire's effect on ecosystems, including grasslands (chapter 2 on page 10). Though general conclusions can be reached regarding fire's impact, there are conflicting results within literature possibly due to different localities of grasslands ecosystems as well as limited resources available to most existing investigations. Based on the established general conclusions from past fire-related studies, this research tries to take the full advantage of cost-effective and efficient spatial technology (remote sensing or RS, and geographic information system or GIS) with the intention to overcome the limitations identified in previous researches through establishing an effective method in quantifying and understanding grasslands fire's impact with RS based approaches.

What are the driving factors of recovery and how their influence change over time? Based on the literature, this research focuses on these major factors to explain vegetation post-fire recovery pattern: climate, topography and grazing activity. In the semi-arid mixed prairie, water availability is the limiting factor of the ecosystem's productivity (Schröder, 2006; Banerjee et al., 2011; Yang et al., 2013; Li & Guo, 2014). Studies (Ford, 1999; Ford & Johnson, 2006) indicate that weather patterns play significant role in post-fire recovery and sometimes supersede fire's effect. Topography determines distribution of soil moisture and nutrient that in turn governs species composition and community structure of the grassland ecosystem (Gibson & Hulbert, 1987). Grazing is another major factor that causes disturbance to grasslands and may interact with fire to affect the post-fire grassland ecosystem. In fact, a few studies examined the interaction of the two with the theory of "pyric-herbivory" (Augustine et al., 2010; Scasta et al., 2012, 2016; Powell et al., 2018). Gates (2016); Gates et al. (2017) tested such theory on the mixed prairie (Montana, USA) found that there was no need to separate fire and grazing and deferral of grazing following fire is "unnecessary or even inappropriate". This study aims to quantify the pattern of vegetation recovery in respond to these factors, their interactions, and how their influence change over time, with the help of field data analysis and RS based approaches.

Chapter 2

Literature Review

2.1 Overview of the Landscape of Fire Studies

Grassland fire study is challenging due to its unique environment. There is a plethora of literature dedicated to forest fire studies. However, resources on grassland fire studies are quite limited and the subject is not well understood (Vogl, 1979). Though grassland structure and fire behaviour are simpler than other ecosystems such as forest and brush, not enough attention is paid to fire studies on native grasslands due to various perplexing reasons of cultural, historical and psychological aspects (Vogl, 1979). As a result, resource managers and general public have little regard for native grasslands' fire management. Meanwhile, grassland ecosystem has its unique challenges in fire studies. Some researchers (Schepers et al., 2014) have suggested that results of fire studies in forest ecosystems often perform better than that in grassland ecosystems. The historic management lineage of GNP further complicates fire studies in this preserved area. Ever since large-scale human settlement in the 18^{th} century, the original prairie ecosystem has been severely altered and detoured from its historic dynamic equilibrium. Bison herds once roamed on the prairie and was a significant contributor to the fuel loading of grassland fires. Then they were replaced by cattle grazing. At the same time, a considerable amount of dead material has been accumulating throughout the park, visible on the Landsat imagery even to the untrained eye. Once humans had been actively putting out small fire events. This significantly increased the probability and severity of large fire

outbreaks. When fire's ecological role was recognized, rangers started to, more often, use it as management tool (Vogl, 1979) to suit their own purposes such as improving forage quality, controlling brush or external parasites, instead of comprehensive consideration of ecosystem's health (Scasta et al., 2012). Some research indicates that fire suppression is still practised in the 21st century with significant hesitation of reintroducing fire back to the prairie ecosystems (Brockway et al., 2002; Wakimoto et al., 2005). As a result, the original fire regime once governed and shaped the prairie ecosystem has been profoundly disrupted.

Fire's impact on terrestrial ecosystems is documented (Bond & Keeley, 2005) as: (1) shaping global biome distribution, (2) maintaining the structure and function of fire-prone communities, (3) acting as an evolutionary force, (4) being employed as one of the first tools by humans to reshape the world. Fire has significant impact on the fauna and flora in the grassland ecosystem, in both direct and indirect ways. Direct effects include mortality of individuals, which are short-term. Indirect effects, such as dynamics of species composition and changes in habitat, are long-term. Indirect impacts are not easy to observe and evaluate, but usually more important than the short term effect.

Fire, coupling with other numerous factors, i.e. topography, soil, fauna (insects, herbivores), together with herbaceous plants (Grover & Musick, 1990; Wright & Bailey, 1982), can restrict the encroachment of woody plant (trees, shrubs), release nutrients bound up in organic matter, accelerating the rate of decomposition in the soil, so as to maintain the establishment and the stability of grasslands (Ford & Johnson, 2006; Ford & McPherson, 1996; Wright & Bailey, 1982). Descriptive studies (Dwyer & Pieper, 1967; Launchbaugh, 1964) show that fire occurrences decrease herbaceous production for one to three years. And herbaceous recovery is influenced strongly by precipitation. Plant species in semi-arid grasslands are more likely subject to fire season and frequency than fire behaviour (Steuter & McPherson, 1995). The reestablishment of periodic fire is fundamental to the

ecological restoration of grasslands on the Great Plans (Ford & Johnson, 2006). However, current understanding of fire's effect on the grassland ecosystem still need to be improved, especially for grasslands under conservation such as GNP.

2.2 Current Approaches and Results

This section first reviews the commonly used methods in fire studies and highlights RS based approaches as potential solution for studying grasslands fires more effectively in the northern mixed prairie. Then major conclusions are summarized from the pertinent literature to provide as the basis of understanding fire's effect in this grasslands.

2.2.1 Methods Used in Fire Studies

Based on historical materials, Wakimoto et al. (2005) tried to reconstruct historic fire regimes and fire behaviours in the northern mixed-prairie. General conclusions about historic fire frequency can also be reached based on rates of fuel accumulation and woody plant invasion (Madden et al., 1999), as well as charcoal remains from lake sediment cores (Umbanhowar, 1996). Meanwhile, in places of grasslands with trees, tree fire scars can be used to study its fire history and historic fire regime. Furthermore, tree-ring studies help establish the drought cycles and duration, which in turn provide evidence of historical climate, fuel loading, and potential fires. However, this remains a challenge if woody plants are scarce; because grasses and forbs that do not carry fire scars and growth ring patterns (Wakimoto et al., 2005), as in GNP.

Wildfires provide first-hand data for grasslands fire studies, such as Redmann (1978). By compiling wildfires occurred in this region (most of them in late summer), Kruger (2001) investigated fire's immediate and long-term effect on forage species as well as other range plant species on the northern mixed prairie. A typical methodology can be found in Wakimoto et al. (2005); Kruger

(2001). By surveying the vegetation and soil properties at burned sites and its adjacent unburned sites, the hypothesis of no differences across sites can be tested with statistical analysis (e.g. t-test). Fire's long-term impact can also be analyzed with field surveys of longer time frame or intervals, e.g. < 5 years, > 5 years, 10 years, 15 years (Wakimoto et al., 2005; Kruger, 2001). However, such wildfire studies have obvious limitations. Besides expensive sampling effort, no systemic evaluation of fire regime can be conducted and it is impossible to know when and where wildfires will occur (Wakimoto et al., 2005).

A large body of literature is dedicated to controlled burning, or prescribed fires, including academic as well as applied researches on various types of grasslands on the Great Plains, for example Anderson et al. (1970); Vogl (1979); Kucera (1981); Collins & Wallace (1990); Ford & Johnson (2006); Knapp et al. (2009); Augustine et al. (2010); La Pierre et al. (2011). Moreover, detailed long term ecological researches have been designed and implemented, such as the famous Long-Term Ecological Research program (or LTER, more details available from Franklin et al., 1990; Knapp et al., 1993, 1998), to understand the fundamental mechanisms of fire's effect on grasslands ecosystems. A good review of ecological effects of prescribed fires can be obtained from Knapp et al. (2009) with their central region covering the northern mixed-prairie. Prescribed fires are effective in identifying basic principles of fire's effect to the ecosystem through systematic manipulations such as extrapolation, synthesis and generalization (Vogl, 1979). Based on the established understanding of ecological processes and mechanisms, ecological models can be developed to simulate vegetation dynamics and quantify various fire regimes, such as the LANDFIRE model from US Department of Agriculture (Rollins, 2009) to study fire regimes of different ecosystems including part of the mixed prairie. Though prescribed fires experiments and fire modelling have significantly improved our understanding of fire's impact, both are resource-consuming and not readily portable to different locales.

In fact, the contribution of remote sensing in fire studies has been recognized since 1970s (Jayaweera & Ahlnas, 1974) for forest fire monitoring and control effort. Performance of various satellite sensors have been tested in fire studies including ERS-1, GOES, DMSP, AVHRR, Landsat (a review can be retrieved at Rauste et al., 1997), SPOT (Yang et al., 2013), and MODIS (Chuvieco et al., 2005). LTER investigated the sensitivity of Landsat product to distinguish burned and unburned grasslands with positive result (Franklin et al., 1990). RS based approaches have obvious advantages compared to conventional field surveys in terms of providing timely and cost-effective imagery at various scales. Related studies have confirmed the robust performance in the sensitivity of RS data in capturing the spectral characteristics of wildfires to study their occurrence, size and severity (van Wagtendonk et al., 2004; Petropoulos et al., 2011; Yang et al., 2013). Besides visible bands (sensitive to blackened charred vegetation), other bands are also proved effective, including near-infrared (NIR) (Franklin et al., 1990) (sensitive to green vegetation) and shortwave infrared (SWIR) bands (sensitive to mositure content) (van Wagtendonk et al., 2004; Yang et al., 2013). Furthermore, various vegetation indices and specifically burn indices have been designed from single RS bands that can be used for fire studies (Chuvieco et al., 2005; Yang et al., 2013; Lu et al., 2016).

2.2.2 Impact of Lacking of Fire

For ecosystems with a long history of fire, there is concern over the negative series of consequences of manmade fire suppression. Studies (Leach & Givnish, 1996; Uys, 2004) in tall grass prairie shows that 5% plant species has been lost due to human fire suppression and the authors argue that this is common in grasslands elsewhere. Taking fire out of grassland ecosystem makes it threatened by the encroachment and dominance of woody plants. According to Barker & Whitman (1988), northern prairies had reoccurring fires every 5-7 years historically. With active fire suppression, aspen and poplar began to invade grasslands in Alberta. Dramatic species loss may occur when

fire suppression results in complete biome change, from grasslands to forests as shown in a study (Peterson & Reich, 2001). In the plant level, fire causes various levels of reduction in above ground biomass. In the community level, fire results in potential local species loss, changes in species composition. Meanwhile, fire affects vegetation by lowering the soil albedo, raising soil temperature, as well as releasing nutrients from organic matter. Study of the conifer forests of southwestern North America (Bond & Keeley, 2005) explicitly describes that: human settlement during the early 20th century, with the policy of total fire suppression, is by itself an experiment on how fire controls vegetation structure, and has resulted in near-total fire extinction. This in turn resulted in major shifts in ecosystem structure and function: (1) tree density increased significantly; (2) major losses in the herbaceous under-storey; (3) losses in species diversity; (4) fuel accumulation, a major potential threat.

2.2.3 Fire Regime of Northern Mixed Prairie

Fire regime was introduced by Gill (1975). Bond & Keeley (2005) modified the concept of fire regime to include five aspects: (1) fuel consumption and fire spread patterns, (2) intensity, (3) severity, (4) frequency and (5) seasonality. All these aspects alone or together may have profound impacts on terrestrial ecosystems.

Scholars have been trying to understand fire regimes to use them as management tools beneficial to local grassland ecosystem. Fire has been reintroduced back to most ecosystems around the world to restore its ecological functions. The assumption is that this restoration can be achieved through carefully designed prescribed fire and fuel management that resembles historic fire regimes.

However, a few questions arises regarding this process. First, historic fire regime is sometimes unclear and is challenging to determine (Wakimoto et al., 2005). Then fire regimes were different historically: prior to human occupation (<15,000 YBP) when grasslands were shaped under grow-

season lightning fires through 30 million years of evolution (Howe, 1994), and first nation's era when most fires were man caused right before Euro-American settlement (Wakimoto et al., 2005). Moreover, current fire regimes are thought to be different from historical regimes according to Howe (1994), detrimental to native species and possibly the whole ecosystem because it did not evolve under such manmade fire regimes (Howe, 1994; Knapp et al., 2009). Moreover, when the fire regime of the target ecosystem is difficult to determine, an estimation is assumed based on the fire regimes of its adjacent ecosystems. However, research findings from one area or vegetation type may not apply to another locality (Knapp et al., 2009, p. 7).

It is challenging to understand fire's effect in the prairie region, especially the historic fire regimes because much of the grasslands area have been profoundly modified by human activities (agriculture, overgrazing) and woody species encroachment. The fragmented landscape severely disrupted the historic fire regime. Though the region had developed under recurrent fires in history, it is challenging to understand historic fire regime due to lack of physical evidences such as fire scars, or trees rings. Most researchers use prescribed fires to understand the fire regime and its impact to grasslands in this region.

2.2.3.1 Fire Intervals

Madden et al. (1999) found that in general, grasslands that receive greater annual precipitation always have a higher fire frequency than areas with less moisture. This is mainly caused by the different rates of fuel accumulation. For grasslands with higher precipitation, more biomass and litter can be accumulated each year, making fire more likely to occur. Whereas in more arid grasslands, fuel accumulation takes a longer time before it is sufficient to carry a fire across the landscape.

LANDSUM is a spatially explicit vegetation dynamics simulator from USDA. It is capable of incorporate various disturbances including fire into vegetation succession. Multiple fire succession

pathways are utilized. The model suggested a fire interval of 4-23 years for the northern mixed-prairie (Missoula Fire Sciences Laboratory, 2012).

Wakimoto et al. (2005) determined and reconstructed historic fire regimes and fire behaviours in the northern mixed-prairie. Under pristine conditions, northern prairies burned on a regular basis, approximately once in every 5-7 years (Barker & Whitman, 1988). Based on fire ecology and prescried burning results in this area, Wright & Bailey (1982) found that grassland fires often occurred in drought years after abundant fuel from previous 1-3 years of above-average precipitation. They reported a fire frequency of 5-10 years in level-to-rolling areas, and 20-30 years in rough hummocky topographies. A few studies suggest that at ponderosa pine sites (prairie ecotone) in South Dakota, fire intervals were about 7-12 years (Wakimoto et al., 2005). Meanwhile, rates of fuel accumulation and woody plant invasion indicate an average fire frequency of 6 years in most part of the northern mixed prairie, and 25 years in the dry western part.

The recovery of ground surface dynamics (vegetation and soil) can also serve as an indicator of historic fire interval explaining the adaptation of the ecosystem to historic disturbances. La Pierre et al. (2011) examined three fire intervals (1, 4 and 20 years) and found that four year fire regime proves consistently as a strong predictor in explaining above ground net primary productivity, even if it is included as simple as a binary parameter. Wakimoto et al. (2005) compiled recent wildfire survey data at this region and reported that grasslands usually can recover after 5 to 10 years, depends on different vegetation cover type. However, they also reported a change in species composition and abundance after 10 years of recovery in areas with more shrub cover. For example, based on the fire scar data in Montana, North Dakota and southern Saskatchewan, a fire frequency of 10-20 years is suggested prior to Euro-American settlement era.

2.2.3.2 Impact of Fire Seasons

Seasonality of the fire can affect grasslands community composition, especially when repeated over several years (Knapp et al., 2009). The main reason is that different grass species vary significantly in their response to the burning season. For example, Ford & Johnson (2006) showed that shortgrass steppe can recover from fire in three to thirty months, dependent on the fire season.

Fire season is governed by the coincidence of ignition and low moisture in the ecosystem. This condition usually happens to be the driest time of the year. However, humans have modified fire season in many ways, which makes the understanding of the impact of fire season more challenging and demanding. When dry, fuels of semi-arid grasslands may favour high rates of fire spread (Rothermal, 1983), whereas green grasses or actively growing grasses promote a discontinuous or patchy fire regime (Andrews, 1986). The high moisture content of green, living plant tissue makes it more difficult to burn, than dry plant or litter which ordinarily promotes fire spread. Therefore, fire intensity and severity during the dormant season tend to be higher, resulting in more widespread damage and mortality to exposed surface crusts than growing-season fire. Whereas, fire during the growing season has been shown to reduce regrowth in vascular plants because large portions of photosynthetically active tissues are killed (Briske, 1991).

Knapp et al. (2009) provided a systematic review of the ecological effects of fire seasons' to all ecosystems in conterminous USA, with the central region overlaps part of the northern mixed prairie in this study. They find that timing of fire can affect certain species through direct injury or mortality, especially during their vulnerable phenological stages. Fire at the period of active growth is most detrimental, simply because new plant tissues are more senstivie to heat, and meanwhile carbohydrate reserves are lower at that time. Grasslands displayed higher resistance to fire when carbohydrate reserves are replenished (Wakimoto et al., 2005). However, diverse species composition in grasslands complicates the situation. Vegetation's post-fire response depend on

three elements: the species' ability in fire resistance, timing in relation to its phenology at fire's occurrence, and total heat from the fire. Vegetation's response to time of fire can be as sensitive as a few days. Benning & Bragg (1993) reported significant differences of big bluestem to burns just four days apart, with fires shortly after the species' start of growth producing an increased stem height and number of flowing than fires applied promptly before its start of growth in the spring.

Researches from Howe (1994) indicate that prescribed fire at the growing season in summer and historical fire frequency cause more harm to warm-season grass species, therefore promoting the early-flowering cool-season grass species; whereas spring fire will shift species composition and favours warm-season grass species. Brockway et al. (2002) also found that dormant-season fire may be the preferable method for restoring fire in shortgrass steppe ecosystems in the southern Great Plains where fire has been excluded for a long period of time. Though more damaging, growing-season burns showed higher plant diversity, probably due to its preference of C3 grasses and greater heterogeneity of burn intensity. As for the soil, early spring burns decreases soil moisture compared to late spring, because with early spring the ground is exposed for longer time which leads to more evaporation. The presence of litter content (thatch) helps to accumulate snow and increases the time of snow-water infiltration to soil in this region. Though burning during the growing season minimizes impact on soil crust, its recovery can be rapid (Ford & Johnson, 2006).

2.2.4 Grasslands Post-fire Recovery

USDA conducted a comprehensive review (Knapp et al., 2009) on the ecological effects of fire, aiming to provide well-round information for range managers to use prescribed fire as a management tool effectively. Part of their investigation covers the Canadian prairie in GNP. In general, they found that post-fire response of organisms depends on the complex interactions between a myriad of factors, including time of prescribed burning, historical fire regime, phenological stage of the

organisms, fire severity of different burn seasons, climatic variation within or across burn seasons.

Researches from Great Plains (such as Madden et al., 1999) indicate that fire generally decreases shrub coverage and increases the cover of graminoid species as well as percentage of live vegetation. In contrast, lack of fires from active suppression causes direct woody species encroachment, such as big sagebrush, ponderosa pine and Douglas fir (Wakimoto et al., 2005).

Ford & Johnson (2006) reported that in general, grass cover recovered quickly from the fire treatment, and the long-term effect of fire was neutral. Burning during the dormant-season had little effect on grass cover, when the burning site was revisited and sampled after as little as two months from prescribed fire; but burning during the growing-season seems to negatively impact grass cover for up to two years after fire. Studies (Anderson et al., 1970; Heirman & Wright, 1973; White & Currie, 1983) on the effects of seasonality of fire (spring fire) on buffalograss and blue grama indicated mixed results, over a time frame of three months to 16 years. Often, early-spring burns (March) produce neutral or positive responses; and late-spring burns (May) produce negative results. Whereas fall burns led to more yield than did spring burns. Negative, neutral and positive responses to fire were evident in both season-long grazed areas (Anderson et al., 1970), and areas protected from domestic livestock grazing (Dwyer & Pieper, 1967). Shortgrass prairie ecosystem recovers relatively quickly from fire disturbance (Ford & McPerson, 1998). Vegetation cover, arthropod, mammal species richness treated with dormant-season fire recovered in approximately two months and showed no significant difference from untreated communities. By studying vegetation response (grass cover) to different timings of fires (dormant season versus growing season), Ford & Johnson (2006) concluded that in the short-term, burning during the growing-season appears to reduce fire severity but exerts greater impact on grass communities (opposite for soil crusts) compared to burning during the dormant-season. Dormant-season fire in the shortgrass steppe is less damaging to grass communities (opposite for soil crusts) than growing-season fire.

Wakimoto et al. (2005) used vegetation similarity values to quantitatively measure the similarity between vegetation cover types between burned and unburned sites. For grassland and shrubland, vegetation similarity values are consistently and significantly difference across treatments, indicating the fact that burned communities cannot return to the unburned status even after 10 years plant succession. Grassland sites only, however does not show significant difference either short-term or long term, i.e. 1-2, 3-5, 6-10, >10 years. With the typical grassland taxonomic complex (wheatgrass, gramma, needlegrass, big sagebrush) in GNP, similarity values across treatments are essentially equal 1-5 years post-fire, and changed slightly >5 years post-fire.

Shannon-Wiener diversity index can be used (Wakimoto et al., 2005) to evaluate fire's impact on grasslands biodiversity. For grasslands and shrubland cover types, burned sites had slightly higher diversity than unburned sites 1-2 years post-fire. For the wheatgrass-grama-needlegrass complex, diversity index remains increased >5 years post-fire. Meanwhile, species richness (total number of species) at burned sites was also slightly higher, and remained so to 3-5 years, 6-10 years and >10 years post-fire. The greater post-fire species diversity and richness indicates a decrease in dominance by a few species previously present on burned sites compared to adjacent unburned sites.

Wakimoto et al. (2005) also found that fire affected the vegetation structure of 62% surveyed sites. Such structure change tended to happen on sites with shrubs. This is probably because shrubs are more susceptible to fire mortality, with some shrub species especially sensitive to fire. They found that shrubs were killed entirely for some sites, converting the vegetation cover from pine-shrubland-grass cover to wheatgrass-needlegrass cover types. Whereas no such change occurred for wheatgrass-grama-needlegrass sites.

Fire showed different effects on various major grassland species. Kruger (2001) found that burned sites showed more cover of blue grama, sandberg bluegrass and green needlegrass one

year post-fire. Such increase became less obviously 2-5 years post-fire. 6-15 years post fire, these species showed mixed result; with some slightly higher and some slightly fewer. Meanwhile, unburned grassland and shrubland had more undesirable species compared with burned sites. 15 years post-fire, burned and unburned sites showed little difference with each other. Comprehensive and detailed species' response to fire can be accessed at Wakimoto et al. (2005) as well as USDA's Fire Effects Information System (USDA, 2018).

2.2.5 Driving Factors of Post-fire Recovery

Climate plays a significant role in vegetation's post-fire recovery. Knapp et al. (1993) showed that burned communities are more limited by water than the unburned. In the semi-arid mixed prairie, water availability is the limiting factor of the ecosystem (Schröder, 2006; Banerjee et al., 2011; Yang et al., 2013; Li & Guo, 2014). In fact, weather patterns (typically increased precipitation) can override fire effects. Ford & Johnson (2006) found that with adequate precipitation the nitrogen enriching function of the soil crusts recovered within two years. Launchbaugh (1964) examined a spring wildfire in shortgrass prairie, when the soil moisture was low, and found that fire caused short-term declines in plant biomass. It took three growing seasons for a burned grass community to return to a level comparable to the unburned state. Similar results of burning in prairie were confirmed by Ford (1999) and also reported in west-central Kansas (Hopkins et al., 1948). Following a wildfire in New Mexico when the moisture balance was more favourable, Dwyer & Pieper (1967) found that biomass production of a species (blue grama) was reduced only by 30% during the first post-fire growing season. Biomass returned of the grass community to pre-burn status with above-average precipitation the second year after the burning event. Prescribed fire in Texas during years with above-normal winter and spring precipitation showed considerable tolerance of fire for buffalograss and blue grama, with no loss at all in the yield at the end of the first growing

season (Heirman & Wright, 1973; Wright & Bailey, 1982). Wright & Bailey (1982) showed that the tolerance of most grass species to fire in the shortgrass prairie, under different moisture regimes, appears to be similar to the species mentioned above. Temperature, on the other hand, seems to play a weaker role in vegetation's post-fire recovery, according to La Pierre et al. (2011).

Other potential factors affecting vegetation's recovery on the northern mixed prairie include topography and grazing. Topography determines distribution of soil moisture and nutrient that in turn governs species composition and community structure of the grassland ecosystem (Gibson & Hulbert, 1987). Topography causes heterogeneity of grasslands and grassland studies often investigate communities at different topographic locations as they show greater variation in vegetation cover and characteristics (Wakimoto et al., 2005; Knapp et al., 2009). Grazing causes disturbance to grasslands and may interact with fire to affect the post-fire grassland ecosystem. Herbivores prefer recently burned grasses because forage on burned sites is more palatable and higher in protein (Anderson, 2006). Also heavy grazing pressure prevent accumulation of fine fuel, thus reducing the likelihood of fires (Fuhlendorf et al., 2009). In fact, grasslands are often disturbed by both fire and grazing. Powell et al. (2018) showed that the northern Great Plains is adapted to both and can recover within two years after fire and grazing pressure, indicating its resilience to the fire-grazing interactions. Meanwhile, studies have suggested the theory of "pyric-herbivory" (Augustine et al., 2010; Scasta et al., 2012, 2016; Powell et al., 2018) to model their interaction in greater detail.

2.3 Research Gap and Research Objectives

As an important ecological factor, fire has been studied extensively in tallgrass, shortgrass as well as mix-grass prairie in the central and southern parts of the North American Great Plains (Augustine et al., 2010; Ford & McPherson, 1996; Knapp et al., 2009; Wright & Bailey, 1982). For different grasslands, the influence of fire may contribute to different vegetation responses. For example,

Oesterheld et al. (1999) showed contrasting productivity responses for subhumid versus semiarid grasslands. Most researches on grassland fires deal with particular local landscapes and ecosystems. We must be cautious when interpreting the results from different researchers on the impact of fire on the grassland ecosystem, because Ford & Johnson (2006) confirmed that impact of fire varies for different types of plants according to their active growth season, with C4 plants least vulnerable to the dormant-season fire and most vulnerable to the growing season fire. And research findings from different localities can vary significantly due to differences in historical and prescribed fire regimes (Knapp et al., 2009, p. 7). Guo et al. (2000) found that aboveground dry biomass, plant moisture, and dominant species together with plant forms are different for cool seasons and warm seasons on a tallgrass prairie. With unique flora and fauna composition, the Canadian northern mixed prairie can be significantly different from other grasslands. However, little is known about fire effects in semiarid mixed-grass prairie in Canada (Ford, 1999). There is lack in knowledge about the pre-settlement fire regime (Glitzenstein et al., 1995) and clear understanding of fire effects on the dynamics of that ecosystem, especially the plant communities (Li & Guo, 2014; Yang et al., 2013).

All previous researches on vegetation responses to fire in this region are based on short-term investigation (less than a year, see Lu et al., 2016; Yang et al., 2013). However, grassland communities have evolutionary adaptations, showing variation in population recovery dynamics from fire season, frequency and behaviour (Glitzenstein et al., 1995). As a result, fire regime should be studied in a more consist and reliable manner, especially in longer term and with finer temporal resolutions. Long-term field studies in climate and disturbances suggested that short-term ecosystem responses are usually opposite to long-term responses (Franklin et al., 1990). Special interest is given in the vegetation recovery, because vegetation patterns play a significant role in maintaining the grasslands ecosystem through its influence in runoff, soil moisture, spatial distribution of

erosion-deposition, nutrients as well as other biophysical activities (Schröder, 2006).

Meanwhile, there is still no clear understanding of the mechanisms behind the interaction of fire and biophysical environment, such as the relative importance of ignition, dry periods, properties of grasses as fuel, and topographic barriers to constrain fire spreading (Bond & Keeley, 2005). Though we know that different fire regimes favour different plant attributes and similar fire regimes favour similar plant attributes (Scholes & Archer, 1997), no two burns are the same, even both are conducted within the same season, due to the presense of other confounding factors Knapp et al. (2009). Fire's impact, its behaviour and its consequences as well as vegetation response in the grassland ecosystem, is to some extent determined by local climate. The detailed mechanisms therein demand more studies on the specific ecosystem under investigation.

Quantifying long-term shift in fire regimes is important to comprehend the driving forces of changes in fire dynamics, and the implications of fire regime changes for ecosystem ecology. Even though past fire occurrences can be traced by various means, it is still difficult to reconstruct historic fire regimes. Studying the effects of fire regime and its change is challenging, especially on the prairie due to the high intra- and inter- annual variation of grass communities, which is determined by a myriad of factors from climate to disturbances. Field experiments can be used to reveal the mechanism behind the interaction of grazing, fire and grass communities. However, effects of fire regimes still need to more investigation (Glitzenstein et al., 1995), especially for ecosystems where comprehensive conservation or management plans are involved as in GNP. Meanwhile, RS provides new ways of grassland fire studies. Time series of burn patches can be mapped with RS approaches (Dubinin et al., 2010). Also (Lu et al., 2016; Yang et al., 2013) have demonstrated the feasibity of using RS in evaluating grassland fires in the nothern mixed-prairie, GNP.

A comprehensive examination of fire effects on the ecosystem is needed to further our understanding about ecosystem dynamics, especially vegetation responses to fire. This research intends

to investigate the vegetation recovery of the C3 dominated northern mixed grassland from a spring fire event, focusing on a longer historic perspective with RS approaches. Field data were collected before the burn and four growing seasons following the burn. Various spectrum bands, vegetation and fire indices developed for Landsat product are tested for their capacity in distinguishing burned and unburned areas as well as studying the long-term vegetation recovery.

By investigating a wildfire that took place in April 27th, 2013 with the help of time series of RS data, this study tries to understand fire's immediate and long-term effect on the northern mixed-prairie and the driving factors for vegetation's post-fire recovery. Specifically, there are three major research objectives:

- To evaluate fire's effect on the northern mixed-prairie using field survey data
- To investigate the theory and application of Remote Sensing approaches in grasslands post-fire recovery
- To examine the driving factors of grasslands post-fire recovery using both field data and RS approaches

Moreover, several minor objectives are also involved in this study. These objectives have inherent logical connection as indicated in Figure 2.1.

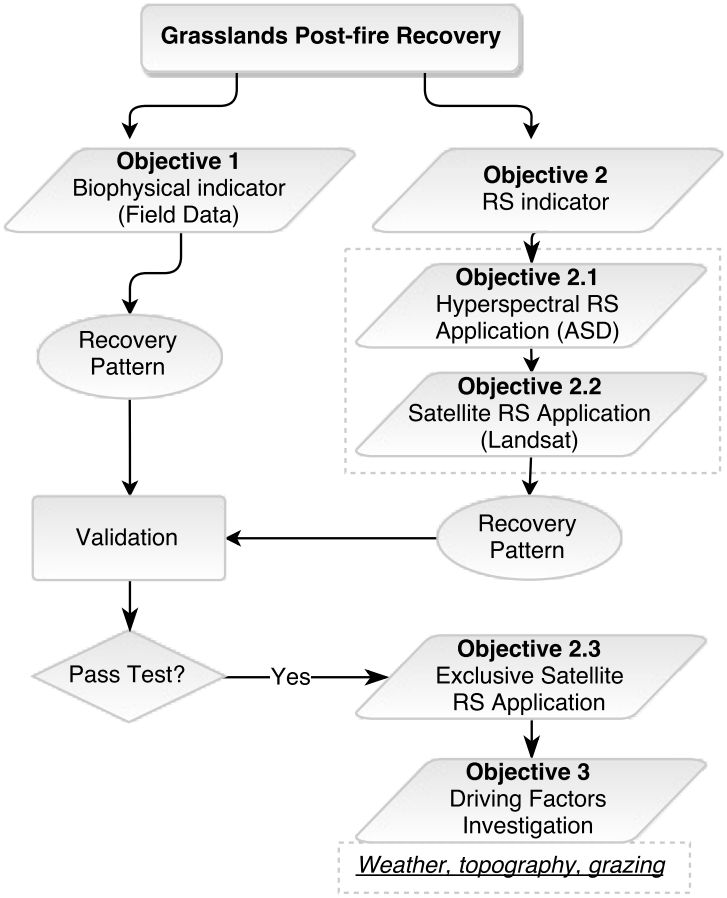

Figure 2.1: The objectives of this research and their inherent logical connection. Vegetation post-fire recovery is examined using the field data in Objective 1, which also serves as the ground reference of RS based approaches discussed in Objective 2. Hyperspectral measurement from field data is also used to establish the theoretical basis of RS approaches. After testing and validating the performance of RS approaches, vegetation post-fire recovery is investigated again with Objective 3, in the context of major driving factors influencing the process of recovery.

Chapter 3

Study Area & Data Collection

3.1 Study Area

This section first introduces the study area with relevant information on the wildfire's location and its physical geography in order to establish appropriate spatial context for the fire's initial propagation and its later influence on the recovery of the grassland ecosystem. Following up is the visual assessment of the fire's disturbance. The assessment itself consists of two parts: the first part focuses on the reconstruction of the fire's propagation path, its spatial pattern and burn severity across the study area; whereas the second part tries to qualitatively evaluate the vegetation's post-fire recovery through visual interpretation of imagery acquired from both the ground as well as the satellite (Landsat 8). These qualitative assessments serve as the introduction of the grassland fire study, providing general overall evaluation of the fire and opening up research questions that can only be answered with quantitative analysis. Quantitative analysis using both field data and RS imagery is the main focus of this research, which will be discussed in the following chapters.

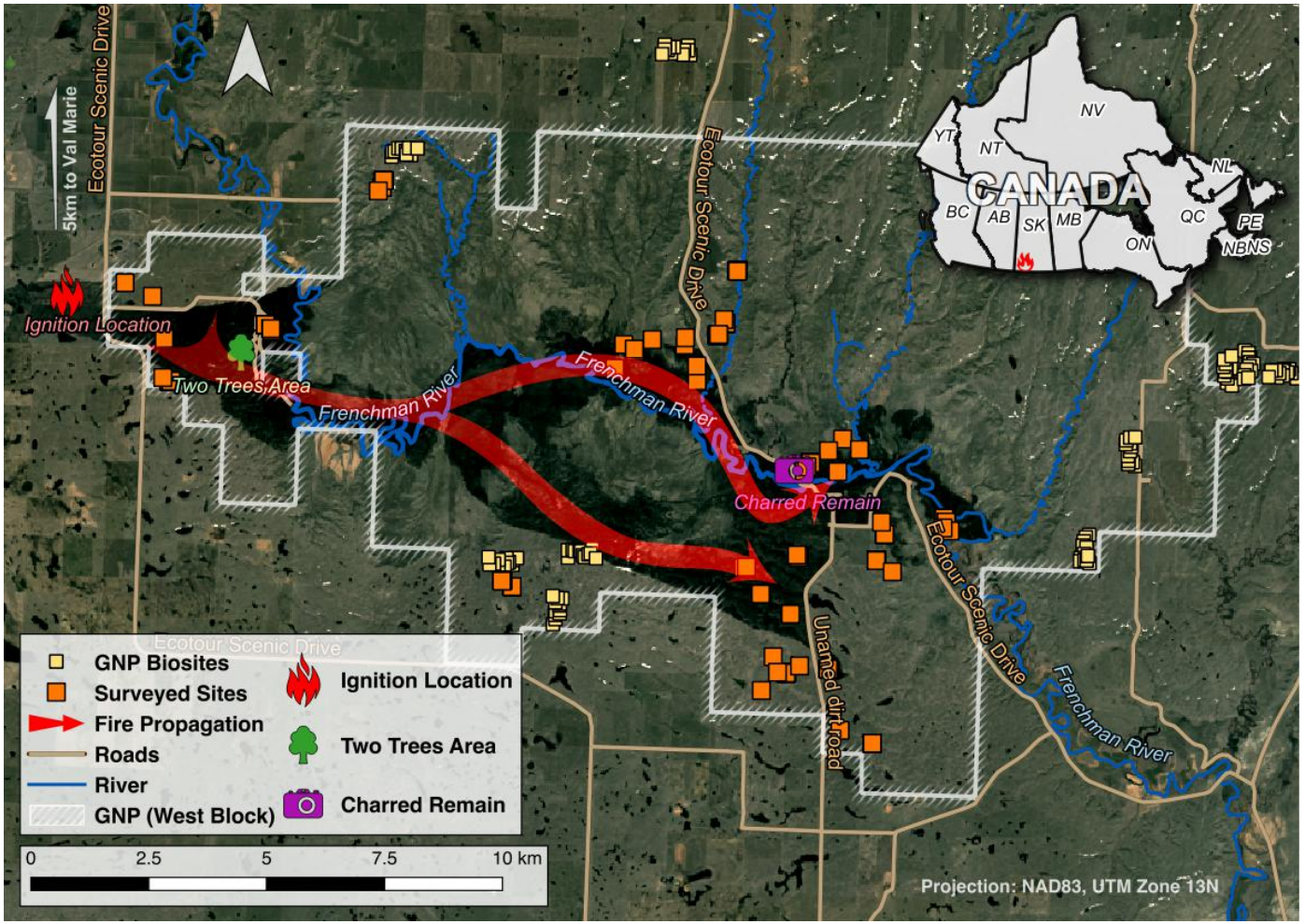

Figure 3.1: Study area for this research is located at the West Block of the Grasslands National Park, Canada. Background of this image is a natural colour composite of Landsat 8 imagery (May 1st), acquired merely three days after the fire's occurrence on April 27th, 2013. The fire started close to the park's west border (marked as "Ignition Location") and quickly spread eastward across the park, burning approximately 1/3 of the west block. Burn severity varies, as indicated by different intensities of the black colour (charred material). Notice the isolated unburned grassland "pockets", of which the most prominent one is formed by the fire's two heads (one along the Frenchman River valley, the other to the south).

3.1.1 Physical Geography

The study area is located in the west block of the Grasslands National Park (GNP, also referred to as "the park" in this research), bordering Saskatchewan in Canada and Montana in USA (Figure 3.1). It is situated in the prairie ecozone and has been providing habitats for rich diversity of flora and fauna that have evolved in a highly dynamic environment including grazing, prairie fildfires, soil erosion, drought and flooding (Anderson, 2006).

Fire plays significant role on the mixed prairie. Grasslands are characterized by rapid growth and slow decomposition rates due to the chemical and physical composition of the plants (Vogl, 1979). Decomposition process of above-ground materials by microorganisms are limited. And fire functions as an important decomposition agent and nutrient cycler of the grasslands ecosystem (Vogl, 1979). A survey (Redmann, 1978) indicated that naturally (lightning) caused fires are relatively common in the grassland here, with one year in six years having abundant fuel and suitable weather conditions to encourage fire's occurrence. Most of these dynamic disturbances had been removed ever since the massive human settlement in the 19^{th} century. Wildfires have been actively suppressed, resulted in near-total fire extinction and major shifts in ecosystem structure and function, with 80% of the native prairie lost for ever (GNP, 2017a). In light of this, GNP was founded in 1988 with its mission to preserve the large still standing pristine mixed grass prairie in North America (Csillag et al., 2001; GNP, 2017a).

The area is semi-arid, with annual precipitation between 300 and 330 mm, and average temperature ranging from 28 °C in the summer to −22 °C in the winter. The dry air, strong sunshine and high winds results in evaporation two times the moisture gained from precipitation, encouraging wildfire occurrence (GNP, 2017b). Poorly distributed precipitation pattern, frequent drought are typical in the mixed-prairie. Wind prevail in all seasons, with velocities exceeding most other parts of the continent. Arctic airmass forms northerly winds that driving blizzards across this region in

winter, whereas in summer winds are hot and dry, resulting in parched and dusty prairie (Kruger, 2001). Dominant landscape of west block of GNP is rolling uplands and river valley, with elevation varying from 770m to 900m above sea level. The nearly level to slightly rolling topography encourages dry winds to carry away wildfires and spread it quickly, with few obstacles (except rivers and paved road surfaces) to slow down or stop the fire's progress (Sauer, 1950; Vogl, 1979). The park is dominated by grasses (family of *Poaceae*) and non-graminoid herbaceous plant called forbs, with few trees and some shrubs along the river valley (Figure 3.1). Both cool season species and warm season species are found on this prairie, with the former shows dominance (Holechek et al., 1998). Cool season grasses start growing in the spring as soon as temperature rises. They become mature and then dormant in the summer due to lack of appropriate moisture. Warm season grasses starts growth in early summer and length of their growing season depends on availability of moisture. The dominant grass species include needle-and-thread grass (*Stipa comata*), western wheatgrass (*Agropyron smithii*) and blue gramma (*Bouteloua gracilis*) (Guo et al., 2005).

3.1.2 The Wildfire and the Visual Assessment

On April 27th 2013, a wild fire spread into GNP from adjacent agricultural lands. The fire consumed 4,500 hectares (11,500 acres) and extended over 16 km (10 miles) (Figure 3.1) in less than four hours, due to high wind and low humidity (Parks Canada, 2013). In the following two months (May and June), above normal precipitation (~230mm, Weather Canada Historical Climate Data) resulted in the rapid vegetation recovery. This wildfire provided an outstanding opportunity to examine the impact of large scale fire on the preserved grassland and how the ecosystem recovers over time. This section first reconstructs the scenario of wildfire's ignition and propagation with relevant weather and topographic data, aiming to explain the spatial pattern and intensity of the burning. Then qualitative visual assessment of the fire's impact on the grassland is discussed with

imagery acquired at both ground level as well as from the satellite.

3.1.2.1 Propagation of the Wildfire

The wildfire broke out accidentally from a farmland adjacent to the park (only 1km away from the park's west border). This was a spring fire when the park was still undergoing the greenup (initiation of spring growth). Therefore, there existed a considerable amount of litter content, including standing dead (or senesced vegetation from the previous growing season) and litter (fallen and/or partially decomposed vegetation); both contributed as fuel load to feed the wildfire. Furthermore, the conservation effort led to the building up of the dead material (similar as in other grasslands e.g. Gibson & Hulbert, 1987), or rather, excessive fuel loading, for more than 20 years, making the park accumulating considerably more litter content than its surrounding farmlands — as can be confirmed from Landsat 8 OLI imagery acquired on April 22nd (five days prior to the fire), which shows clearly much greener cropland next to the park's northwest boundary. The main reason behind this phenomena is the lack of historical disturbances such as large herbivore grazing herds and burning. Though the park is making active effort by introducing both disturbances back, practice for both factors are not well understood, with fire being especially under-studied.

The weather at the time of fire's occurrence further encouraged its fast spread. Weather record shows that during the fire's occurrence relative humidity averaged at 23% with a strong westerly wind blowing at 40km/h. The forward rate of spread under such high wind would be over 100 times the zero wind spread rate (Albini, 1976). Once the fire spread for 1km eastward and crossed the park's boundary, its consuming rate accelerated due to the abundant fuel load within the park as well as the alignment between the wind direction and the east-west direction of the Frenchman River valley. As a result, the fire quickly started to propagate within the park. The burn patch is clearly visible (Figure 3.1) on Landsat 8 OLI imagery from May 1st. The fire originated from its

ignition location and travelled eastward, taking a severely elongated shape under the influence of the wind direction (Albini, 1976).

Topography also played a significant role in shaping the fire's propagation path and its burning intensity. Figure 3.1 shows that after the fire crossed the park's boundary, it kept travelling eastward in a narrow path along the Frenchman River valley for about five kilometres. Then it split into two fire fronts and continued spreading as a north head and a southern head. The northern head kept consuming the dry fuel along the valley. In contrast, the southern head took a southwest turn and travelling in an almost straight linear, a commonly observed feature for flanking fires under high wind's influence (Albini, 1976). When the southern head was stopped by the unnamed dirt road[1] (shown in Figure 3.1), it travelled northward merging into the fire's northern head. Then the fire continued spreading for another three kilometres along the river valley and finally stopped close to the park's boundary at the other side. Notice different levels of burn severity indicated by the intensity of the black colour (charred material) on the burn patch (Figure 3.1). Along the fire's propagation path, most severe burning occurred at the first five kilometres; followed by the moderate burning severity at the northern head and lowest severity at the southern head. Also present on the map are isolated unburned grassland appearing as "pockets" on the burn patch. The largest "pocket" is formed by the fire's two heads. Since this is a dormant-season burning, less burn patchiness ("pockets") is observed than a growing-season fire. (Wakimoto et al., 2005) argues that burn patches today may be more uniform due to the lack of grazing of large ungulates such as bison in history which reduced grassland litter content differentially through preferential grazing behaviour.

[1]The term "dirt road" is the park's convention for any unimproved road with no surface material applied, i.e., neither paved nor a gravel road.

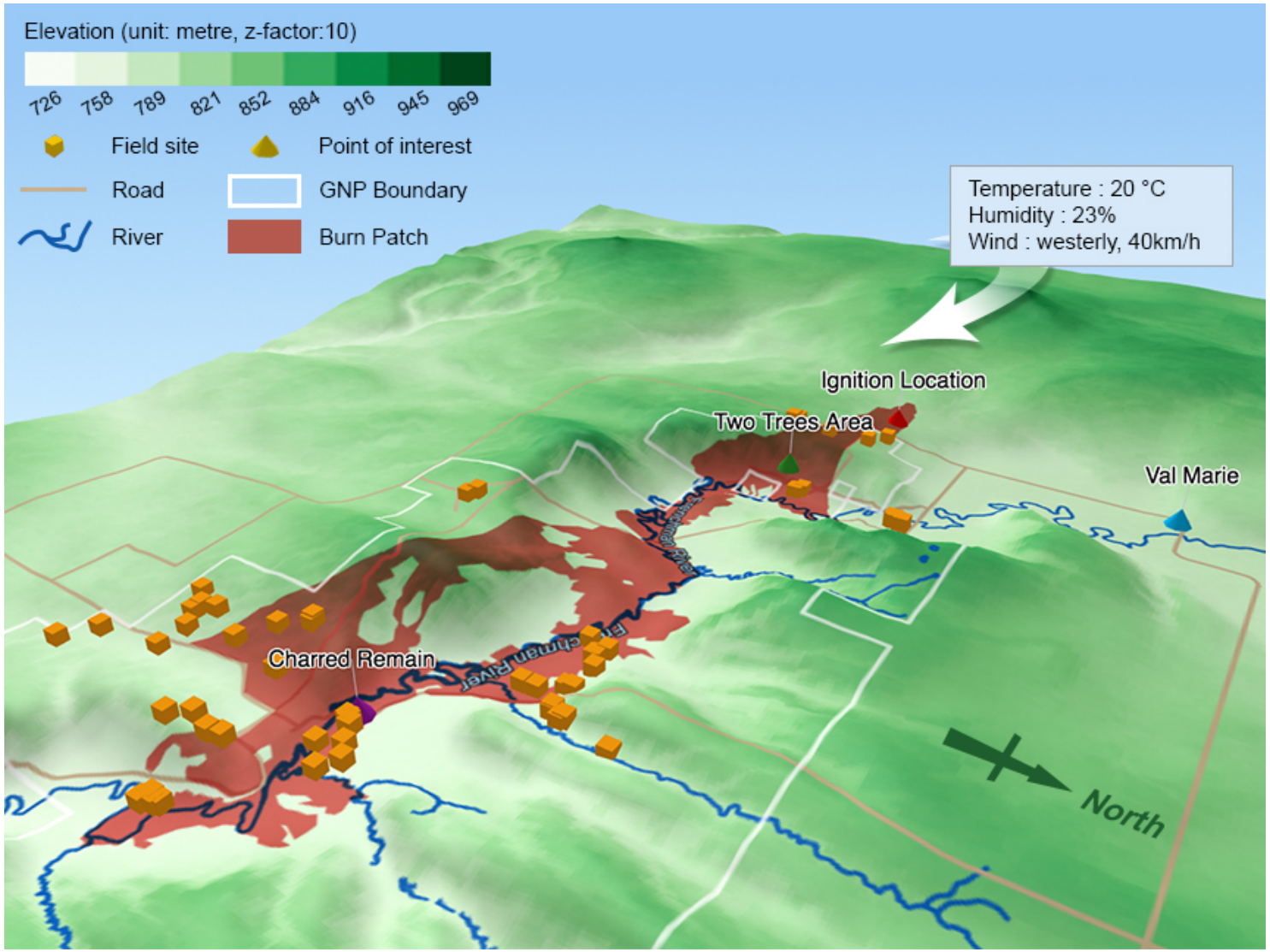

Figure 3.2: Ignition, spread and intensity of the wildfire under the influence of weather and topography. The 3D visualization of the terrain is effective in understanding the fire's propagation and the burn intensity. Weather data was acquired from Weather Canada on the day of fire's occurrence. DEM data was from NASA SRTM Global v3 in 2012. Burn patch was digitized from Landsat 8 OLI image on May 1st, 2013.

The fire's propagation and severity pattern can be better explained with the 3D model of the study area shown in Figure 3.2. Once the westerly wind carried the fire cross the park's border, it quickly spread downward into the river valley (the Two Trees Area), meanwhile fanning outward along the river where more fuel (senesced vegetation) were found. However, the hills from both north and south formed a "hill pass" which prohibited the fire's further spreading. As a result, it was trapped for a certain amount of time, causing the severe burning at that location as well as the three-kilometre narrow linear burn scar at the "hill pass". Once the fire resumed its propagation eastward beyond the "hill pass", it broke into two heads. The northern head continued to consume along the meandering of the Frenchman River. The moderate burn severity of the northern head was mainly due to the much heavier fuel load along the river valley and the constraint from the north. The fire was confined within the river valley because the slopped area on the northern side was less vegetated, hence less fuel available for combustion. Meanwhile, the southern head was formed by the fire spreading to the uphill under the influence of strong wind. It kept travelling for another six kilometres with the least burn severity. The less burn intensity was caused by the steep slope present in that area where less vegetation were found. Slopped grasslands in the park tend to be less vegetated due to limited access to soil moisture, nutrient, and sometimes impact of soil erosion — as presented here in the southern fire head. The less fuel load weakened the propogation rate of the southern fire head so much that it made a full stop at the unnamed dirt road. Then it took a northward turn into the valley and merged with the northern fire head. Finally, the fire died out at another "hill pass" which impeded its further propagation, possibly also caused by a much lower wind speed.

3.1.2.2 Visual Assessment of the Burning

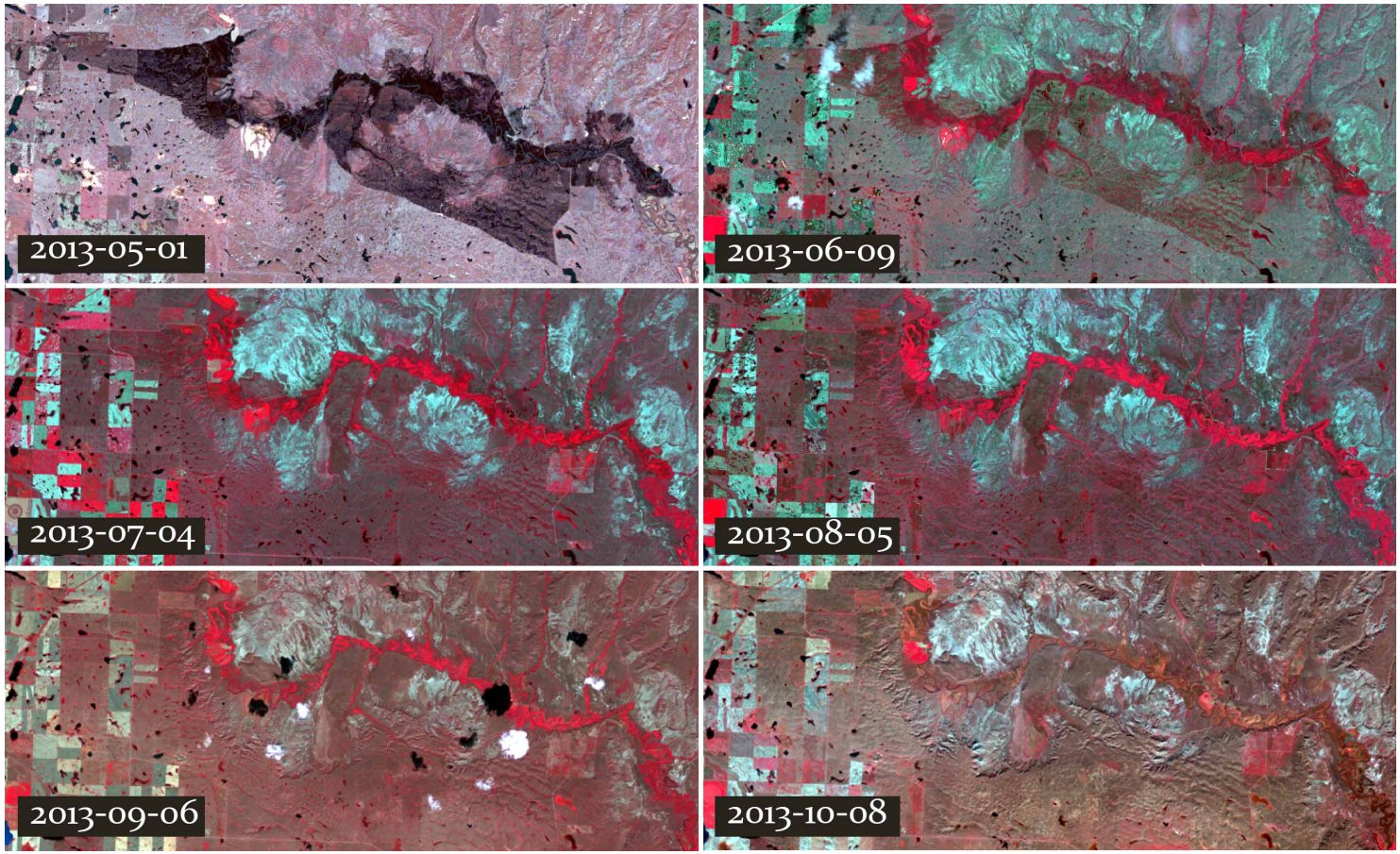

Figure 3.3: Visual assessment of the wildfire and vegetation's rapid regrowth. This series of six standard false-colour composite images are prepared from Landsat 8 OLI sensors. They represent the fast process of grassland recovery on the monthly basis from immediately after the fire till five months afterwards. Notice image in May shows the very defined boundary of the burn patch, especially the almost linear shape at its bottom stretching from northwest to southeast. The linear feature was primarily caused by the strong westerly wind blowing at the speed of around 40 km/h. However, the linear feature was not prominent any more one month later (June), barely visible two months later (July), and not traceable at all three months later (August). The grassland becomes homogeneous to the naked eye after three months, indicated in September's and October's images. The burn patch faded quickly and completely due to vegetation's rapid recovery.

Visual assessment of the burning suggests a quick post-fire regrowth of grasslands. There is no apparent visual difference between burned and unburned communities two months after the fire. GNP promptly assessed the fire's impact and actively monitored the effect of burning throughout the park. They photographed several locations the following day after the fire and revisited two and half months later (Parks Canada, 2013) to get before- and after-burn images for visual pairwise comparison[2]. Their data included the Two Trees Area that is only three kilometres east of the ignition location (Figure 3.1). The boundary of the burn patch at the Two Trees Area was quite prominent at their first visit. However, the well-defined boundary was lost completely to the healthy green vegetation two months later, indicating vegetation's rapid recovery at the ground level. Meanwhile, the quick recovery was captured by the Landsat satellite. Figure 3.3 shows a time series of standard false-colour composite from the Landsat 8 OLI imagery. The burn patch was barely visible two months later and completely disappeared three months later. However, rare traces of the fire can still be found at the ground level. In fact during the field trip in 2017 I observed a few charred shrubs at their roots located along the Frenchman river valley (Figure 3.4), bearing the mark of the wildfire even after five growing seasons. Nevertheless, overall at the landscape level it seems the grassland has no memory of the wildfire's disturbance that occurred a few months earlier.

Though effective and straightforward, visual interpretation can be misleading and belies the fire's potential profound impact on the ecosystem at levels that human eyes fail to capture; such impact may reach far into the future of the ecosystem (Pickett et al., 1989), especially in light of historical fire regime of four years, suggesting the time frame of grassland fire studies should be able to cover at least one post-fire recovery cycle for effective evaluation. As a result, the initial

[2]Materials are not presented here due to copyright concerns. Source of the material was originally accessible at http://www.pc.gc.ca/eng/pn-np/sk/grasslands/ne.aspx. However, please be noted that the link was broken as of February, 2018.

investigations conducted by the park and also Lu et al. (2016) need to be extended and improved with a systematic assessment of this fire's impact on the grassland ecosystem.

Figure 3.4: Partially charred shrub remain from 2013's wildfire still visible (highlighted in red) after 5 growing seasons. Picture taken on June 8th, 2017 by Meng Li during the field survey at GNP.

Furthermore, this research will facilitate the park to have an improved understanding wildfire's impact on grassland ecosystem. GNP has active management plans (GNP, 2017a) every five years to restore the historical disturbance regime by incorporating prescribe burning and grazing, with the intention to reproduce disturbances occurred in the historic past. However, the effects of fire on the mixed prairie still remain unclear, especially in the long term perspective. By evaluating the effectiveness of RS based approaches in the grassland fire study, stakeholders will be equipped with faster and robust solutions enabling them to examine the fire's impact from cost-effective and long-term RS dataset, as well as developing better management plans to maximize the ecological integrity of the grassland ecosystem.

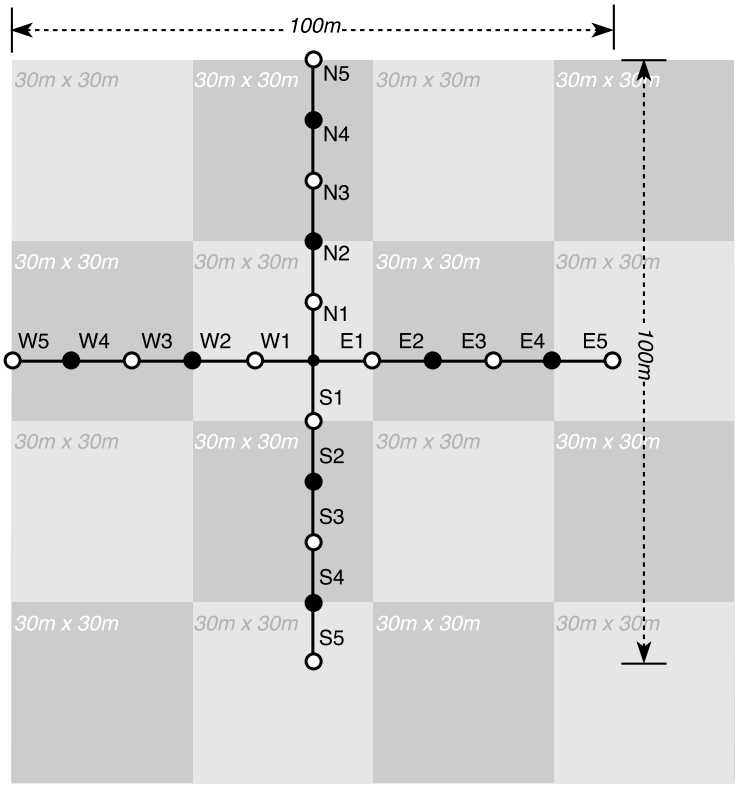

Figure 3.5: Field design used in this study. Biophysical parameters are collected at all quadrats or plots; whereas biomass are only collected twice at each wing indicated as closed circles. In the background are 16 squares (4 by 4) indicating footprint of pixels covering the field site from satellite product of 30 metre spatial resolution (e.g. Landsat product).

3.2 Data

3.2.1 Field Data

Guo's research team from University of Saskatchewan has been conducting ground level measurement within GNP for more than 10 years. Of which, measurement spanning from 2012 to 2017 are used in this study. Field sites were selected following two principles: (1) based on biosites established by GNP (refer to Figure 3.1), and (2) stratified random sampling.

Each site is 100m x 100m in size (Figure 3.5, also refer to Appendix A on page 128) in order to effectively capture the minimum spatial variation in products from moderate resolution satellites

(e.g. Landsat). Each year about 10 - 12 field sites were selected with at least 130m apart from each other (refer to Figure 3.1) to avoid autocorrelation (He et al., 2006; Yang et al., 2013). Each site contains 20 quadrats distributed as four wings (north, south, west, east) with five quadrats for each wing.

3.2.1.1 Biophysical Parameters

Field measurements were taken at each quadrats and later averaged into a single value at the site level in this study. Primary datasets included biophysical parameters (grass life form composition, dominant species, biomass, max height, LAI, and ground reference), soil parameters (temperature, moisture and electric conductivity), as well as presence of grazing activities (through feces of large herbivores). Using a 50cm x 50cm square quadrat, vegetation's life form composition is determined as ground cover percentages of different components: green grass (graminoid species), standing dead, litter, forb, moss, lichen, shrub and bare soil. For key biophysical parameters, measurements were estimated visually by the same recorder in the field season to ensure consistency and reliability of the dataset. Photos of vegetation structure were also taken for later reassessment if required. LAI was measured using the LI-COR LAI-2000 Plant Canopy Analyzer. Soil data were collected using Decagon Pro-Check Sensor Readout and Storage System. Three readings were recorded at each quadrat and averaged into a single data entry in the post-processing stage. Field dataset from 2012 to 2017, i.e. one year before the fire and five years after the fire, are incorporated in this research primarily to evaluate fire's effect as well as providing ground truth for validating RS-based analysis.

Since there are no definitive measures of grasslands post-fire recovery, this research compiled all available biophysical parameters and arrived at the decision to use plant form information as the major indicator of post-fire recovery. Though other parameters are also included in the research.

Plant form information were collected from the field survey across six years as percentage cover with 50cm by 50cm quadrat consistently following the same protocol. Due to limited effort in sampling the field sites, as well as human errors in judgement and recording, secondary parameters were created from the original dataset: (1) percentage of live component which is the sum of green grass cover, forb cover and shrub cover; (2) percentage of dead component which is the sum of standing dead and litter; (3) ratio of green and dead component; (4) standardized difference of green and dead component. The latter two parameters are used to factor in both live and dead components and serves as a comprehensive indicator of post-fire recovery.

3.2.1.2 Ground Reference Data

Hyperspectral data lays the theoretical foundation for satellite RS based solutions. It functions as the ground reference to evaluate and improve the performance of RS products. The dataset records reflectance values of land surfaces at a broad range of wavelengths: from 350nm to 2,400nm at 1nm interval. The fine resolution allows us to thoroughly investigate suitable wavelength windows for modelling vegetation's post-fire recovery. The suitable windows will function as the guideline for selecting potential RS platforms and data products capable of supporting the grassland fire study.

Hyperspectral dataset was collected in the field survey using Analytical Spectral Device portable (FieldSpec Pro FR model). Measurements were taken under clear sunny condition within the time-frame between 10AM and 2PM. Each measurement was the average of ten replicates. The raw reflectance data were processed using ViewSpecPro v6.0.11 and exported in the ASCII format which then analyzed in the R computing environment.

Ground reference data of all samples are compiled and grouped into burned and unburned categories (Figure 3.6). Mean reflectance curves are computed within each category for all available years. In order to find wavelengths that are sensitive to certain post-fire recovery biophysical

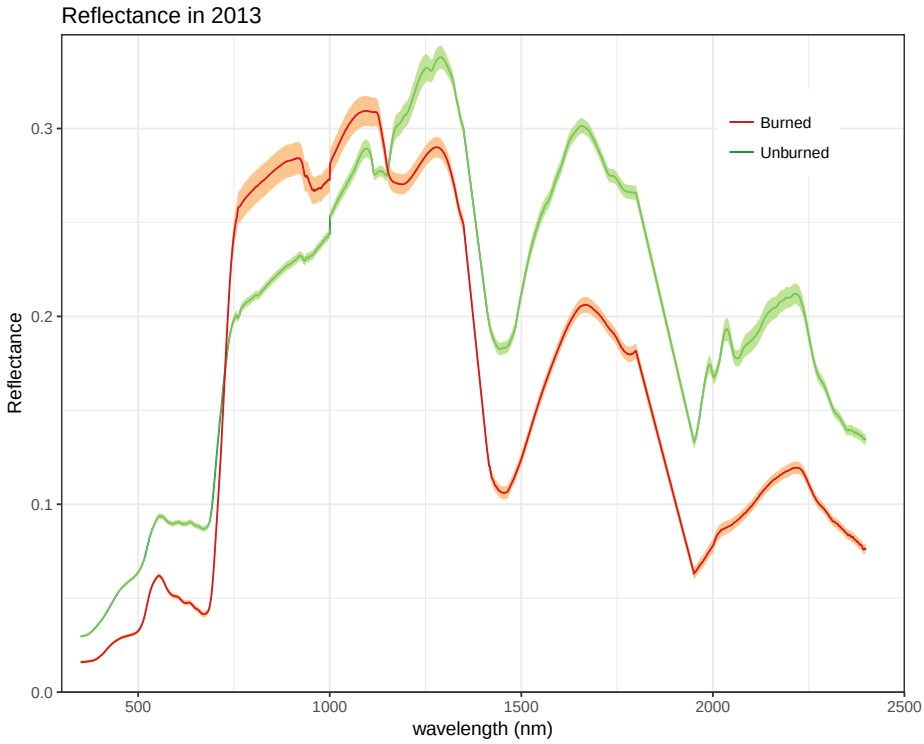

Figure 3.6: Example of processing ground reference data.

parameters, simple linear regression is used in the R computing environment. Considering the performance of all biophysical parameters, these fire-sensitive parameters are used: percentage of live component, the ratio of green and dead components, as well as the standardized difference of green and dead components. The selected biophysical parameters were regressed by the reflectance values at each narrow band. Coefficient of determination (r^2) and p-value were compiled for each narrow band and plotted for diagnostics. Based on these statistics, "sensitive" narrow bands were determined. To further examine the feasibility of using actual satellite RS product in modelling post-fire recovery, band configurations of Landsat 7 and 8 are also included in the analysis to check their agreement with the sensitive narrow bands established earlier.

3.2.2 RS Imagery

Landsat 7 (2012) and Landsat8 OLI (2013-2017) product were used in this study and atmospheric correction was performed when needed. Landsat scenes were downloaded in `GeoTIFF` format from USGS's EarthExplorer data portal [3].

Table 3.1: Acquisition Date of Landsat images used in this study. Dates in *italics* are paired with the field survey of the same year.

Product	**Acquisition Date**
Landsat 7	2012 *June 30th*
Landsat 8	2013 May 1st, June 2nd, *June 18th*, July 4th, Aug 5th, Sep 6th, Oct 8th 2014 May 11th, *June 12th*, July 14th, Aug 11th, Sep 12th, Oct 14th 2015 Apr 28th, *June 8th*, July 10th, Aug 11th, Sep 12th, Oct 14th 2016 Apr7th, Apr 23rd, June 10th, June 17th, *July 3rd*, July 19th,July 28th, Aug 4th, Aug 13th, Aug 29th, Sep 14th, Sep 30th 2017 Apr 10th, May 3rd, May 19th, May 28th, *June 4th*, June 20th, July 6th

In order to check the performance of satellite RS product, each year's field survey data was paired with an imagery with its acquisition date as close as the field season. However due to weather condition (eg. cloud, shadow) acquisition time of the images not always within the proposed month, adjacent images were used instead (dates shown in *italics* in Table 3.1).

[3] EarthExplorer data portal is accessible at https://earthexplorer.usgs.gov/.

Table 3.2: Spectral indices widely used in burn severity analysis included in the study (part one).

Spectral Index	**Formula**
Normalized Difference Vegetation Index (NDVI)	$NDVI = \frac{NIR - Red}{NIR + Red}$ (3.1)
Global Environmental Monitoring Index (GEMI)	$GEMI = \gamma(1 - 0.25\gamma) - \frac{R - 0.125}{1 - R}$ (3.2) $\gamma = \frac{2(NIR^2 - R^2) + 1.5NIR + 0.5R}{NIR + R + 0.5}$
Enhanced Vegetation Index (EVI)	$EVI = 2.5\frac{NIR - R}{NIR - 6R - 7.5B + 1}$ (3.3)
Soil Adjusted Vegetation Index (SAVI)	$SAVI = (1 + L)\frac{NIR - R}{NIR + R + L}$, (3.4) $L = 0.5$

Table 3.3: Spectral indices widely used in burn severity analysis included in the study (part two).

Spectral Index	Formula
Modified Soil Adjusted Vegetation Index (MSAVI)	$MSAVI = \frac{2NIR + 1 - \sqrt{(2NIR+1)^2 - 8(NIR - R)}}{2}$ (3.5)
Burned Area Index (BAI)	$BAI = \frac{1}{(0.1 + R)^2 + (0.06 + NIR)}$ (3.6)
Normalized Burn Ratio (NBR)	$NBR = \frac{NIR - SWIR_2}{NIR + SWIR_2}$ (3.7)
Char Soil Index (CSI)	$CSI = \frac{NIR}{SWIR_2}$ (3.8)
Mid-Infrared Burn Index (MIRBI)	$MIRBI = 10SWIR_2 - 9.8SWIR_1 + 2$ (3.9)

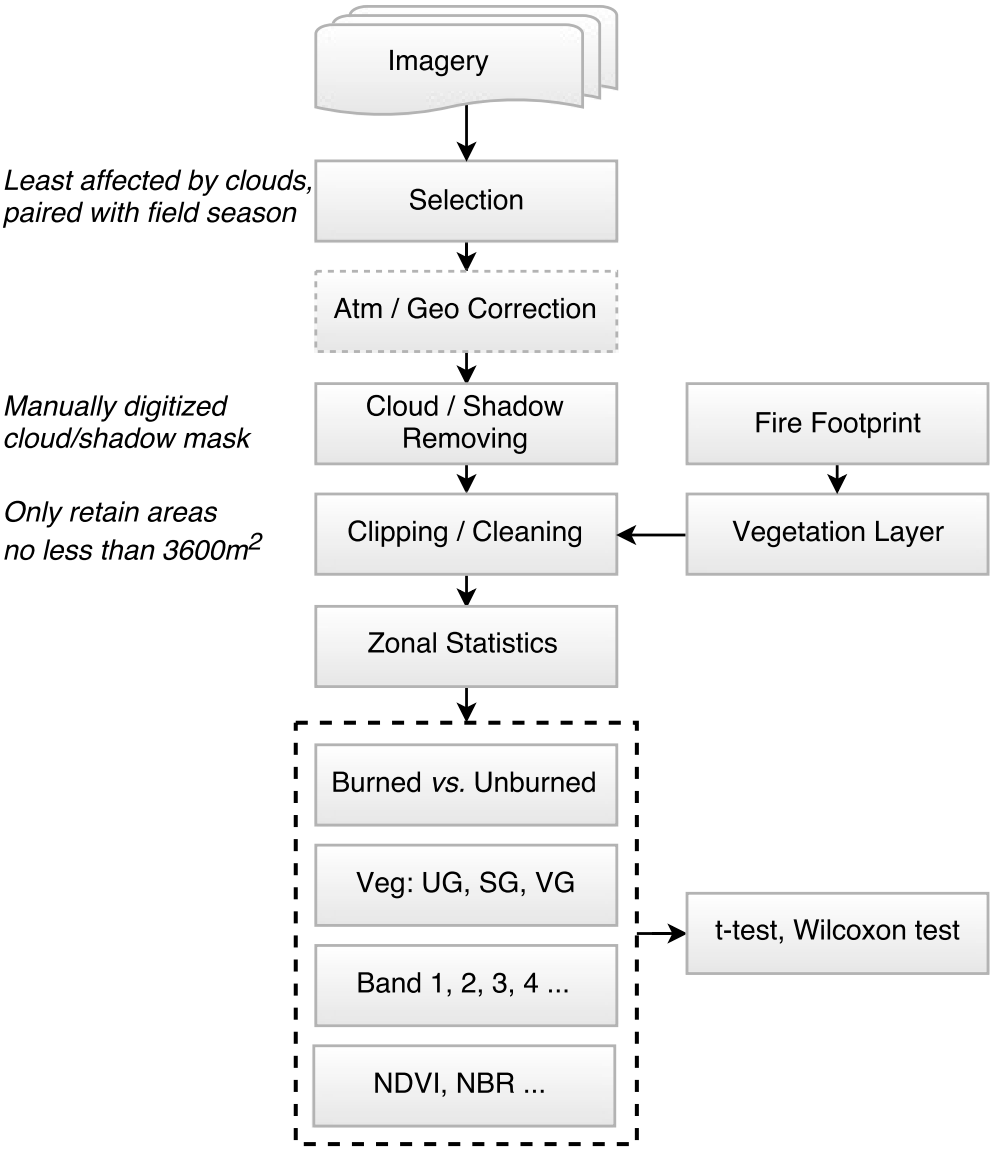

Figure 3.7: Procedure of processing RS imagery in this study

Because the field data were collected at two 100m transacts perpendicular to each other, centers of fields sites were buffered with 100m radius and zonal statistics were used in ArcGIS 10.5 to get the average reflectance values for individual Landsat bands. Moreover, most commonly used Vegetation Indices (Table 3.2 and Table 3.3) were calculated (Figure 3.7) using GIS packages (`GDAL` for imagery manipulation, `numpy` for calculating cloud-and-shadow-free footprint and actual VI calculation, `ArcPy` for other processing).

3.2.3 Ancillary GIS Layers

Table 3.4: Ancillary GIS layers used in this study.

Group	Layer	Usage	Source
Reference	GNP boundary	Study area is defined with this boundary.	GNP, 1998
	Contour	DEM and TIN models are derived.	GNP, 1998
	Rivers, streams	They are used as reference.	GNP, 1998
	Roads, trails	They are used as reference, e.g. field design.	GNP, 1998
	Biosites	biomonitoring sites are considered when designing field sites in this research.	GNP, 1995
	Air photo	It is used as reference, e.g. interpretation of fuel load.	FlySask, 2015
Research	Vegetation survey	Grassland types and information on topography are used in this research.	GNP, 1994

Several ancillary GIS data layers were used in this study. They can be categorized into two major groups shown in Table 3.4, together with their utilization in this research. Most GIS layers are obtained from the park and served as reference layers to support this research. Vegetation survey data is the only layer critical to this research. It allows refined analysis on the different post-fire recovery scenarios based on grassland communities types, i.e. valley grassland, sloped grassland and upland grassland. Since these categories are classified base on the topography, this vegetation was also used as a proxy of topography to study the driving factors of grassland post-fire recovery. However, during this research I identified several errors within this dataset. These errors were probably due to the limited access to resources for the park to conduct the field survey in 1993. Metadata of this layer suggests several revision efforts from the park yet the issues still remain unfixed. Due to the fact that this was the only dataset available, I manually corrected the misclassification of three vegetation community types with the reference from DEM built with the

park's contour lines and other resources.

3.2.4 Meteorological Data

Climate plays the most significant role in semi-arid mixed grasslands. To effectively explain the post-fire recovery pattern, several parameters are collected, including temperature, precipitation, and drought indicators. Temperature and precipitation were downloaded from historical dataset authored by Environment Canada with the time span in accordance with the field seasons. Drought indicators include evapotranspiration, effective precipitation and moisture deficit. These drought-related datasets were based on Environment Canada's climate data (Environment Canada, 2017) and acquired from FarmWest (Farmwest, 2017) at the monthly resolution. Figure 3.8 shows the compiled meteorological dataset used in this study.

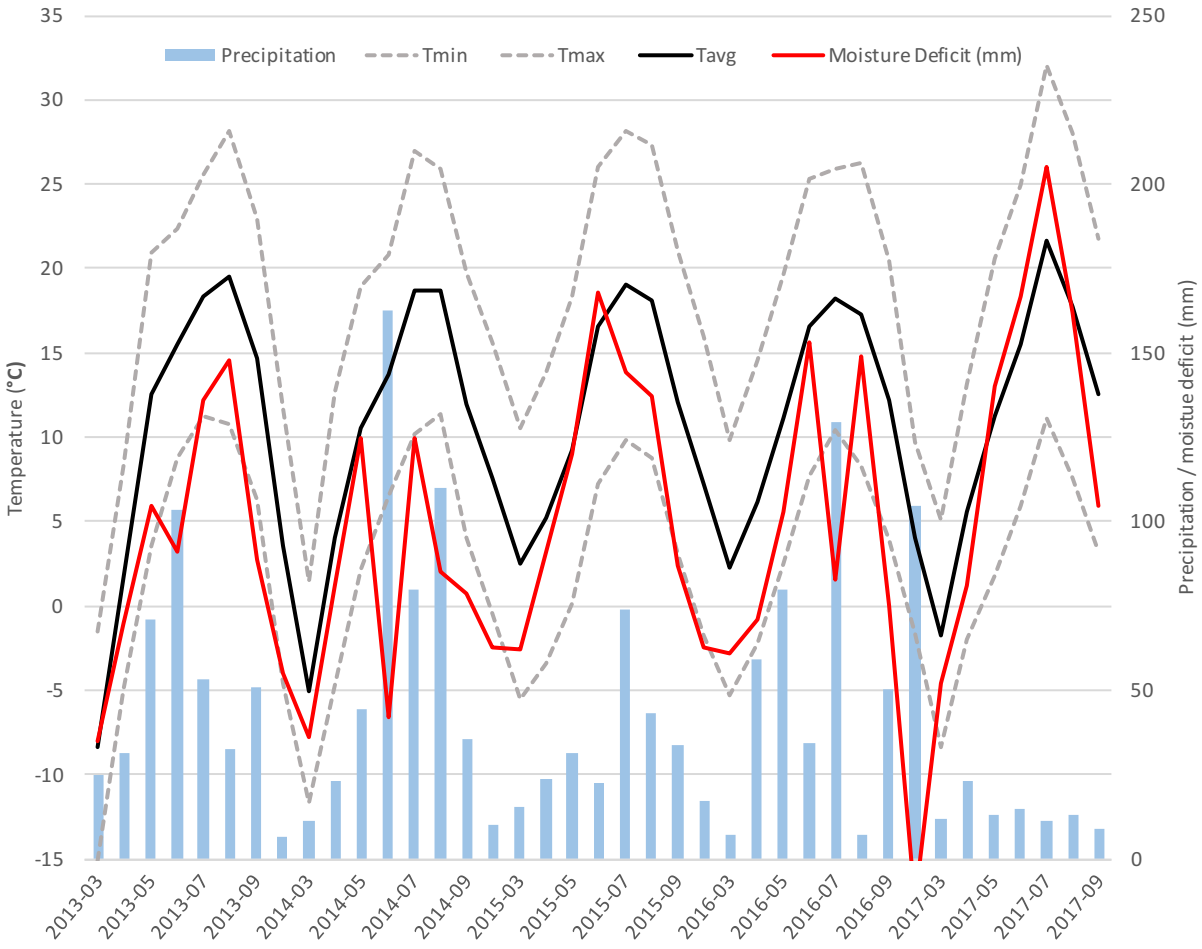

Figure 3.8: Monthly meteorological variables from 2013 to 2017. The X-axis displays months of year. The primary Y-axis shows temperature for Tmax (maximum temperature), Tmin (minimum temperature) and Tavg (mean temperature). The secondary Y-axis indicates either amount of precipitation or the moisture deficit. Data source: Environment Canada.

Chapter 4

Methods

4.1 Overview of Methodology

The methodology is designed to effectively address the objectives of this research outlined in chapter 2 (on page 27). The overall objective of this research is to establish a framework capable of quantifying grasslands post-fire recovery using RS and GIS approaches. In order to achieve this, there are 3 closely related objectives. Objective 1 is to study grasslands post-fire recovery pattern using field data and offers as the ground truth for Objective 2 which is to establish a RS-based framework capable of studying grasslands recovery. Objective 2 itself comprises 3 sub-objectives: Objective 2.1 to verify the feasibility of RS in the fire study by conducting a theoretical experiment using hyperspectral measurement from the field survey, Objective 2.2 to actually test the performance of satellite RS product against the ground truth derived from Objective 1, Objective 2.3 to further unlock the potential of satellite RS product with advanced spatial analysis that are beyond the capability of field experiments. Both Objective 1 and 2 try to describe grasslands post-fire recovery pattern. Whereas Objective 3 aims to answer the question of *How the recovery took place?* by examining all potential driving factors.

The methodology used in this research can be described in greater detail as Figure 4.1 in a standard flowchart with different components (input data, derived data, processes, decisions) defined as well as their connections. Notice that symbols are colour coded according to different purposes:

gray for research data (both original and derived), orange for Objective 1, light blue for Objective 2.1, light green for Objective 2.2, dark green for Objective 2.3, and red for Objective 3.

Most analyses carried out in this research (Figure 4.1) were powered by open source solutions. Examples of software and packages include `QGIS`, `Inkscape`, `R`, `Python` and related scientific libraries. Examples of open data formats include `CSV` and `GeoTIFF`. Even this manuscript is prepared using LaTeX typesetting. Predominant use of open source solutions in this research is intended explicitly to fully exploit their advantages in a tighter and more flexible coupling of data, software and analytical functionalities and final presentation (Brunsdon & Singleton, 2015) that can be packaged together to facilitate dissemination amongst scientific community, as well as related stake holders. RS dataset typically carries massive amount of information and is multi-dimensional in its own right: two dimensions of X-Y coordinate plane, dimension of pixel's bit depth to describe the digital number (DN) for reflectance values, dimension of spectrum bands, dimension of time, as well as associated quality accessment (QA) bands that flag the quality and intended usage of the associated RS product. Hyperspectrum dataset will further complicate data anlaysis with its detailed measurements at thousands of spectrum bands. The challenges posed by organizing, processing and analyzing RS datasets can be effectively addressed with custom built solutions powered by open source packages. Indeed, open GIS will shape the research landscape in face of "spatial" big data deluge in spite of impediments at its current stage (Sui, 2014; Willmes et al., 2014).

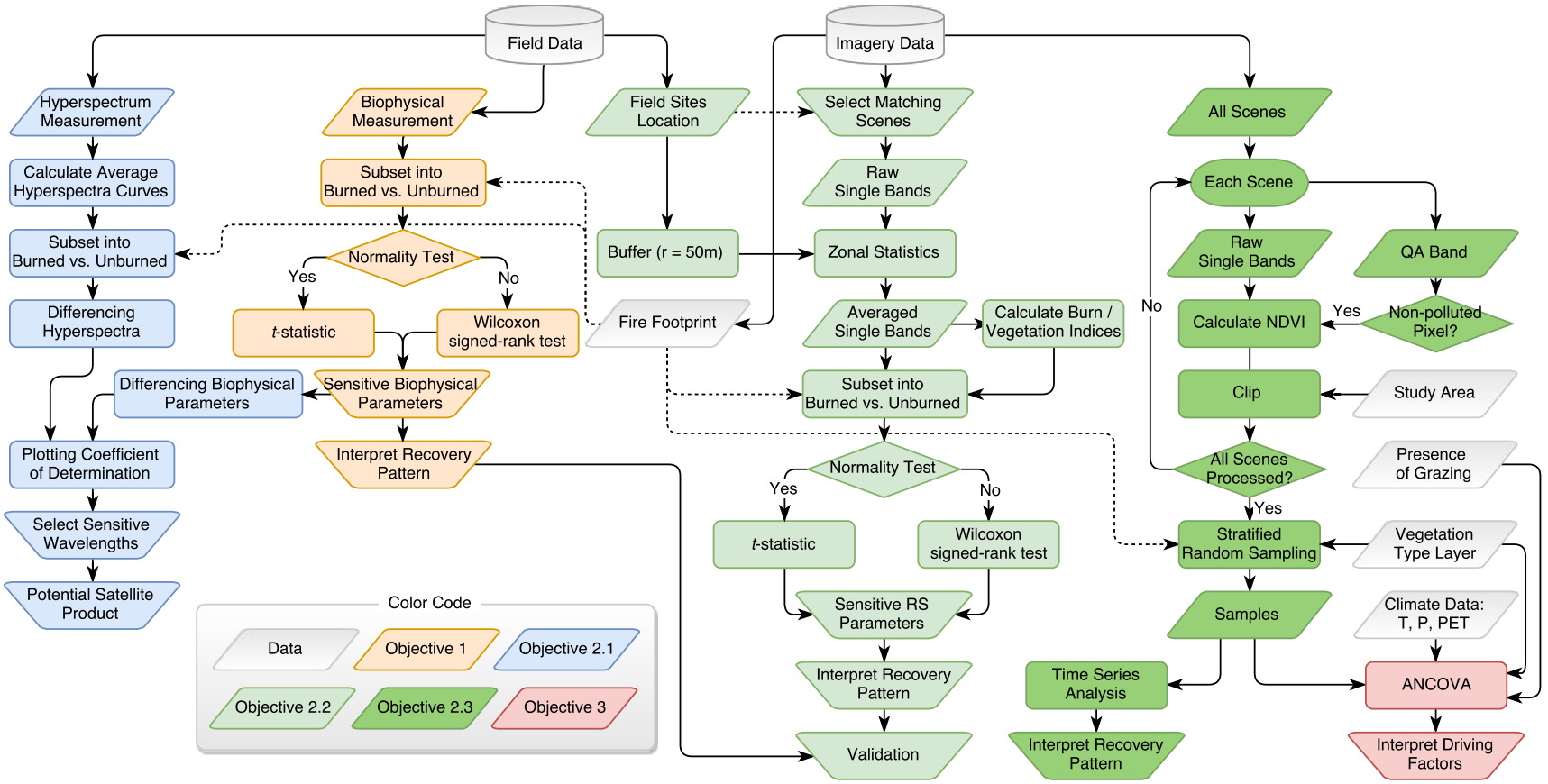

Figure 4.1: Overview of methods used in this research. This flowchart is colour-coded according to different objectives outlined in chapter 2 on page 10. Specifically, grey for research data (both original and derived), orange for Objective 1 (to study grasslands post-fire recovery pattern using field data), light blue for Objective 2.1 (to verify the feasibility of RS in the fire study by conducting a theoretical experiment using hyperspectral measurement from the field survey), light green for Objective 2.2 (to actually test the performance of satellite RS product against the ground truth derived from Objective 1), dark green for Objective 2.3 (to further unlock the potential of satellite RS product with advanced spatial analysis that are beyond the capability of field experiments), and red for Objective 3 (to answer the question of 'How the recovery took place?' by interrogating all potential driving factors).

4.2 Methods for Objective 1

By studying grasslands post-fire recovery pattern using field data, Objective 1 provides the ground truth for RS-based methods discussed in Objective 2.

In order to fulfil Objective 1, field samples (biophysical parameters) from 2012 to 2017 are collated and pre-processed (data cleaning and reformatting according to a standardized schema) using Microsoft EXCEL spreadsheet program. Field data were organized in the `csv` format to avoid parsing issues and facilitate automation. Fire's footprint information was extracted from Landsat imagery (acquired on May 1st, 2013, or four days after the fire) and assigned to the field data. Each year's field data were in turn imported into the `R` environment for statistical analysis.

It's worth-noting that in order to reduce sampling errors, two higher level biophysical parameters were created by aggregating from the original parameters measured in the field. Specifically, "live component" is the sum of "green grass cover", "forb cover" and "shrub cover" (notice moss and lichen were excluded from the aggregation); whereas "dead component" accounts for "standing dead cover" and "litter cover". Furthermore two comprehensive biophysical parameters were devised to factor in both live and dead components: the simple ratio index (or SRI_{bio}), and normalized difference index (or NDI_{bio}) defined as below:

$$SRI_{bio} = \frac{live\%}{dead\%} \tag{4.1}$$

$$NDI_{bio} = \frac{live\% - dead\%}{live\% + dead\%} \tag{4.2}$$

Here the subscript "bio" is used to explicitly indicate the fact that these are burn indices built with biophysical parameters, instead of using satellite product like normal VIs in the remote sens-

ing context.

An `R` script is prepared to analyze each year's data. First it loads a specific year's `csv` file as `data.frame` and checks its data quality by excluding any invalid records with the sum of all its biophysical parameters unequal to 100% — a frequently observed human input error for the field dataset. All samples were subsequently divided into two groups based on treatments as either burned or unburned. During this procedure any partially burned sites were excluded from the subsequent analysis. Since field data are recorded at the quadrat level (eg. "N3" being the third quadrat on the "North" wing) which is unfit for the site-level analysis in this research, `aggregate` function with the option `FUN="mean"` is used to get a new aggregated site-level `data.frame`.

The script then carries out the analysis to determine whether any biophysical measurement exhibits statistically significant differences between treatments. Specifically, these steps are performed:

1. Select the first biophysical parameter and perform `Shapiro-Wilk Normality Test` to check the data's statistic distribution for both burned and unburned samples groups.
2. When both groups conform to normal distribution, use `Student-t` statistic to test the null hypothesis that there are no significant differences between burned and unburned samples.
3. Otherwise when normality assumption is violated, adopt `Wilcoxon Rank Sum and Signed Rank Test` with the same null hypothesis.
4. Report any statistic results.
5. Go to step 1 and process the next available biophysical parameter.

Once analyses for all years have completed, statistics on each biophysical parameter's performance are assembled. The result shows the magnitude as well as the `p-value` of a biophysical parameter one year prior to the fire as well as `n (n=1,2,3,4,5)` years after the fire. The one year pre-burn statistic is intended to cancel any lurking variables' potential influences on the analysis

by providing as the baseline for evaluating the biophysical parameter's post-fire performances in the following years.

Statistic results are also used to produce a ternary plot (using `ggterm` package in `R`) that can be used to further understand the post-fire recovery dynamics at a higher level. Specifically, percentage of live component, dead component and the rest are plotted to emphasize how the configuration of these major components has evolved from the fire until the fifth growing season, serving as a visual guide on interpreting the post-fire recovery pattern.

Finally, sensitive parameters are selected and provided as main indicators for interpreting grasslands fire recovery pattern. This result will be established as the foundation for subsequent grasslands post-fire recovery analysis using RS approaches.

4.3 Methods for Objective 2.1

Objective 2.1 is to verify the feasibility of using RS in the fire study by conducting a theoretical experiment using hyperspectral measurement from the field survey. Hyperspectral data data offers a broad range of wavelengths (from 350 nm to 2,400 nm) with 1 nm interval that can help us find sensitive wavelengths suitable for monitoring vegetation's post-fire study. This is the theoretical foundation for satellite RS approaches, through acting as the reference to evaluate and potentially improve the performance of RS products.

The underlying theory of this analysis can be summarized as a formula as:

$$lm(resp \sim expl) \tag{4.3}$$

where

- $resp = (Bio_{year\_i,burned} - Mean(Bio_{year\_i,unburned})) - (Bio_{2012,burned} - Mean(Bio_{2012,unburned}))$,

- $expl = (Ref_{year\_i,burned} - Ref_{year\_i,unburned}) - (Ref_{2012,burned} - Ref_{2012,unburned})$, and
- $i = 1, 2, 3, 4, 5$.

lm is a linear regression model fit to the data. Basically we want to get its r^2 to determine what wavelengths (indicated as Ref or reflectance values) can better explain the variation of fire-sensitive biophysical parameters. Wavelengths with better performance provide as the reference for selecting suitable RS data products through their spectral response functions (or SRF), eg. Barsi et al. (2014). Conclusions from this section will be applied in Objective 2.2 with suitable RS data product.

For the response variable $resp$, $Bio_{year\_i,burned}$ stands for a chosen biophysical parameter at each burned site in i_{th} year. The selected parameter is derived from the Objective 1. Similarly, $Bio_{year\_i,unburned}$ is for an unburned site. $Mean$ function computes the mean value of $Bio_{year\_i,unburned}$. Notice there are two subtraction operators. The inner subtraction calculates within-year differences in biophysical parameters between treatments, whereas the outer subtraction computes the difference for year i from the baseline year 2012 which is before the fire. The same pattern applies for the explanatory variable $expl$, with the only difference is reflectance values are used instead of the biophysical parameter. The following discusses this procedure in details.

First hyperspectral data are screened for any errors due to either inappropriate procedure or hard-ware related issues. Quadrats with erroneous hyperspectral data are excluded from the following analysis. Major errors include these scenarios: *(1)* multiple calibration/optimization processes during data collection, *(2)* quadrats exhibiting too diverse hyperspectral signatures, *(3)* sensor related errors. It is unfortunate that hyperspectral data for 2012 could not be used due to a device related problem. Efforts were made to correct the dataset including consulting ASD Inc. but to no avail. All `*.ASD` files are at quadrat level and organized according to different years and site locations. An `*.ASD` file is a proprietary binary format with its specification constantly chang-

ing across years within time frame of this research. No reliable open source `R` package is capable of accessing the file. As a result, each `*.ASD` file is manually loaded with ASD Inc.'s ViewSpecPro v6.0.11 package and exported in the `*.csv` format which in turn being analyzed with an `R` script.

An `R` script is prepared to analyze each year's data. For the technical detail of implementation, please refer to Appendix **??**. Essentially the script computes `Coefficient of Determination` (or r^2) between the difference of a selected biophysical parameter (sensitive to grasslands recovery from analysis in Objective 1) across treatments and the difference of reflectance values across treatments for all hyperspectral data's narrow bands. Please note that two atmosphere-related wavelength regions are excluded from the analysis, resulting three spectra ranges used for this research: 350 nm ~1,350 nm, 1,410 nm ~1,800 nm, and 1,950 nm ~2,400 nm.

The script first loads biophysical `*.csv` files as `dataframe`s for burned and unburned samples and exclude any invalid records with inappropriate biophysical parameters (partially burned sites, `NA` values for target biophysical parameter). After that it computes the r^2 plot following these steps:

1. Calculates derived sensitive biophysical parameter for burned and unburned samples and aggregate data from quadrat-level to site-level using `aggregate` function with `FUN="mean"`, resulting two new `data.frame`s: P_{bio_burned} and $P_{bio\_unburned}$.
2. Compute mean values of $P_{bio\_unburned}$ as $M_{bio\_unburned}$.
3. Calculate the variance of burned biophysical parameter by subtracting the baseline $M_{bio\_unburned}$ from each site in P_{bio_burned}. This will be the "response variable" $resp$ in the regression analysis.
4. From biohysical `*.csv` files' field name list, load hyperspectral reflectance data from disk for burned and unburned sites.
5. Calculate the mean of reflectance for unburned sites as $M_{ref\_unburned}$.
6. Compute the variance of reflectance by subtracting the baseline $M_{ref\_unburned}$ from reflectance

values of each burned site. This will be the "explanatory variable" $expl$ in the regression analysis.

7. Loop through each wavelength and compute r^2 as following:
   (a) Fit a linear regression model using $lm(resp \sim expl)$.
   (b) Gather the linear model's summary and henceforth r^2.
8. Plot the r^2 graph. Optionally superimposing these information:
   (a) Mean reflectance curves for burned and unburned sites.
   (b) Popular satellite bands configuration.

The regression analysis will result in a series of plots showing the performance of all individual wavelengths (at 1nm interval) in explaining variances of fire-sensitive biophysical parameters, which provides as the theoretical foundation of using satellite RS approaches for grasslands fire study, especially useful in finding suitable satellite RS data. Results and conclusion from this analysis will directly serve Objective 2.2, 2.3 and 3.

4.4 Methods for Objective 2.2

Objective 2.2 is to actually test the performance of satellite RS product (suggested from Objective 2.1) against the ground reference derived from Objective 1. The core statistical methods used in this section is very similar to Objective 1, except RS related analysis for preparing RS parameters. First from satellite imagery database, images less effected by clouds and shadows are selected as candidates, which are further narrowed down to select those that most close to the corresponding to field survey dates. Then field data and satellite RS data of the same year are linked together based on their geographical locations. Field site locations are buffered with 50m (arm's length, Figure 3.5 on page 39). `Zonal Statistics As Table` with `Arcpy` is performed with the buffer as the zones against all individual bands of its matching RS scene, resulting in averaged single

band reflectance for each site. Tabular results were assembled together again with `Arcpy`. Through predefined formulae (Table 3.2 on page 44), Vegetation/burn indices are calculated from averaged single band reflectance values. The averaged single and reflectance and Vegetation / Burn Indices are assembled together and analyzed in the fashion similar to biophysical dataset performed in Objective 1. After the statistical analysis, results from this section are compared against ground truth established in Objective 1 to validate the performance of RS based approach — whether RS product can demonstrate equivalent performance in grasslands post-fire recovery study, with its strength and limitation comparing to field experiment. The strength of RS based approach will be exemplified in detail in Objective 2.3.

4.5 Methods for Objective 2.3

Objective 2.3 is to further unlock the potential of satellite RS product with advanced spatial analysis that are beyond the capability of field experiments. One of the greatest strengths of RS data is capability in providing data of large sample size both in spatial and temporal extents. This is not possible for field data and overcomes limited sample size of field data analysis. To properly establish a RS analysis routine for grasslands post-fire recovery, a `Python` script is coded using open source libraries to automating RS data processing and `ArcGIS` software is employed to generate random data samples for further analysis in the `R` environment.

The `Python` script first reads all satellite scenes available to this project. For each scene, it scans its quality assessment (QA) band and masks out pixels that are affected by clouds and shadows. The "non-polluted" cloud- and shadow-free pixels are then used to compute sensitive VI product established in Objective 2.2. The result VI scene is then clipped with the study area boundary to yield VI maps for all acquisition dates. Please refer to Appendix C on page 141 for the implementation detail.

`ArcGIS` is used to perform a stratified random sampling with the `Create Random Points` tool. The sampling methods follows a factorial design with three factors: *(1)* vegetation type of three levels: `VG` for low-lying valley grassland, `SG` for sloped grassland, `UG` for upland grassland, *(2)* presence of grazing activity of two levels: `0` for ungrazed samples, `1` for grazed samples and *(3)* presence of fire of two levels: `0` for burned samples, `1` for unburned samples; and with 15 replications. This sampling results in 90 samples. Also a constraint is applied for the sampling defined by `Minimum Allowed Distance` option ensuring that samples are at least 120 metres apart to avoid spatial autocorrelation. The final 90 samples are screened manually and improved upon as necessary.

VI values (eg. NDVI) are then computed for those samples using `ArcGIS`'s `Extract Multi Values to Points` tool using `Python` scripts to automate the procedure for multiple years. VI results are then analyzed using `R` environment. Boxplots are used for exploratory analysis.

Time Series Analysis (TSA) is demonstrated as an advanced example to illustrate the capability of RS approach in understanding the long-term temporal pattern of grasslands post-fire recovery. Methodology used in TSA can be described in Figure 4.2 (Nau, 2015; Coghlan, 2017). All the data processing and analysis involved in TSA was carried out using `ts` and `stl` packages in the `R` computing environment.

4.6 Methods for Objective 3

Objective 3 aims to answer the question of *How the recovery took place* by interrogating all potential driving factors. Though more sophisticated analyses can be potentially applied here, this section only demonstrates most relevant methods that highlights the dynamic changes in major driving factors during grasslands post-fire recovery.

The methods of this section can be summarized as these two ANOVA expressions:

$$ANOVA_{year\_i}(Bio \sim Climate + Topography + isBurned + isGrazed) \tag{4.4}$$

$$ANOVA_{year\_i}(VI \sim Climate + Topography + isBurned) \tag{4.5}$$

Where $ANOVA_{year\_i}$ is the analysis for year i. "+" signs are used to indicate that interaction terms between explanatory variables are ignored from the ANOVA analysis. Equation 4.4 is used for analyzing driving factors using the field data. Whereas Equation 4.5 is for the satellite RS data. Explanatory variables in field data analysis includes climate variables (temperature, precipitation, potential evapotranspiration), topography (VG, SG, UG) and presence of burning and grazing. Satellite data analysis is similar as field data analysis, only without grazing data due to lack of dataset. Response variable VI here include all VIs listed in Table 3.2 on page 44. Driving factor analysis are carried out with both field data and satellite RS data to compare results with each other and provide different perspectives on the trajectory of grasslands post-fire recovery.

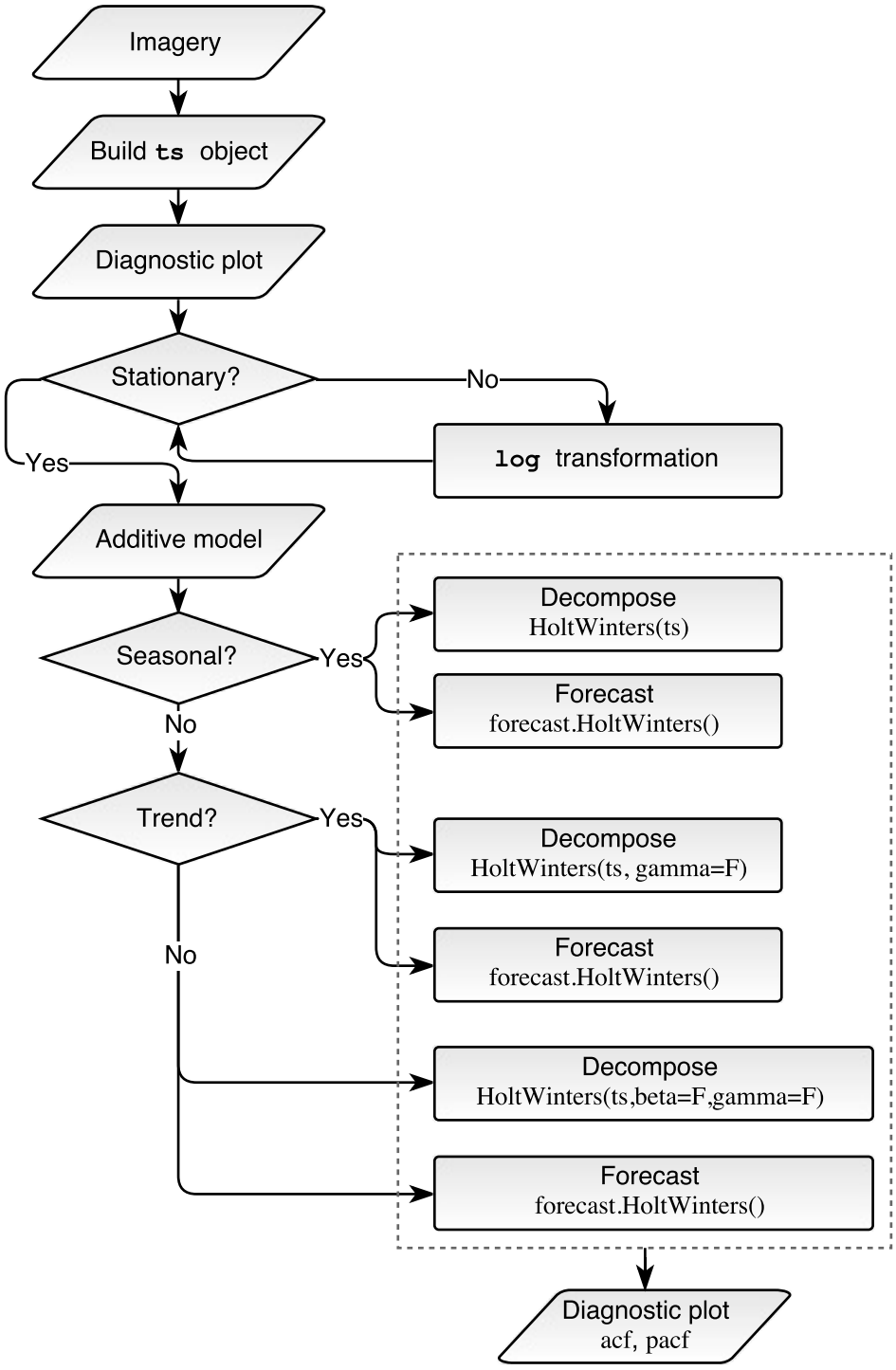

Figure 4.2: Time Series Analysis is experimented on the NDVI dataset derived from satellite imagery to study the temporal pattern of vegetation's post-fire recovery as well as making future projections. The whole process involves three steps: preparing time series data, fitting models and forecasting.

Chapter 5

Results and Discussion

5.1 Grassland Post-fire Recovery with Field Data

To investigate the vegetation's post-fire recovery stated in Objective 1, field data were collected and analyzed one year before the fire and five continuous years after the fire with methods described in section 4.2 (on page 53). A diverse selection of both original and derived biophysical parameters are evaluated in order to find fire-sensitive indicators. Meanwhile grassland post-fire dynamics are also reported.

Results from this section are organized as follows. First, an overview is provided to illustrate grassland recovery at a higher organizational level with aggregated components. Following up is the break down of major components. Results from soil crust and soil properties are also added due to their significant role governing grasslands recovery. When results from different treatment were consolidated, an interesting phenomenon was observed which could be better interpreted as fire's positive impact on grassland resilience. Finally a summary is provided to highlight key findings in this section.

5.1.1 Overview of Vegetation Dynamics

Table 5.1 shows the dynamics of biophysical parameters for burned and unburned samples across six years, from pre-burn growing season (2012) to the 5^{th} post-fire growing season (2017). Most

biophysical parameters are not significantly different between treatments. In fact, only one third of the statistics passed the significant test if weak significant results ($p = 0.1$) are also included. Although some of the weak or non-significant result can be attributed to limited sampling effort (small sample size and human input errors), as well as biotic and abiotic factors other than burning, fire still demonstrates significant correlation with certain biophysical parameters and proves as an important factor shaping the grassland dynamics.

Result shows few significant differences for green grass, forb, and shrub in across treatments (burned v.s. unburned sites). This might be caused by limited sample sizes available to this study as well as data quality issues during the field work. Misclassification of these components is sometimes observed. Additional analysis proves that when the three components are combined altogether as 'live vegetation', significant result was achieved. As a result, in order to reduce such sampling errors, two higher level biophysical parameters were created through aggregation of the original field dataset. Specifically, live component is the sum of green grass cover, forb cover and shrub cover; whereas dead component accounts for both standing dead cover and litter cover. Table 5.1 indicates these derived parameters have relatively better performance than original individual parameters.

To understand the post-fire recovery dynamics at a higher level, a ternary plot (Figure 5.1) was generated based on Table 5.1. Here "live" and "dead" components are the derived biophysical parameters discussed previously. Other parameters are summed up as the "rest" component. Such aggregation procedure allows us to trace the dynamics in configuration of these three major components throughout five post-fire growing seasons. As a result, a higher level understanding of grassland post-fire recovery can be achieved.

Table 5.1: Biophysical characteristics in burned ("B") and unburned ("U") treatments. Values show averages of biophysical parameters. Significance test are performed to compare statistics across treatments. Statistic result of 2012 is included serving as the baseline for the subsequent five post-fire growing seasons. Notice some parameters were not collected consistently throughout the study period. Though most statistic results are not significant due to small sample size and data quality issue, fire's impact can still be observed from certain key biophysical parameters. Check section 5.1 for more discussion.

	2012		2013		2014		2015		2016		2017	
	U	B	U	B	U	B	U	B	U	B	U	B
Grass (%)	16.7	22.7	24.4	45.8*	32.9	31.2	20.6	22.4	32.0	36.3	16.3	14.1
Forb (%)	7.1	3.9○	6.8	13	6.1	11.6	4.3	5.6	3.8	3.7	4.7	7.3
Shrub (%)	0.7	2.6*	1.3	0.2	2.3	3.9	2	5.3*	7	5.8	1.9	3
Live (%)	24.5	29.2	32.5	59**	41.3	46.7	26.9	37.2*	42.8	45.8	22.8	24.4
Canopy Height (cm)	—	—	—	—	25.2	37.1*	27.4	37.1*	27.1	42.2○	22	22.6
Litter Depth (cm)	—	—	—	—	3.5	2	5.8	6.9	—	—	—	—
Stand Dead (%)	52.1	49.8	25.6	0.1**	17	17.3	12.9	8.2	21.8	13.9	14.8	17.8
Litter (%)	11.4	12.2	21.8	14.6	23.1	14.2	43.7	43.2	21.5	36.1○	61.9	55.5
Dead Total (%)	63.5	62	47.3	14.7**	40.1	31.5○	56.6	51.4	43.3	50	76.7	73.3
Lichen (%)	3	3.2	0.3	0○	0.4	0.1	5.7	1.4*	1.8	0.9	0.1	0
Moss (%)	7.4	1.0*	13.1	9.2	10.9	4.4*	0.1	0	10.5	0.2*	0	0
Bare soil (%)	1.6	2.8	3.3	16.1○	0.9	9.2*	8.9	2.6	1.4	2.5	0.2	1.5○
LAI	1.7	2.3	0.4	0.3	1.6	2.3	1.2	2.0*	1.2	2.0*	1.3	1.5
Soil Moisture (m^3/m^3)	0.2	0.2	0.2	0.3	0.2	0.2	0.1	0.1	0.1	0.2***	0.1	0.1○
Soil Temperature (°C)	23.3	25.4	23.4	22.8	23.2	21.9	31.2	32.6	25.8	24.1	30.3	30.7
Soil EC (dS/m)	0.1	0.2**	0.1	0.3	0.1	0.2.	0	0	0	0.1**	0	0

Significant codes: "***" 0.001, "**" 0.01, "*" 0.05, "○" 0.1

Figure 5.1 has three axes ("Dead", "Live" and "Rest") defined by the three high level components. The three axes are arranged from head to toe to form a triangular coordinate system. This technique is often used (e.g. the famous "soil texture triangle" in geologic studies) to visualize the relationships between components in a three-component mixture where components are restricted by each other in that their sum is a predefined fixed number. All data points are plotted according to their 3-tuples in the form of $(dead, live, rest)$. Notice years are color-coded and lines are drawn to connect burned and unburned treatments within each year. Here length of the line indicates the degree of difference across treatments' three component configuration (or cross-sample configurational difference). That is, the longer the line is, the more configurational differences there are between burned and unburned field sites for that specific year.

There exists a clear trend in the cross-sample configurational difference in time. One year prior to the fire (2012) saw a small value in such difference. The wildfire in the following year (2013) led to the sudden and largest difference found in the entire time frame of this study. Afterwards, the difference is getting less pronounced until almost non-existent across samples in the 5^{th} growing season (2017). The progression of vegetation's post-fire recovery suggests a full recovery of 4-5 years. This agrees with some researches conducted in the same region. It may also reflect the historic fire regime (interval) under which the prairie adapted through long term evolution.

The wildfire may have caused hysteresis of the ecosystem. Some ecologists believe that multiple alternative stable states exist in communities with the active state triggered by addition or exclusion of certain interactors or disturbances. More discussion about alternative stable states theory can be found in (Cain et al., 2011, pp. 25-47). Therefore, communities can shift to alternative successional trajectories that might never return to its original community type, but might instead develop into a new community type. Hysteresis describes such behavior of incapable of returning back to the original community type, even with the original conditions fully restored

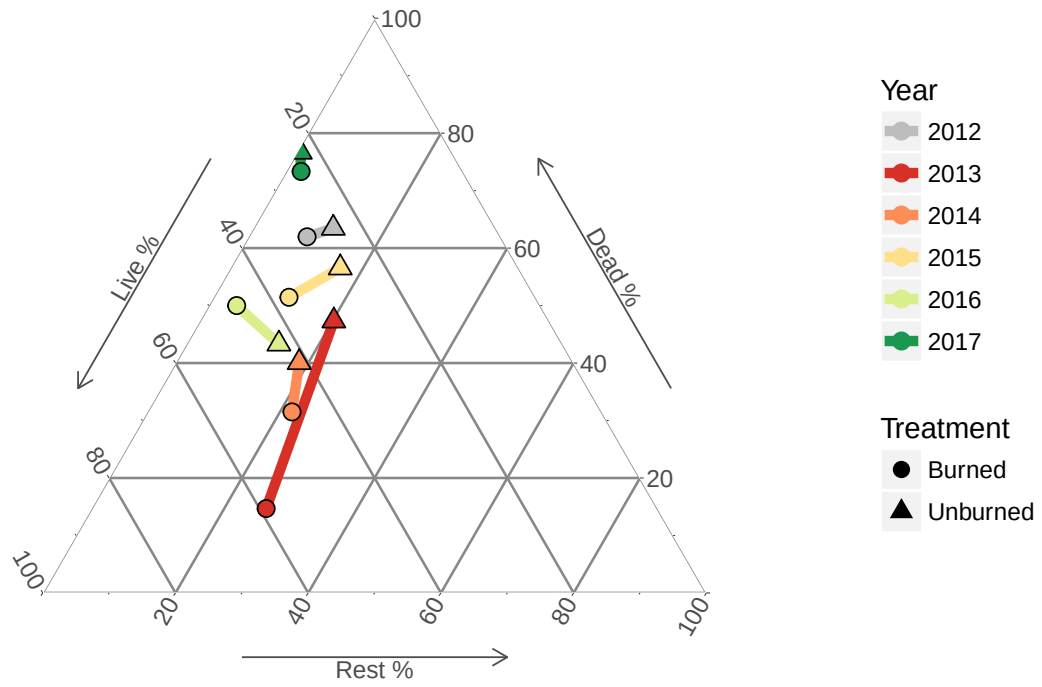

Figure 5.1: Overview of post-fire dynamics with higher level components in the pre- and post-fire grassland ecosystem (2012-2017). "Live" and "dead" components are the derived biophysical parameters through aggregation. Other parameters are summarized as "rest". The figure clearly illustrates the dynamics of cross-sample configurational difference of these three components throughout five post-fire growing seasons. Field data from year 2012 is also added as the baseline (one growing season prior to the wildfire).

back to the community. Figure 5.1 suggests such characteristics. Notice the overall progressively upward post-fire recovery pattern, with only a small setback occurred in 2015 due to the water stress. But the recovery trajectory carries on after 2015. However, configuration in 2017 overshoots beyond that of pre-fire 2012 with significant margin, suggesting a potentially different configuration or alternative state of the ecosystem from its original version. Since there is no other major disturbances present to modify the configurational structure, the hysteresis can be only explained by 2013's wildfire. However, more field dataset both in higher quality and longer time series is needed to provide direct vegetative composition data and observe whether there are shifts in the

communities structure, other than the shifts in the configuration of various high-level categories reported here.

Meanwhile, the figure also portrays the general trend of balance between live and dead component of the ecosystem across time. Since both are major components in the ecosystem, they restrict each other's presence. The fire promoted the percentage of live component significantly in 2013, as indicated by the burned sample positioning at the bottom of the chart (with its value around 60%) . However, the position of burned samples after 2013 have been progressively moving up in the figure (along negative direction of the live-axis), showing a steady decreasing trend. Meanwhile, the dead component displayed the exact opposite increasing trend accordingly. These trends indicate the effective removal of dead material by the fire and later the accumulation process.

Figure 5.2 investigates vegetation's post-fire dynamics at a finer resolution with original unaggregated result from Table 5.1. It illustrates the trends of most biophysical parameters across treatments (solid line for the burned, and dashed line for the unburned) from 2012 (pre-fire baseline) to 2017 (5^{th} growing season). Significance test result is indicated as filled ($p = 0.05$) and open ($p = 0.1$) circles. Figure 5.2(a) provides as an overview, whereas (b), (c) and (d) show the dynamics of soil crust, live and dead component respectively.

Also shown in Figure 5.2(a) is the short-term precipitation (April, May, June) during the field season, because research water availability is the key limiting factor in productivity of the prairie ecosystem (Schröder, 2006; Banerjee et al., 2011; Yang et al., 2013; Li & Guo, 2014). And biophysical parameters used in this study are closely related to productivity.

5.1.2 Post-fire Recovery of the Live Component

It is not surprising to observe fluctuations in biophysical parameters at unburned sites (dashed lines) due to inter-annual variation in the precipitation pattern. This is more obvious for the green

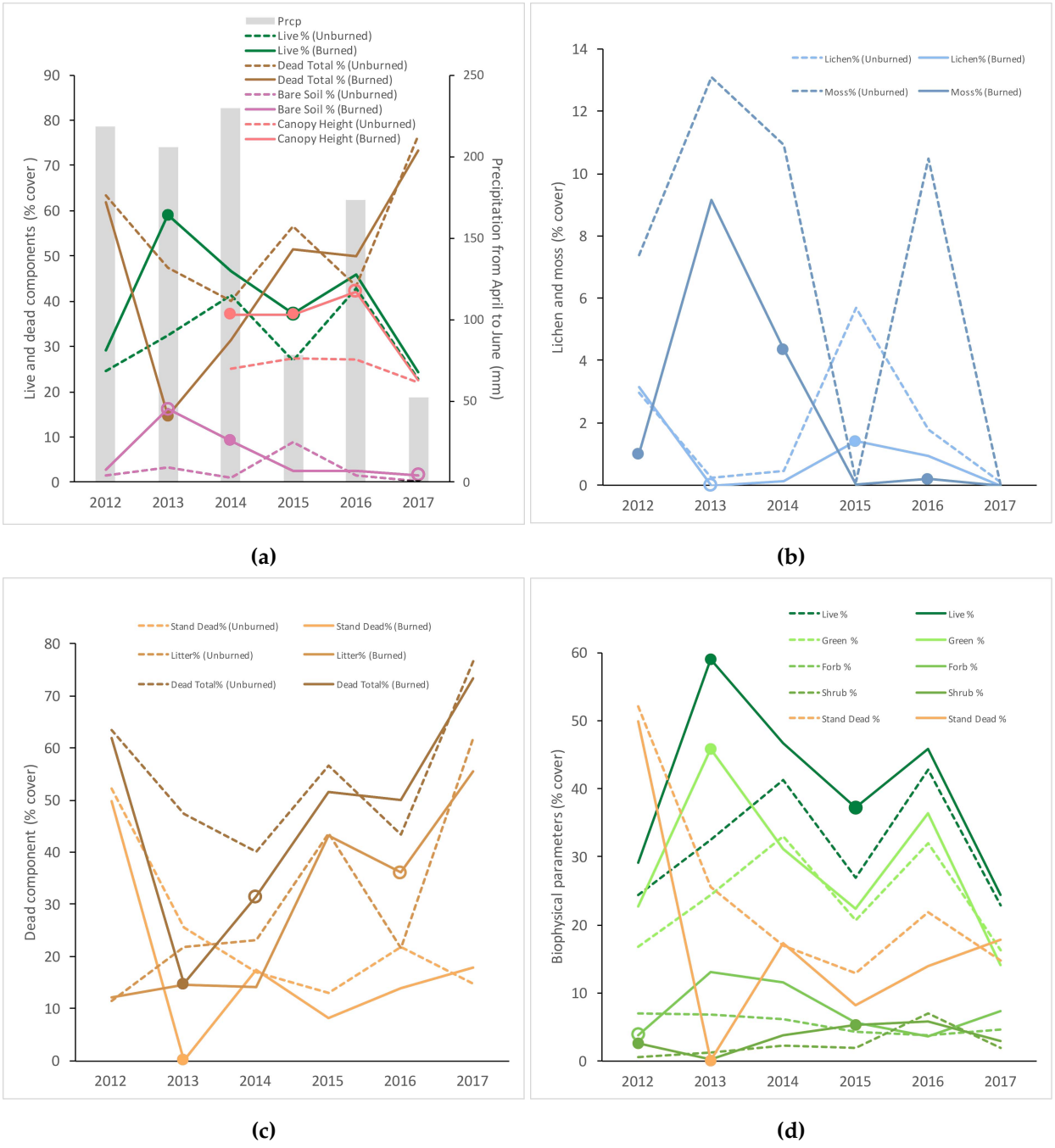

Figure 5.2: Dynamics of biophysical parameters: overview (a), soil crust (b), live component (c), and dead component (d). All parameters are compared at the same growing season between burned (solid lines) and unburned sites (dashed lines) across five post-fire growing seasons (2013-2017). Data from 2012 is included to serve as the baseline. Sigfinicance test is indicated by filled ($p = 0.05$) and open ($p = 0.1$) circles. Notice the apparent correlation between the growing season precipitation and total live component.

grass cover in 2015 and 2017 when both years saw a significant decrease in green grass cover because of the below-normal precipitation during the growing seasons. In fact, result shows that same-month precipitation explains 68% variation in green grass cover and 72% variation in the dead component cover. Though both tests were passed at a weak significance level ($p = 0.1$). However, if the well-documented time lag (Guo, 2002, 2004; He et al., 2008) is considered between grassland phenology and climate variables, the statistics would be much stronger and significant.

There was abundant precipitation following the fire, making green grass cover at both burned and unburned sites experience large amount of increase. GNP reported that the "above normal precipitation [in May and June] resulted in a rapid re-growth of vegetation, giving the Park a lush green look" (Parks Canada, 2013). In fact, live vegetation cover increased by as much as 82% in merely two months after the wildfire. Statistics also shows significant increase of live vegetation at burned sites into the third growing season, howbeit at a lower extent (but still 65% higher than that of the unburned). This suggests that the dead material began to accumulate quickly at the burned sites, resulting in the less pronounced difference in the live vegetation component between burned and unburned sites in the third year. This finding may seem to agree with researches on the tallgrass prairie where fire substentially increases herbaceous production due to modified pattern of soil nitrogen as well as improved light availability (Blair, 1997; Johnson & Matchett, 2001). However, it contradicts the finding by Augustine et al. (2010) on the semi-arid shortgrass in North American Great Plains (about 1,000 km south of the study area in northeastern Colorado). Their prescribed fire showed no influence in herbaceous plant production in both the first and second post-fire growing seasons. This discrepancy may be caused by differences in climate, vegetation types and various grazing pressure in these two ecosystems.

Results consistently show that burned sites have significant 20% more green grass cover. This demonstrates fire's positive impact in promoting grassland health. Meanwhile, it describes the

evolutionary adaptation of the prairie grass communities to disturbances like fire. Fire consumed all the standing dead and other components, broke down biomass into nutrients and opened up space for green grass to colonize on burned sites. This can be clearly confirmed from the dynamics of exposed bare soil, which was significantly high at burned sites in the first two growing seasons. Overall it took merely one growing season for the green grass cover to restore to the unburned status, however canopy height at burned sites are consistently more than 10% higher even at the fifth growing season.

Fire overrides climate as the most significant force in shaping the post-fire vegetation community. Notice that in the second growing season due to above-normal precipitation the unburned sites experienced fast increase in green grass composition and decrease in the standing dead composition. However, the opposite scenario happened at burned sites, with the green grass composition decreased by 15% and the standing dead increased by the same amount.

Though most non-significant result makes it difficult to interpret forb and shrub composition dynamics, still general conclusions can be reached. Figure 5.2(c) shows that fire increased forb's composition in the following two growing seasons. There was a high peak of increase in forb's composition at the first growing season, coinciding with the high increase in green composition. This is obviously due to fire removing most dead component and allowing green vegetation colonize the disturbed area. In the subsequent growing season, we observe forb's cover tend to be higher at burned sites. At the third growing season, there is no difference between treatments. Therefore, it took two growing seasons for forbs to converge to the unburned level, contrasting with grass' one year recovery. As for the shrub, it underwent longer recover process simply due to severe loss of biomass from the burning. Charred wood was still visible in the burned area during field season in 2017 (author's personal observation). Please note that the shrub composition at the would-be-burned sites was a little higher than the unburned sites in 2012. That is expected be-

cause the fire propagated mostly along the Frenchman River valley. As a result, some of surveyed burned sites were located in the low-lying valley area where there were more shrub presence than sites outside the valley. In fact, shrub contributes little in our research sites, with its composition always as low as 5%. Notice that at the third growing season shrub cover at burned sites was significantly higher. In fact, a few samples have exceedingly high level of shrub (cover greater than 40%) and were excluded from the analysis. This is also when the water stress was present, with green grass and forb having converged to the same level as unburned sites.

5.1.3 Post-fire Dynamics of the Dead Components

Fire effectively removed the dead component in the immediate growing season. Individual statistics of standing dead and litter component don't produce consistently significant result. But when combing the two components together there exists significant decrease in the dead component in the burned sites. This can be confirmed from the personal observation in the field as well as related grassland fire study in this area (Lu et al., 2016; Yang et al., 2013). Fire effectively removed the standing senesced grasses from the past year as well as the dead material covering the ground surface. This opened space for new vegetation to take over, with unobstructed light conditions as well as nutrients from the fire-consumed ashes. Dead component at burned sites was 30% less than at unburned sites. The standing dead, which is the most combustible material to fuel the fire, was completely removed at burned sites. In the second post-fire growing season, total dead component at burned sites was still 10% less, though at a weak significant level ($p = 0.1$). Figure 5.2(c) shows obviously that standing dead at burned sites has easily build up after one growing season and reaches the same percentage as at unburned sites. Overall it took two growing seasons for the dead component to converge to their unburned counterparts, ie., restore to its unburned status.

Fire effectively removed the dead component in the immediate growing season. Manually

designed parameters (dead component) is better at depicting trends with statistic power.

5.1.4 Post-fire Dynamics of Soil Crust and Soil Properties

Fire may have profound impact on the soil crust. Its recovery took longer than four growing seasons, indicated by the seemingly unclear and sporadic trend in soil parameters across samples. Fire initially burned most above-ground biomass, exposing bare soil which continuing remained high for two growing seasons. This made lichen composition close to none. Although precipitation helped moss composition to recover but still they are significantly lower at burned sites. The water stress in 2015 affected both burned and unburned sites. Unburned sites had the live component reduced, most moss removed, and lichen exposed. However, burned sites had significantly less lichen. Precipitation at the fourth growing season helped moss at the unburned sites to recover to its un-stressed level, but failed to do so at burned sites. This indicated that burning affected the long-term soil dynamics even into the fourth growing season. In contrast, Ford & Johnson (2006) found that soil crust in burned and unburned sites were at similar level after two years of fire events. The discrepancy between this research and theirs probably was due to three reasons. First, their research site was located in southern Great Plains at Kiowa National Grassland, New Mexico — 1,500km south of GNP. The environmental variables are quite different from that of the mixed prairie, causing variations in time of recovery. Second, their grassland was classified as shortgrass steppe. The predominant cover of warm-season C4 plants have distinct biophysical properties than C3 plants found in the mixed prairie at GNP. Third, during their study timeframe, several months of drought occurred followed by several months of heavy precipitation. This particular weather pattern will certainly make their findings less comparable to results identified here in this research.

In semi-arid mixed grasslands, its productivity is often water limited due to its impact on bio-

logical activity within the ecosystem (Schröder, 2006). Acting as a protective blanket (Vermeire et al., 2011; Yang et al., 2013), the dead material traps water from precipitation and also helps retain water from evaporation at soil surface. When the dead material has been removed by fire, soil surface at the burned sites receives more solar radiation and also evaporation loss will increase. Vermeire et al. (2011) was able to demonstrate that for burned sites soil temperature rose by 0.5 °C during drought and was similar during a wet growing season. Meanwhile, a consistent increase by 1% was reported in soil moisture at burned sites. However, this study does not have significant result to indicate such change. This may be caused by a few reasons. The device used in the field data collection is known to be not sensitive enough to detect the small changes in the soil parameters. Also field sites were sampled at different dates usually in a period of two weeks. Weather pattern and time of day can both impact the measurement.

Unfortunately soil measurement in this study was of low accuracy to provide useful insight. Considerable errors come from low precision sensor being used, inconsistency in measuring time (different time of day, month of year), as well as influence from topography and short-term weather conditions. As a result no significant results were found for soil temperature and moisture (except in 2016). However, Vermeire et al's study showed 0.58 °C significant higher temperature at burned sites.

5.1.5 Fire and Grasslands Resilience

Result suggests that fire enhanced short-term health and resilience of the grasslands. GNP received below-normal precipitation in 2015, causing a water stress that impacted both burned and unburned sites of that year. Now the grassland ecosystem has undergone two years of recovery from the wildfire's disturbance in 2013. And in the third year water stress settled in, causing a minor disturbance. As a result, grasslands were experiencing a compound effect from both wildfire

and water stress. However, result indicates the wildfire' impact masking the effect of water stress at burned sites.

It is interesting to observe that in 2015 the live component at burned sites was significantly 10% higher ($p = 0.05$) than at the unburned sites. The significant increase coincides with a very low percentage of exposed bare soil as well as higher shrub coverage at burned sites. Whereas unburned sites saw an increase in exposed bare soil and lower live component. These opposite scenarios across treatments suggest better performance of burned sites in withstanding water stress. As a result, fire promoted grasslands' resilience, and positively caused grasslands ecosystem to perform better under water-stressed condition. Though the underlying mechanism of such improvement in grasslands resilience needs to be further researched, yet still it is possible to hypothesize that fire modified the local hydrological cycle through its effect on grassland covers; moreover, it probably enhanced water utilization, which can be further supported with more discussions in section 5.3.

Fire's improvement in grasslands resilience lasted no more than four years. Another water stress condition appeared in 2017 with similar below-normal precipitation. However, data analysis didn't show significant differences across treatments. This indicates the fire's influence only lasted for four years in term of its impact on grasslands health and resilience.

5.2 Grassland Post-fire Recovery with RS Approaches

The previous section 5.1 (on page 63) investigated grasslands post-fire recovery using dataset collected manually in the field. Results therein offers fundamental insights on the process of grasslands recovery at the ground level. Moreover, conclusions drawn from that section provide ground reference for establishing satellite RS based solutions to be discussed in this section. Field experiment exhibits obvious limitations. It is often not only time and resource consuming, but produces small and sometimes insufficient sample size unsuitable for vigorous statistical analysis which has

been demonstrated explicitly in the previous section. RS approaches on the other hand, inherently overcomes these limitations both in terms of cost-effective data acquisition and consistent dataset that can facilitate analyzing grassland post-fire recovery both in breadth and depth. For instance, we can leverage on the archived historical satellite dataset for studying grasslands fire at a larger spatial scales and across longer time frames that is beyond the capability of field experiments.

This research tries to evaluate grasslands post-fire recovery by establishing satellite RS solutions systematically from both theoretical and practical perspectives. First (in section 5.2.1 on page 76), using hyperspectral measurement from the field survey, theoretical analysis verifies the feasibility of using satellite RS products to quantify grasslands recovery based on their nominal wavelength windows. Key fire-sensitive wavelengths were identified, confirming the effectiveness of commonly used RS product from Landsat sensors in fire studies. Then (in section 5.2.2 on page 81) grassland post-fire recovery analysis originally discussed in section 5.1 (on page 63) was repeated — not with field data but instead using selected Landsat imagery paired with field surveys in accordance to the timeline. Both the original individual single band reflectance and relevant VIs are examined to exemplify and validate the capability of satellite RS products in grassland fire study. Finally (in section 5.2.3 on page 89), I want to leverage on the unique power of satellite RS based solutions by answering more challenging questions that could not be solved through field experiments. This allows us to tap into the potential of RS data and gain more insights on grasslands post-fire recovery from new perspectives.

5.2.1 The Theoretical Foundation

In order to examine the feasibility of RS in capturing grasslands post-fire recovery, hyperspectral ASD dataset from field surveys were collected and analyzed. In essence, I want to find suitable windows of wavelengths that correlate well with fire-sensitive biophysical parameters identified

in section 5.1.

In order to quantify the performance of RS product in detecting grasslands post-fire recovery, a few assumptions are made here. First, Landsat sensors are selected as the primary candidate for RS application in this research, mainly due to its impact in RS research community in forms of its longevity, popularity and ease of access. Second, due to the complex nature of evaluating grasslands post-fire recovery, three biophysical parameters were selected as the proxy of ground truth in vegetation recovery, also called *fire-sensitive biophysical parameters*. Third, simple linear relationship exists between measured ASD reflectance and fire-sensitive biophysical parameters. Technically the across-treatment difference of biophysical parameters is regressed against the across-treatment difference of ASD reflectances. From the linear regression models run at each narrow wavelength window, the coefficient of determination (r^2) indicates the capacity of that wavelength in quantifying grasslands post-fire recovery; meanwhile the $p - value$ tests whether the model is statistically significance, i.e., not due to random effects. As a result, performance of thousands of narrow wavelengths can be examined and those bearing strong relationship with biophysical parameters will be regarded as effective fire-sensitive predictors in quantifying grasslands post-fire recovery.

Three biophysical parameters are involved in testing the performance of Landsat bands: percentage of the live component, SRI_{bio} and NDI_{bio}. A series of analytical plots were produced and compiled into tables to facilitate interpretation and conclusion.

It is important to consider the pre-fire condition when quantifying grasslands post-fire recovery. However, due to device-related issue that cannot be corrected as pointed out in section 4.3, pre-fire ASD data in 2012 could not be used in this part of research. Even though related scripts have implemented the functionality of removing the effect of pre-fire condition using baseline data, the current dataset available to this research could not support such analysis. As a result, the proposed methods were carried out without factoring in the baseline scenario. Nevertheless, RS data

from 2012 suggests insignficant differences across treatments; therefore the exclusion of baseline data should not severely impact the following analysis. Apparently quality dataset can be collected in the future to improve the result and findings from this research.

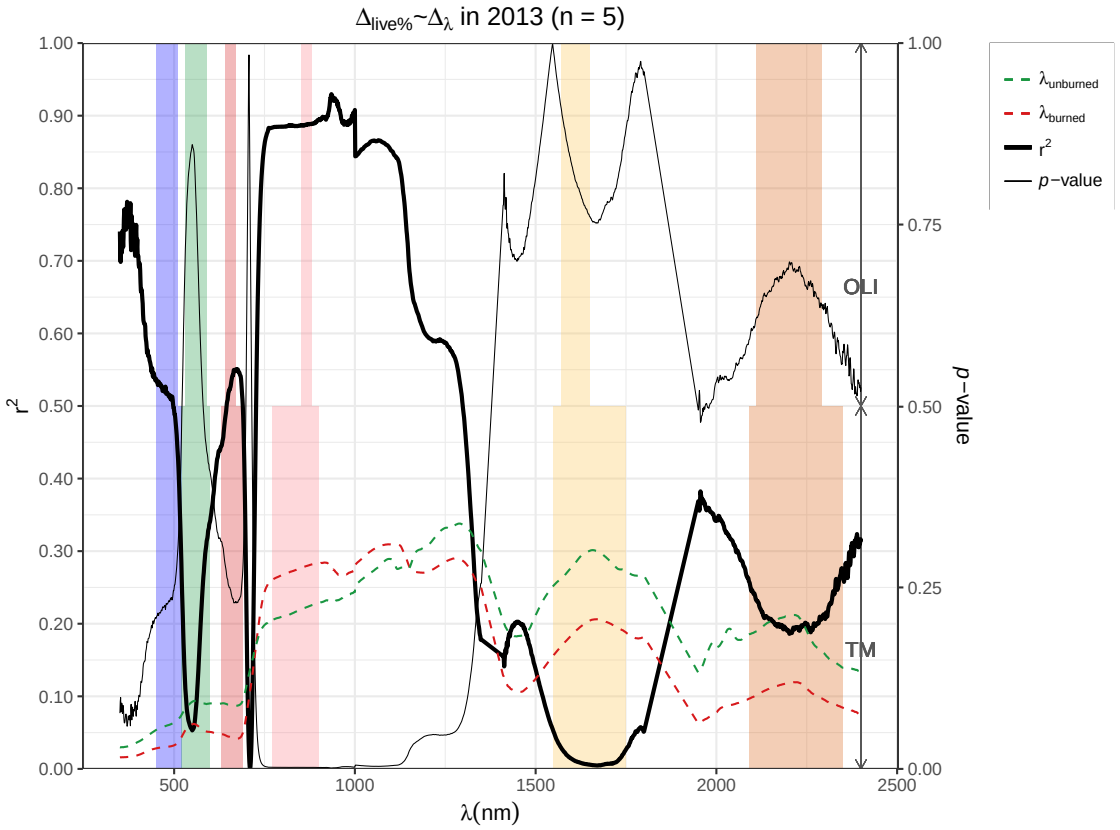

Figure 5.3: Power of all wavelengths in explaining the variation of fire-sensitive biophysical parameters. The biophysical parameter used here is the percentage of live component (live%). The thick black line shows the r^2 curve. The thin black curve indicates p-values from significance tests. Averaged reflectance curves for burned (red dashed line) and unburned (green dashed line) are superimposed as references. Color bands shown in the background are band configurations for Landsat sensors (OLI of Landsat 8 on the top; ETM+ of Landsat 7 below) plotted according to their designated wavelengths. A sensitive window from 750nm to 1,250nm can be clearly identified from the figure. The analysis was carried out using a small sample size (n=5). Better result can be achieved if more samples are available.

Figure 5.3 shows an example of the analysis result for year 2013 with live component as the biophysical parameter. Due to limited sampling effort in the field survey, only five burned samples were included in the analysis. The explanation power of narrow bands (wavelength ranging from

350 nm to 2,400 nm at 1nm interval) is indicated as thick black line. Three regions show strong r^2 values: violet region (r^2 peaks at 0.80), red region (r^2 peaks at 0.55), and NIR region (r^2 peaks at 0.93). However, the thin black $p - value$ line indicates only NIR region as statistically significant ($p = 0.05$), excluding the other two windows. Notice that regressions for producing this graph were carried out using only five samples due to limited field sampling effort (five burned samples and five unburned samples). Overall, we can conclude that reflectance at NIR region (750 nm to 1,000 nm) can explain approximately 90% of the variation of live component percentage ($p = 0.05$). It is not surprising to know that this window also happens to cover the NIR band of Landsat product, shown as light pink color bands in the background (wide band at bottom for Landsat 7 ETM+ sensor and narrow band on top for Landsat 8 OLI sensor). The scattering of NIR radiation in green vegetation's spongy mesophyll (Jensen, 2005, p. 302) is commonly used as a robust measure of green vegetation, which in this case can also serve as an effective parameter in evaluating post-fire recovery when live component is used as the measure of recovery.

Similar plots were prepared as in Figure 5.3 for all the years and other two fire-sensitive parameters. Results were assembled and organized together according to Landsat bands as Table 5.2. Please note that data analysis suggested additional two sensitive windows at SWIR region: $SWIR_a$ at 1,300nm and $SWIR_b$ at 1,950nm located at two atmospheric water absorption regions (Jensen, 2005, p. 302). Also included in the table are weak significance tests with $p = 0.1$ due to the limited sample size from the field survey (indicated as n in the table). Though some statistics are not significant at $p = 0.05$, they will probably pass the test if more or better data samples are available to the analysis. This can be seen from field data in 2015 that has comparatively larger sample size and thusly more significant results being reported.

Overall, Landsat product demonstrated its effectiveness in studying grasslands post-fire recovery, with the most sensitive bands to be red, NIR, and two SWIR bands. When live component

Table 5.2: Sensitivity of Landsat Bands evaluated using three fire-sensitive biophysical parameters. "*" indicates significance level at $p = 0.05$; whereas "○" stands for $p = 0.1$. SWIR_a and SWIR_b are not Landsat bands, but two water absorption regions at with their central wavelengths at 1300nm and 1,950nm respectively. Sample size (indicated as n values) available to the regression models are also included here as reference.

Variable	Year	n	Blue	Green	Red	NIR	SWIR_a	SWIR_1	SWIR_b	SWIR_2
Live%	2013	5	0.53	0.10	0.27	0.89∗	0.20	0.02	0.37	0.20
	2014	5	0.80∗	0.75∗	0.98∗	0.82∗	0.58	0.00	0.85∗	0.44
	2015	9	0.49∗	0.02	0.73∗	0.76∗	0.42○	0.07	0.58∗	0.33
	2016	4	0.99∗	0.65○	0.93∗	0.56	0.75	0.20	0.70	0.52
	2017	5	0.48	0.60	0.48	0.65○	0.00	0.17	0.25	0.37
SRI_{bio}	2013	5	0.67○	0.86∗	0.65	0.00	0.89∗	0.87∗	0.73○	0.82○
	2014	5	0.52○	0.90∗	0.94∗	0.27	0.65	0.32	0.65○	0.58
	2015	9	0.38	0.80∗	0.62∗	0.80∗	0.50∗	0.20	0.63∗	0.40○
	2016	4	1.00∗	0.90○	0.96∗	0.43	0.86○	0.35	0.80○	0.64
	2017	5	0.82∗	0.89∗	0.82∗	0.63	0.05	0.07	0.02	0.20
NDI_{bio}	2013	5	0.62	0.97∗	0.63	0.01○	0.92∗	0.98∗	0.82	0.92∗
	2014	5	0.45	0.12	0.85∗	0.27	0.55	0.22	0.05	0.40
	2015	9	0.29	0.02	0.52∗	0.62∗	0.25	0.03	0.40○	0.15
	2016	4	0.98∗	0.85○	0.93∗	0.27	0.94∗	0.47	0.90∗	0.82○
	2017	5	0.48	0.61	0.47	0.71○	0.02	0.20	0.25	0.35

(live%) is used as the parameter of measuring vegetation recovery (top section of Table 5.2), the most sensitive window is 750 nm–1,000 nm, which corresponds to Landsat's NIR band. The second sensitive window is 625 nm–690 nm, overlapping with Landsat's red band. Green and blue region also showed some explanatory power but not consistent throughout five years study period. Though dynamics of the live component should be captured by Landsat's green band from a theoretical perspective, result demonstrated the worst performance of that particular band in 2013 and 2015, when both years experienced abnormal events (fire in the former case and water stress condition for the latter). When both live and dead component are considered (middle section of Table 5.2 for SRI_{bio} and bottom section for NDI_{bio}), the most sensitive window still proves to be the red region. However, the second most sensitive region is in the SWIR region, specifically starting

from 1,375 nm forward, with the most sensitive peak wavelength at 1,375 nm which is only about 250 nm shorter than Landsat's SWIR1 band. The second sensitive region is less concentrated, with its window close to Landsat's SWIR1 and SWIR2 bands, making both turn out to be useful. This finding also confirms the algorithms of various SWIR involved burning indices such as NBR, CSI and MIRBI (Table 3.2 on page 44). Also from the biophysical perspective, the burned area tends to exhibit abnormal moisture content compared with unburned samples, which can be captured by SWIR reflectances as this region is sensitive to vegetation's in vivo water content (Jensen, 2005, p. 309-311). Though soil meter used for field data collection failed to capture the significant differences across samples due to various errors, RS data outperforms and compensate on this dataset.

5.2.2 Post-fire Recovery with Landsat Product

5.2.2.1 Performance of Individual Bands

Spectral reflectance from satellite imagery demonstrated significant power in distinguishing different treatments for five consecutive seasons. Across five post-fire growing seasons, spectral reflectance of all Landsat bands were significantly lower at burned sites than the unburned (Figure 5.4, left), except near infrared band (NIR) which saw higher reflectance in burned sites howbeit most results were not statistically significant. Moreover, for the aforementioned non-NIR bands, the difference of spectral reflectance between treatments generally displayed a decreasing trend (Figure 5.4, right). This implies that fire's impact is fading in the process of vegetation recovery, with burned sites converging to the unburned, making both treatments appear homogeneous. For the forth season some statistics became weaker (Red, $SWIR_2$) and eventually in the fifth season all statistics were non-significant, implying the fact that the burned communities almost fully recovered. The author checked two images for 2017, one in early growing season (June 4^{th}) and another in maximum growing season (June 20^{th}) and both showed non-significant results.

Table 5.3: Performance of satellite products at burned (“B”) and unburned (“UB”) sites

	2012		2013		2014		2015		2016		2017	
	UB	B	UB	B	UB	B	UB	B	UB	B	UB	B
Blue (%)	5.2	5.6	5.3	3.4*	5.7	5.2*	7.2	5.6***	7.4	6.4*	5.6	5
Green (%)	7.3	7.5	8.2	6.2**	8.5	7.9	10	8.5**	5.7	4.6**	8.3	7.6
Red (%)	7.6	7.8	8.4	5.2*	9.1	8.2*	11.3	8.5***	6.2	4.7○	9.2	8.4
NIR (%)	23.1	21	22.6	28.1	22.3	22.7	23	27.1*	21.1	21.2	22.7	20.9
SSWIR (%)	25.1	24.9	27.3	20.5**	27	23.5***	30.8	25.8***	25.4	21.5**	27.8	24
LSWIR (%)	13.4	14.8	16.9	12.7*	17	14.9**	20.3	15.2***	15.2	12.5○	16.9	14.6
NDVI	0.5	0.5	0.5	0.7*	0.4	0.5	0.3	0.5**	0.5	0.6	0.4	0.4
NBR	0.2	0.2	0.1	0.4○	0.1	0.2	0.1	0.3***	0.2	0.2	0.1	0.2
EVI	1	1	1.1	0.8*	1.4	1.1○	0.7	1.6	1.3	0.9***	1.4	1
SAVI	0.3	0.2	0.3	0.4	0.2	0.3	0.2	0.3**	0.3	0.3	0.2	0.2
MSAVI	0.3	0.2	0.2	0.4	0.2	0.2	0.2	0.3**	0.3	0.3	0.2	0.2
BAI	3.1	3.3	3.1	2.9	3.1	3.2	3	2.8	3.4	3.5	3.1	3.3
CSI	1.7	1.4	1.3	2.4**	1.3	1.5	1.2	1.9*	1.4	1.8	1.3	1.5
MIRBI	0.9	1	1	1.3*	1.1	1.2*	1	1	1	1.1	1	1.1
GEMI	0.6	0.5	0.5	0.7	0.5	0.5	0.5	0.6**	0.5	0.6	0.5	0.5

Significant codes: ”***” 0.001, ”**” 0.01, ”*” 0.05, ”○” 0.1

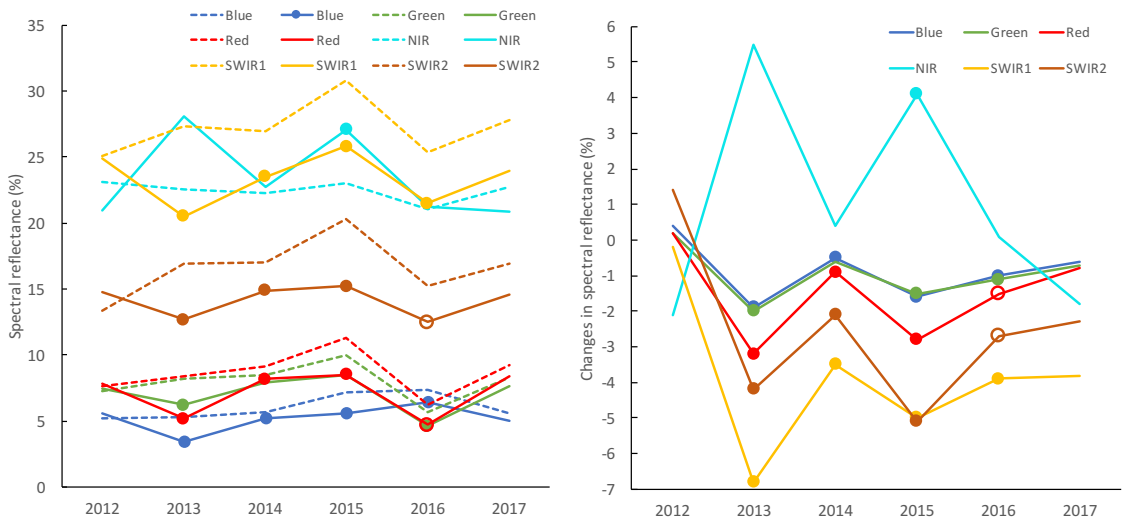

(a) Raw reflectance of Landsat bands **(b)** Changes in reflectance between treatments

Figure 5.4: Dynamics of Landsat single band reflectance across post-fire growing seasons (2013-2017) for burned sites compared with unburned sites, with pre-burn 2012 serving as the baseline. Figure *a* shows raw reflectance of Landsat single bands for burned (solid lines) and unburned (dashed lines) sites. Filled circles indicate significant difference with $p = 0.05$ between the burned and unburned, empty circles for $p = 0.1$, whereas absence of circles for non-significant results. Figure *b* portrays the relative change between treatments. Notice differences in reflectance is getting less pronounced across years. Such decreasing trend can be easily observed in figure *b*.

Notice the anomalies occurred following 2015 where the converging trend was disturbed. This is caused by the water stress in 2015, which affected the post-fire recovery. However, the converging trend continued consistently after 2015. Some claim fire as a "global herbivore" (Bond & Keeley, 2005). Here the statistics suggests that drought can also mimic fire's impact. At a glance, it can be regarded as a minor "fire". It decreased the reflectance signature of both treatments, proving itself as a "global herbivore". However, we observe more pronounced contrast between treatments, with burned sites still have much higher reflectance as in previous growing seasons, suggesting fire's profound impact. Needless to say, more research need to quantify the impact of drought, fire and herbivore, the three most common and interconnected disturbances in shaping the grasslands.

Responses from three visible bands (especially the red band) are significantly smaller at burned sites than the unburned. This is because burned sites tend to have more live component (green vegetation) and less dead material (standing dead and litter). Chlorophyll and other pigments in healthy green vegetation absorbing red spectrum for photosynthesis, making reflectance in that region significantly lower than the unburned sites that find less live component. On the other hand, the light-coloured standing dead and other non-photosynthetic vegetation (NPV) have higher reflectance at visible bands and appear brighter. However, across time the difference of reflectance in visible bands between treatments became less pronounced, from 3.2% in 2013 to 0.8% in 2017 (Figure 5.4 right). As the grasslands recovered, burned sites started to build up their own dead material and the contrast in the visible bands was getting less obvious.

SWIR1 and SWIR2 are vivo water content related (Fourty, 1997) with healthy vegetation exhibit more absorption (less reflectance). Figure 5 displayed similar result as three visible bands, emphasizing the more live component during vegetation's recovery from the burning. And both bands experienced similar converging trend between treatments.

NIR is the only band showed increased reflectance at burned sites, simply because of the more healthy live component at burned sites. Though we expect to see a consistent and significant higher reflectance in NIR at burned sites, satellite data suggested otherwise. Yang et al. (2013) investigated fire's effect in the same study area and also reported that NIR increase at some burned sites showed no statistical significance. Across five post-fire growing seasons only 2015 saw a significant increase in NIR by 4% at burned sites. The insignificant result for other growing seasons may be due limited sample size, and large variations in the live component at the burned sites. It is worth noting that removing an outlier (a burned site with extremely low response in NIR) in 2013, led to a significant increase in NIR response by 6% at the burned sites.

In SWIR2 region, solar radiation can be significantly absorbed by the water content in green

vegetation or soils. Meanwhile, researches (Key & Benson, 2006; Schepers et al., 2014) also suggest that dry soil exposure after burning would increase SWIR2 reflection. Water absorption in SWIR1 is considerably weaker. However, this study showed the opposite relationship. There was significant decrease in both SWIR bands at burned sites. This can be explained by the increased composition in green vegetation for the burned sites which had higher water content than unburned sites. As a result, SWIR regions in burned sites had more absorption and less reflectance. Although for unburned sites the significant amount of the dead material help to retain water. However, in this study we don't see this effect from SWIR bands. This is probably because SWIR bands couldn't penetrate the vegetation structure and pick up the water's signal in the dead material at the soil surface. Furthermore, Landsat 8 imagery acquired five days after the burn also indicated lower SWIR responses for burned sites. This is probably due to the presence of charred soils found at the burned sites which had lower reflectance in both SWIR regions than unburned sites where senescent grasses were dominant (Lu et al., 2016). Overall, we observe lower reflectance in SWIR region for burned sites from right after the burn, till the third year. This finding contradicts Schepers et al. (2014), probably due to difference in ecosystems and vegetation types.

5.2.2.2 Performance of VIs

Although individual spectral bands demonstrated promising capability in separating treatments, commonly used broad-band vegetation and fire indices showed mixed results with most statistics non-significant, demonstrating the pressing and challenging issue of finding a suitable vegetation index in monitoring vegetation recovery from the fire. Detailed result can be summarized in Table 5.3 and more visually in Figure 5.4.

The algorithm of NDVI involves NIR and red bands, and has been widely used in the literature as an important index for studying green vegetation as well as fires. In this study, although NIR

band didn't have a good performance from the statistical perspective, we did find a good performance of NDVI. We saw a significant increase in NDVI for the burned sites in the first (by 44%) and third growing season (by 49%). NDVI for burned sites in the second and fourth growing season also increased but was not statistically significant.

NBR is a widely-used fire index expressed as the normalized difference between NIR and LSWIR. It is able to distinguish green vegetation from soil based on their contrasting reflectance signatures at these two bands. This study confirms its performance in such ability. NBR at burned sites had as much as 1.5 to 4 times higher values than unburned sites. Though its performance varied from weak in the first year to not significant in the second year, and became strong in the third year. This result proves NBR as a reliable long-term fire index suitable for studying grassland fires.

EVI is another commonly used vegetation index which was developed to overcome the limitation of NDVI. However, this study demonstrates that EVI's performance is not as good as NDVI in studying fires at GNP, even though burned sites had significant lower reflectance in blue band. Instead of increasing as we see in NDVI, EVI in this case is lower in burned communities. Its weak performance may be affected by high percentage of dead material dominant in GNP grasslands.

Both SAVI and MSAVI are developed as a modification of NDVI to correct the influence of soil brightness in ecosystems with low vegetation cover and exposed soil surface. However, this study find both didn't perform well in distinguishing burned and unburned grass communities. We see these indices are greater at burned sites. From a theoretic perspective, they should have good performance for the first two years because percentage of bare soil exposure is relatively high at burned sites. However, it is interesting to find both indices can only distinguish burned sites in the third year with statistical significance. This is also when bare soil percentage was lowest in burned sites. The poor performance may due to a few reasons. First the soil brightness correction

(a) Vegetation/burn indices

(b) Vegetation/burn indices

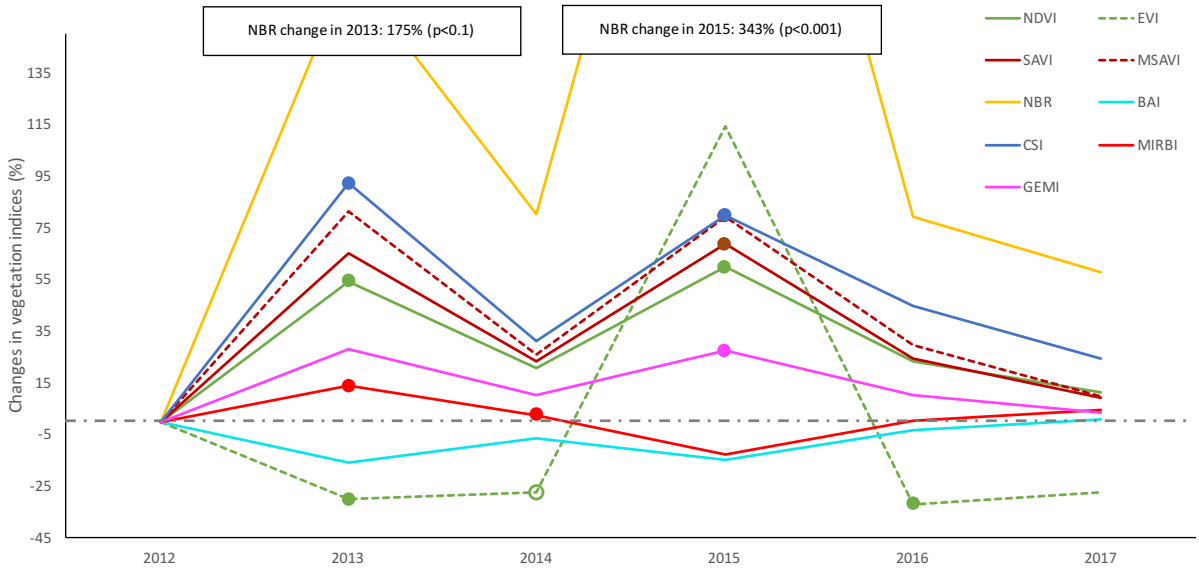

(c) Changes in vegetation/burn indices

Figure 5.5: Dynamics of vegetation/burn indices (separated into figure *a* and figure *b* according to their value ranges) across post-fire growing seasons (2013-2017) for burned sites (solid lines) compared with unburned sites (dashed lines), with pre-burn 2012 serving as the baseline. Filled circles indicate significant difference with $p = 0.05$ between the burned and unburned, empty circles for $p = 0.1$, whereas absence of circles for non-significant results. Notice in plot *c* most indices displayed greatest difference right after the fire (2013) and keep converging to the 0% (dash-dot horizontal) line afterwards, indicating less pronounced differences between treatments, which also can be confirmed by the significance test (absence of circles).

factor (parameter L) for calculating SAVI may need fine tuning in this study. Second, these indices are developed to overcome the influence of soils at the cost of being less sensitive to vegetation changes that are essential in study post-fire vegetation recovery in this study.

The Burned Area Index (BAI) was designed to detect the char signal (Chuvieco et al., 2002). However, this study finds out BAI is not suitable for grasslands fire study in GNP. This is probably due to BAI being developed for ecosystems other than grasslands in GNP. Grasslands ecosystem has higher turnover rate. Grass communities are well adapted to disturbances like fire. As a result, their fast recovery will block the char signal being captured by remote sensors, thus making BAI not useful in study fires in this region.

Char Soil Index (CSI) is another index to detect the char signal, but meanwhile considers influence of soil signal. In this study, CSI in the burned communities are greater than the unburned, though this is only statistically significant in year one and year three. We also see the CSI values are decreasing from year one to year three. This study confirms CSI's performance in studying grassland fires.

Mid-Infrared Burn Index (MIRBI) was a fire index developed for savannah ecosystem, where NIR is less useful because of senescent vegetation in the fire season. Literature shows MIRBI to be relatively stable in performance over time. MIRBI also performed well in this study, showing significant greater values in the burned sites than the unburned, though not significant in the third year. Also, we observe a decreasing trend in MIRBI over time for the burned sites.

GEMI index is designed to reduce atmospheric effects and sensitive to dark surfaces such as burned areas. But it failed to capture the land surface changes in this study for the first two years where char soil was abundant. Instead, it shows a significant increase for burned sites in the third post-fire growing season.

5.2.3 Advanced application of satellite RS solutions

Results in previous sections have already successfully validated satellite RS based solutions as an effective and reliable method of studying the grassland fire, especially with a large wealth of long-term RS archives available to us, not succumbing to the limitations found in field experiments. This opens up new possibilities in treating the subject with sophisticated satellite RS based solutions capable of answering more challenging questions. Here in this section two exercises are done to further take the advantage of Landsat RS product. First (section 5.2.3.1), a series of satellite NDVI was calculated and sampled to provide more robust analysis on the grasslands post-fire recovery. Then (section 5.2.3.2), a time series of satellite NDVI was built and Time Series Analysis was employed to reveal the long-term pattern of grassland post-fire recovery in terms of its trend.

5.2.3.1 Robust Post-fire Analysis with Satellite NDVI

A `Python` script scans all available Landsat imagery acquired for this research and computes NDVI for non-polluted pixels. Stratified random samples are collected (Figure 5.6) from calculated NDVI scenes to perform further statistical analysis. Result can be illustrated with Figure 5.7.

Without the impact of limited sample size observed in the field data analysis, here NDVI demonstrates its apparent strength in portraying grassland post-fire recovery. The within-year seasonality caused by vegetation phenology is clearly seen. Also can be observed is the overall decreasing trend from 2013 to 2016, reflecting the climate variation of the same period. Though 2017 is also an extremely dry year in this area, the impact of drought didn't settle in till late July (refer to Figure 3.8) which is outside the analyzed time frame. Apparently grasslands recovery is closely tied to climatic variables. Though both burned and unburned grassland underwent the similar recovery scenario, yet they carry significant differences. Burned grassland always maintained higher NDVI values compared with its unburned counterpart, which can be explained by

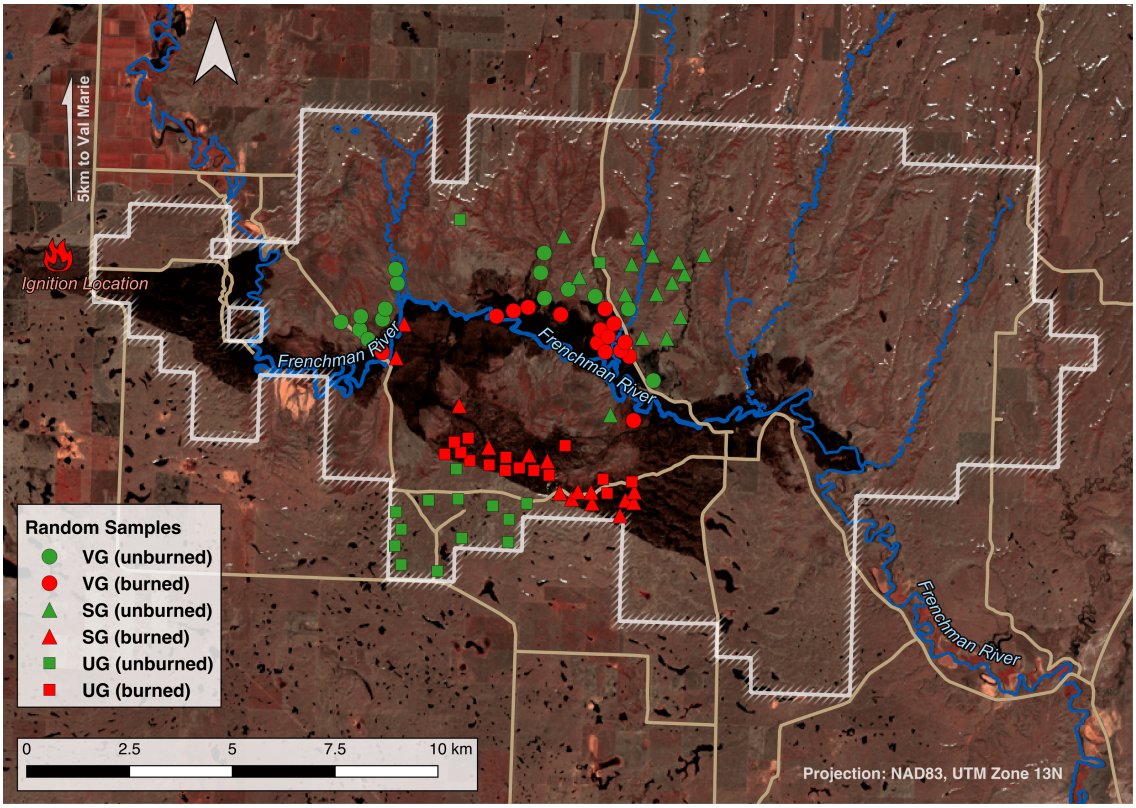

Figure 5.6: Stratified random samples are collected from satellite NDVI scenes. The background shows the burned area with the standard false colour composite of Landsat 8 scene on May 1st, 2013.

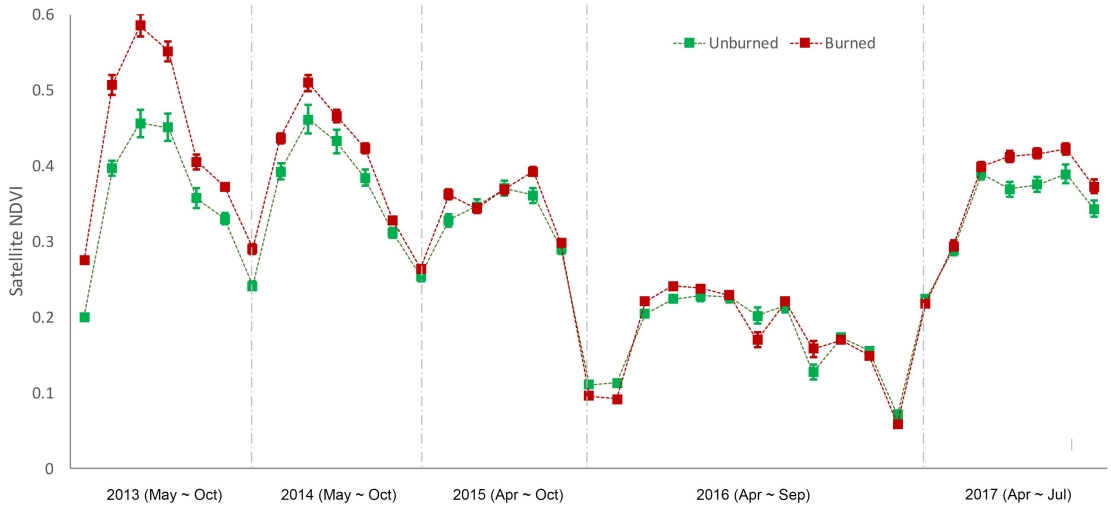

Figure 5.7: Satellite NDVI demonstrates the effectiveness of NDVI as a post-fire recovery indicator (error bar indicates one standard error). Notice there are more imagery available for year 2016.

the fire's positive impact to the ecosystem. When peak NDVI values (corresponding to the maximum growing season) are considered, we observe such positive influence gradually dying out across time, from 30% higher in 2013 to 10% higher in 2014 and eventually almost non-existent in 2016. This result may suggest a fire regime with a period of four years to be ideal for the prairie ecosystem. But fire's impact is more profound when we look at the start of the growing season — burned communities consistently exhibit higher NDVI values. This can either means the burned site has the earlier start of growing season, or the burned site always tends to grow greener vegetation. Since there is no apparent phase shift (a.k.a. time delay in the signal) between the two curves, the former hypothesis may not seem to be a plausible explanation. However, Peet et al. (1975) and Knapp (1984) indeed reported the greenup being advanced by one week or as much as one month at burned sites due to relatively warmer soil temperatures during the day. Therefore in order to clarify on this, better satellite RS datasets need to be analyzed, especially with fine-tuned temporal resolution at the greenup period for the study area. Nonetheless, we can certainly observe the impact of grassland fire even at the fifth growing season, with both climate variation (2013-2017) and a minor disturbance (water-stress condition in 2015 and 2017) considered.

5.2.3.2 Time Series Analysis with Satellite NDVI

In order to further model grassland post-fire recovery, the NDVI samples prepared in the previous section were manually transformed into time series data. The previous analysis suggested a recovery cycle of four years. Henceforth, data from 2013 to 2016 are considered for TSA. Moreover, in order to test the performance of the TSA 2017's data was withheld from the analysis and used for model validation. The time series was built with a frequency of six (from months of May to October) for year 2013 to 2015. Since VG grassland demonstrated the most pronounced change, its TSA results are shown here in Figure 5.8 and Figure 5.9, together with the diagnostic plots in

Figure 5.10 and Figure 5.11. Holt Winters forecast model was used to validate the TSA, with result shown in Figure 5.12 and Figure 5.13.

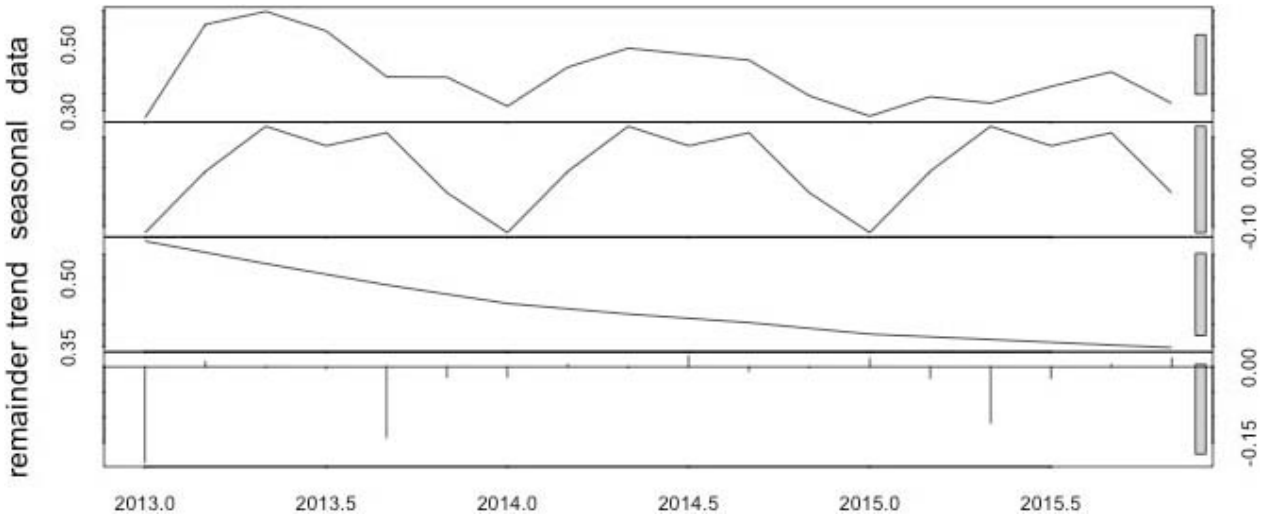

Figure 5.8: TSA results for burned VG grassland. This graph shows the original dataset and its decomposition into seasonal and trend components, as well as the remainder. The trend component depicts a clear decreasing trend in satellite NDVI for burned communities (the amplitude of the trend is $0.50 - 0.35 = 0.15$).

TSA was able to decompose the original dataset into three parts: seasonal signal, trend and remainder. The second component clearly identified a consistent decreasing trend in the satellite NDVI for burned VG sites which could not be observed for unburned VG sites. Results for SG and UG sites exhibited similar characteristics as VG, howbeit not as pronounced as VG. Diagnostic plots didn't detect any lags touching the critical bounding box, suggesting that the fitted TSA model was able to extract the above-mentioned three components effectively, with the remainder containing noises (little and non-significant autocorrelation at the temporal scale). Moreover, the fore-casted result for year 2016 from Holt Winters forecast model showed good agreement with the actual NDVI trajectory in 2016. This further validated TSA as a useful tool in quantifying grassland post-fire recovery from a long-term perspective, which can only be achieved through satellite RS dataset. This also opens up new opportunities to investigate historic grassland fires.

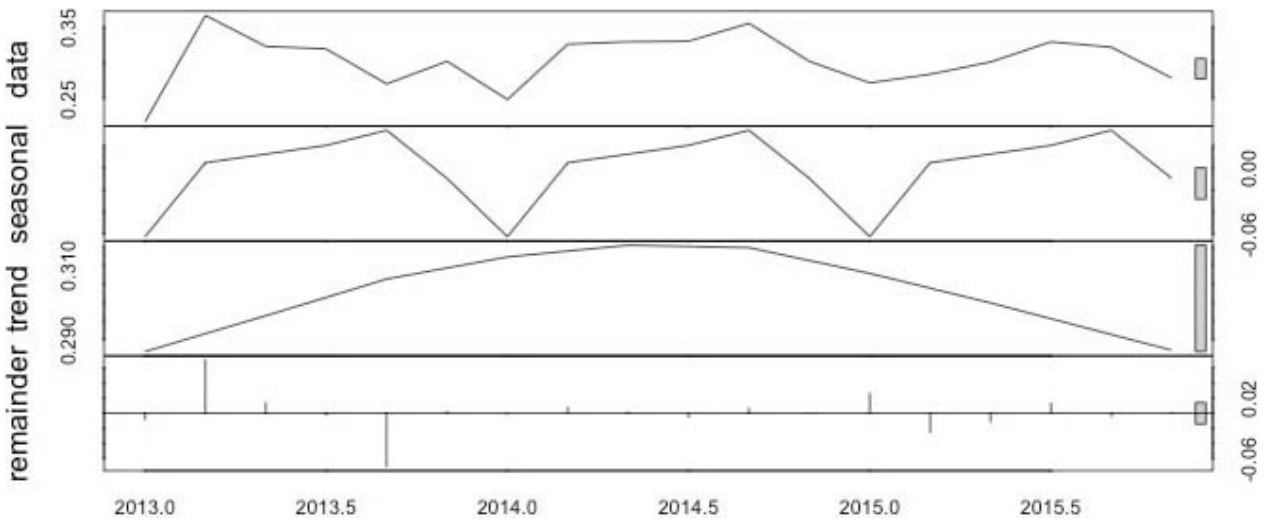

Figure 5.9: TSA results for unburned VG grassland. This graph is similar as the above one, but plotted for unburned grassland. Satellite NDVI for unburned sites display slightly different pattern than burned sites based on seasonal component; and no clear trend can be observed (the amplitude of the trend is negligible, as small as $0.31 - 0.29 = 0.02$).

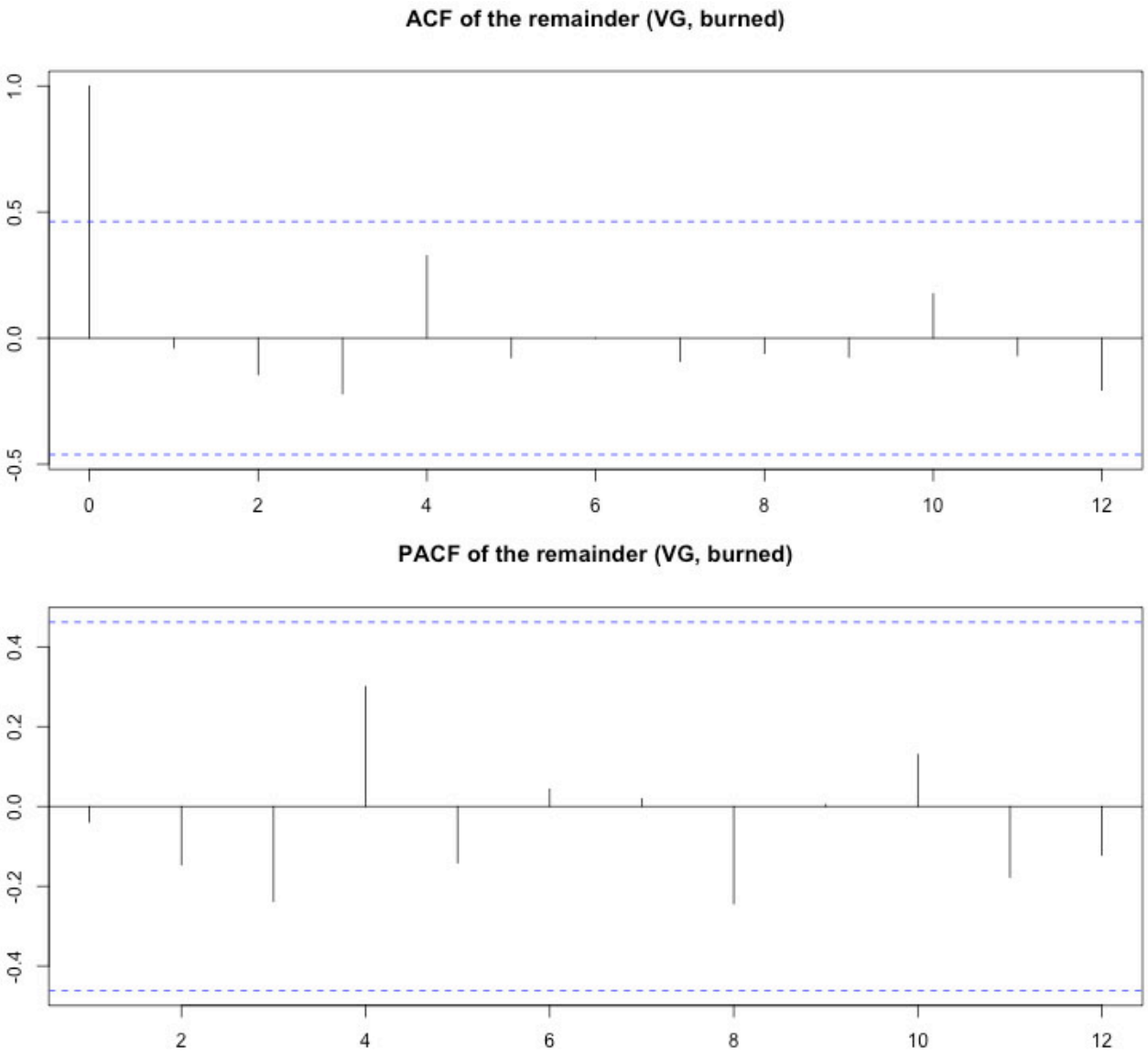

Figure 5.10: TSA diagnostic plots for burned VG. Diagnostic plots are correlograms of the in-sample forecast errors at various lags (1-12 here). It is used to evaluate the performance of fitting models. In this example, errors seem random and exhibit little autocorrelation, with no bars touching the significace bounds shown as dashed blue lines.

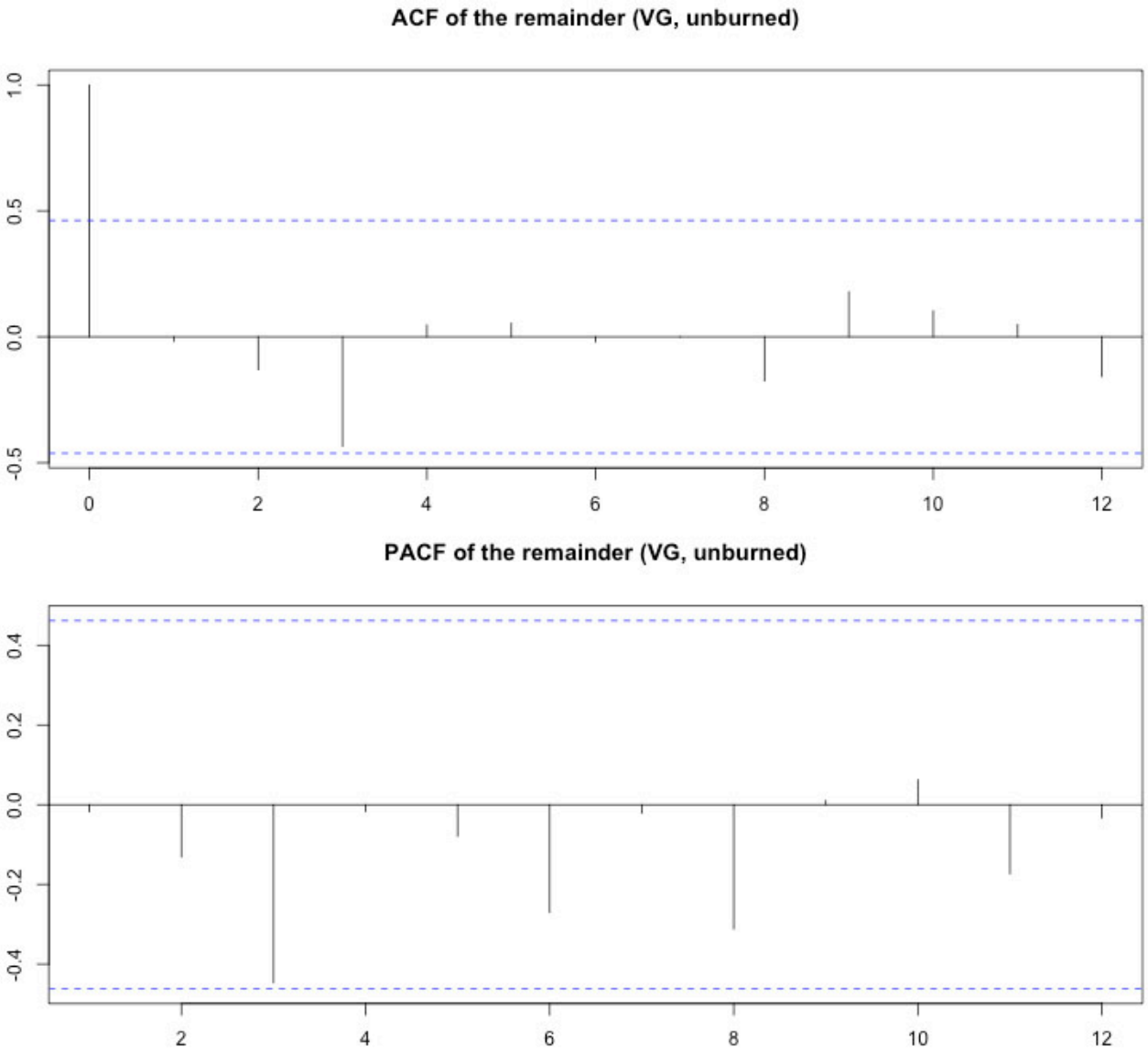

Figure 5.11: TSA diagnostic plots for unburned VG grassland. This graph is similar as the above, but for unburned grassland. TSA model for this dataset seems less robust compared to the burned model, because autocorrelation at lag 3 almost touches the significance bound.

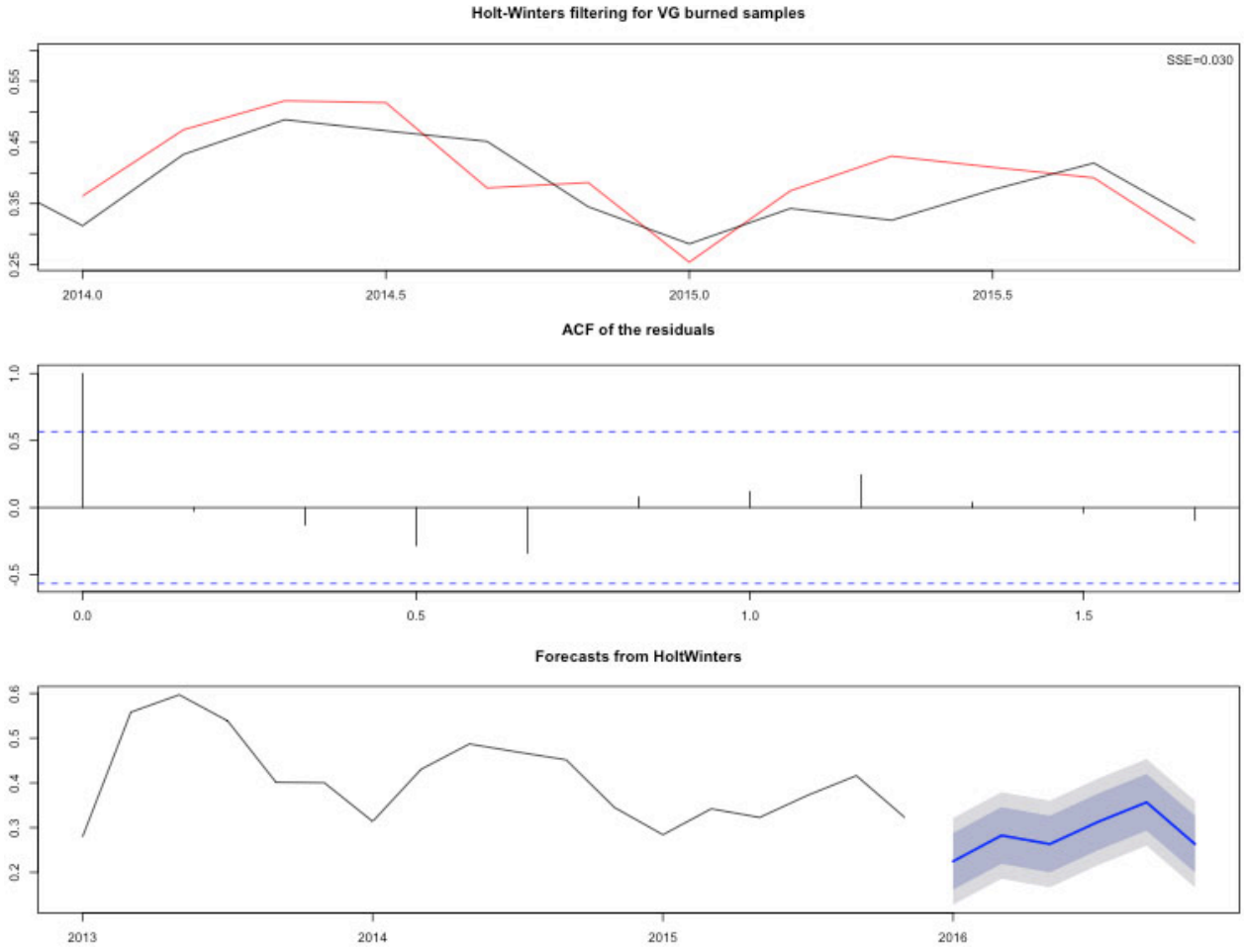

Figure 5.12: Holt Winters forecast model for burned VG grassland. The top graph shows the original dataset as black line, model's prediction (fitted values) as red line. The middle graph is the diagnostic plot. The bottom graph shows the model's future forecast (2016's growing season) of satellite NDVI at burned sites (dataset for year 2016 is too small to be incorporated into the TSA, and is withheld for validation). The blue line is the forecast, with 80% prediction intervals as dark gray, and 95% prediction intervals as light gray. The forecast shows good agreement with the actual satellite NDVI for year 2016.

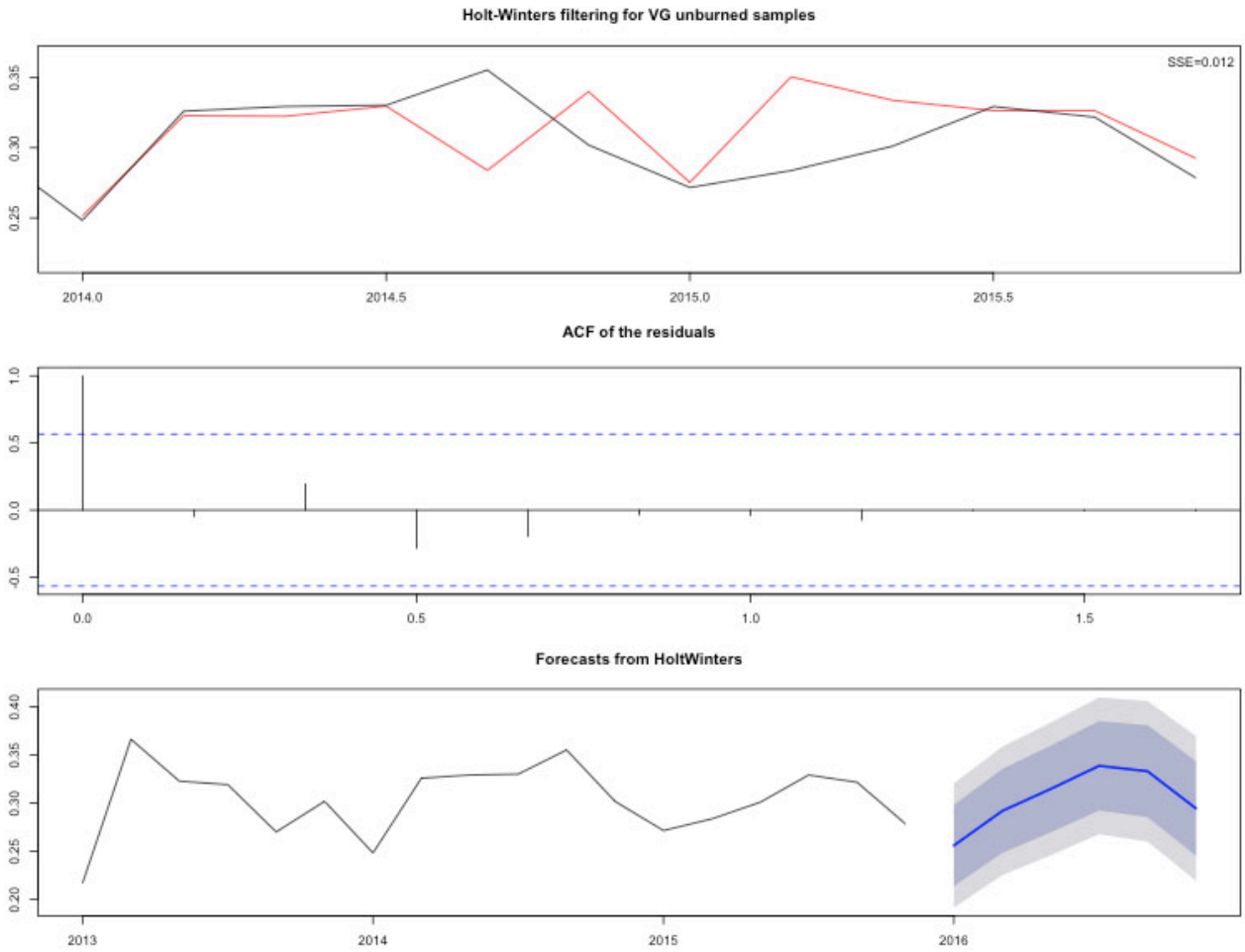

Figure 5.13: Holt Winters forecast model for unburned VG grassland. This figure is similar as the above figure for burned sites.

5.3 Driving Factors of Grassland Post-fire Recovery

This section tries to investigate the driving factors influencing vegetation's post-fire recovery. Factors examined include meteorological variables, grazing and topography. This purpose of this section is to provide a concise summary of how the burned grasslands recovered. Though many aspects need to be reviewed and considered in the analysis, this research purposefully simplifies this process, aiming to provide a overall high level understanding of the recovery dynamics under these driving factors, and by no means a well-rounded investigation.

5.3.1 Results from Field Data

ANOVA was carried out to evaluate how variance of green grass percentage could be explained by the variances of climate variables (mean temperature, precipitation and moisture deficit), presence of grazing, and topography. Table 5.4 shows the result. For unburned sites, the major driving factor of green grass recovery was topography, which explains as high as 60.4% of green grass's variance. Mean temperature showed weak significance ($p = 0.1$), indicating weak explanatory power.

In contrast, burned sites experienced a totally different scenario. Precipitation was the only significant variable and it could explain as much as 25.4% of variance in green grass percentage.

Same analyses were also done for forb cover percentage and shrub cover percentage but with no significant results. This was due to several aspects. Number of field sites was considerably limited. Field surveys in some years were not designed for this study which has further impaired quality of the result. Human errors were unavoidable during the field survey, with certain percentage of misclassification. For small components as forb and shrub, their statistics were prone to such errors. The overcome these issues, live component percentage was analyzed and Table 5.5 shows the updated result.

Table 5.4: Explanation power of various driving factors in the variance of green grass percentage between burned and unburned samples. All years' data were included in the analysis

Explanatory variables	Burned	Unburned
Topography	7.40%	60.4 %***
Presence of grazing	0.40%	1.90%
Mean temperature	0.20%	4.8%.
Precipitation	25.4 %*	2.00%
Moisture Deficit	4.20%	1.00%
Residue	62.30%	29.80%

Significant codes: "***" 0.001, "**" 0.01, "*" 0.05, "○" 0.1

Table 5.5: Explanation power of various driving factors in the variance of live component percentage between burned and unburned samples. All years' data were included in the analysis

Explanatory variables	Burned	Unburned
Topography	0.0%	60.5 %***
Presence of grazing	3.0%	5.4%*
Mean temperature	2.3%	3.5%.
Precipitation	2.4%	6.0%*
Moisture Deficit	15.1 %	2.9%
Residue	77.2 %	21.8 %

Significant codes: "***" 0.001, "**" 0.01, "*" 0.05, "○" 0.1

The result for live component was different from that for green component. For unburned sites, though topography was still the major driving factor and could explain 60.5% of variance of live component, both grazing and precipitation also displayed as significant factors howbeit with limited impact. Grazing's influence might be downplayed here due to limited quality of grazing data. The significance of topography's impact might be from the fact that topography determines the water and nutrition redistribution.

At burned sites, there was no significant explanatory variables. Precipitation was a strong variable for explaining green component but here it has little impact for live component. The major

driving factor seems to be moisture deficit. But it failed to pass the significance test. Overall, the non-significance results demonstrated fire's long term (five years) impact on the mechanism of grasslands ecosystem. Fire generally makes the grasslands more productive and resilient, thus making other factors less significant.

5.3.2 Results from RS approaches

ANOVA was carried out to check how variance of green grass percentage could be explained by the variances of climate variables (mean temperature, precipitation and moisture deficit), and topography. Grazing was not included because: (1) field data analysis in the previous section indicates that grazing is not a significant factor influencing grasslands post-fire recovery; (2) no grazing datasets are available to support RS analysis. Table 5.6 shows the explanation power of these factors in determining the variance of satellite NDVI. Once again results show that RS approach (through stratified random sampling) can overcome the limitation of small sample size typically exhibited in field data analysis, thusly producing robust result with more statistical power.

Temperature proves to be always the significant factor in explaining NDVI variances. This might seem to conflict with the established finding that grasslands are a water-limited ecosystem. However, the context has now become as inner-annual trajectory of NDVI, whereas temperature becomes the most important factor in plant's growth and senescence. However, we still can observe the moderate impact of water availability from the factors of precipitation and/or moisture deficit.

It is interesting to observe the contrast between burned and unburned samples in 2013. Precipitation was a strong factor that explains 17% of NDVI variances for unburned samples. However, it is not a significant factor for burned samples. Based on the field data analysis from the previous section on fire's positive impact on the grasslands, the same can be stated here. Here are a few interpretations. In 2013's growing season fire effectively removed the dead component, making

green grass to establish quickly which improved the water use efficiency, thus reducing precipitation as a strong indicator of NDVI. Meanwhile, fire also sped up the nutrient cycling and enhanced grasslands productivity, with less reliance on precipitation as the unburned samples.

Table 5.6: Explanation power of various driving factors in the variance of satellite NDVI between burned and unburned samples. Each year's data was separate in the analysis.

Year	Samples	Precipitation	T_{mean}	Topography	Moisture Deficit	Residuals
2013	Burned	0.5%	49.3%**	1.7%	2.40%	46.2%
	Unburned	1.30%	47.8%**	2.8%	8.8%	39.3%
2014	Burned	30.8%***	41.5%***	3.1%	12.6%**	11.9%
	Unburned	27.0%***	40.3%***	1.60%	18.0%**	13.0%
2015	Burned	12.1%*	46.4%***	5.8%	11.9%*	23.7%
	Unburned	22.8%**	41.0%***	1.5%	18.9%**	15.7%
2016	Burned	1.6%	57.5%***	0.3%	16.2%***	24.4%
	Unburned	5.5%*	46.0%***	2.1%	15.1%***	31.30%
2017	Burned	43.9%***	1.8%	5.9%	25.0%**	23.4%
	Unburned	42.8%***	1.1%	0.8%	22.3%**	32.9%

Significant codes: "***" 0.001, "**" 0.01, "*" 0.05, "." 0.1

Moisture deficit proves to be a significant factor of explaining NDVI variances. In the water-stress condition of year 2015, moisture deficit has more influence on unburned samples' NDVI. However, its influence on the burned samples is much less. We observe that for three years (2013-2015) the explanation power of moisture deficit for burned samples were much lower than unburned ones, but became relatively similar in the following two years. This not only reconfirms fire's positive impact on water use efficiency, but also demonstrates such effect is gradually fading away and almost non-existent after three years.

Fire enhanced the positive relationship between productivity and climate variables (precipitation and temperature). Though precipitation and temperature can explain 50% to 70% of variance for both burned and unburned samples. Yet burned samples' NDVI can be better by precipitation and temperature. This may be due to fire caused secondary succession which facilitated establish-

ment of live component that correlates well with temperature and precipitation.

Fire enhanced grasslands resilience. The explanation power of precipitation and temperature for burned samples in 2015 decreased significantly, even less than that of the unburned. This drop in explanation power can only be attributed to the fire's presence, implying the fact that burned samples' productivity were not impacted significantly during water stress as found for unburned samples. This again has validated the previous finding about fire's enhancement on grasslands resilience.

Chapter 6
Conclusions & Future Work

This thesis has spent five chapters previously to describe how RS can play a significant role in grassland post-fire recovery assessment — specifically on how field data were collected to quantify grassland recovery which also establishes as the ground reference for RS based approaches; how RS based approaches are feasible in modelling grassland recovery from the theoretical perspective using hyperspectrum data; and finally using the actual satellite RS product to verify the reliability and robustness of its performance in grassland fire studies. Results and findings from different sections may get segmented and not synthesized holistically to reveal the whole landscape of the research. Therefore, this final chapter aims to draw primary findings from previous sections and place them within a coherent context of grassland post-fire recovery studies, highlighting the overall conclusions and contributions of this research, the current progress of related studies, as well as the future directions.

6.1 Review of Results

To fulfil the overall objective of studying grasslands post-fire recovery with RS approaches, this study first designed field experiment and examined fire's impact on the grassland ecosystem. Results therein offers fundamental insights on the process of grasslands recovery at the ground level. Then based on the conclusions from field data analysis as ground reference, RS based solutions are explored as it overcomes the inherent limitations found in the field experiment, i.e., resource con-

suming and insufficient sampling effort. RS based solutions are discussed from both theoretical and practical perspectives. Theoretical foundation of RS based solutions are explored using hyperspectral field measurement to prove the feasibility of using RS sensors in grassland fire studies. Actual Landsat RS imagery were acquired to further validate the robust performance of RS based solutions. Also advanced RS applications were demonstrated to help improve our understanding in the trajectory of grassland post-fire recovery, and also potentially reveal the current fire regime. This proves the unique strength of RS based solutions in studying grassland fires in breadth and depth, besides of its advantage in cost-effective data acquisition and reliable database. Finally, this research also tried to answer the question of *how the grassland ecosystem recovered under major driving factors*. Again both field data and RS data were analyzed. The results not only confirmed the general agreement between the two datasets, but demonstrating RS dataset with more robust and reliable result.

This study found that vegetation was able to recovery quickly from the spring burning. Starting from the first post-fire growing season, we see the grasslands ecosystem has begun the quick process of regeneration, and even resulted establishment on previously bare soil. This demonstrates the strong resilience of the mixed prairie due to its adaption to frequent grassland fires in the past. Fire effectively removed the dominant dead component in the ecosystem and promoted the regeneration of the grasslands, indicated by the increased green live component in the burned communities. However, the difference between burned and unburned communities get less pronounced across time as vegetation recovers. In the third post-fire growing season, the burned communities started to converge to the physiology of the unburned communities, suggesting a fire frequency of four years in the mixed prairie would be appropriate as the best regime in promoting native species in the ecosystem. Remote sensing product proved to be effective in detecting post-fire vegetation recovery. Some vegetation indices are sensitive in such detection. NDVI as a most widely used

vegetation index is a good indicator, suggesting the possibility of studying fire ecology in even longer time frame in light of the rich and cost-effective remote sensing data archive available. In contrast NDVI based indices such as EVI, SAVI and MSAVI are not suitable for studying post-fire vegetation recovery in the mixed prairie. By incorporating SWIR regions, MIRBI, NBR, CSI are also effective fire indices suitable for this study, with MIRBI being the best indicator.

Overall, Landsat product demonstrated its effectiveness in studying grasslands post-fire recovery, with the most sensitive bands to be NIR, red, and two SWIR bands. Landsat NIR and red bands are the primary and secondary strong predictors of variation in live component if green vegetation is the main focus of vegetation post-fire recovery. When dead component is also considered as part of vegetation recovery, Landsat SWIR bands can be used as they correlates well with SRI_{bio} and NDI_{bio}. There are two other SWIR bands that sometimes demonstrated stronger relationship than the current Landsat SWIR bands. But overall sensitive wavelength windows for SRI_{bio} and NDI_{bio} are less concentrated than that of live component, indicating the challenge of developing the best RS index for quantifying live-dead dynamics of grasslands post-fire recovery. Li & Guo (2015) has reviewed the RS approaches in quantifying non-photosynthetic vegetation (dead materials). They mentioned the claim from related researchers (Gao & Goetz, 1994; Asner, 1998) on the feasibility of detecting NPV based on wavelegnths from 400nm to 2,500nm. However, in reality NPV estimation is always complicated due to presence of water, soil mineralogy, soil organic carbon etc. (Daughtry et al., 2004; Cao et al., 2010; Li & Guo, 2015). This is especially the case in mixed-praire (Li & Guo, 2015).

Remote sensing product proved to be not only viable solution from the theoretical perspective, but also demonstrated its effectiveness in detecting post-fire vegetation recovery. All Landsat bands except NIR were sensitive in distinguishing burned and unburned samples and in portraying vegetation's post-fire recovery. Some vegetation indices are sensitive in such detection. NDVI

as a most widely used vegetation index is a good indicator, suggesting the possibility of studying fire ecology in even longer time frame in light of the rich and cost-effective remote sensing data archive available. In contrast NDVI based indices such as EVI, SAVI and MSAVI are not suitable for studying post-fire vegetation recovery in the mixed prairie. By incorporating SWIR regions, MIRBI, NBR, CSI are also effective fire indices suitable for this study, with MIRBI being the best indicator. From the theoretical perspective, SWIR, Red and NIR bands are robust bands sensitive to post-fire recovery and new vegetation indices can be proposed based on them.

Driving factors analysis explained the trend of detailed grassland post-fire recovery. Main driving factors include climate variables, fire and grazing. At burned sites, there was no significant explanatory variables. Precipitation was a strong variable for explaining green component but here it has little impact for live component. The major driving factor seems to be moisture deficit. But it failed to pass the significance test. Overall, the non-significance results demonstrated fire's long term (five years) impact on the mechanism of grasslands ecosystem. Fire generally makes the grasslands more productive and resilient, thus making other factors less significant. Moisture deficit proves to be a significant factor of explaining NDVI variances. In the water-stress condition of year 2015, moisture deficit has more influence on unburned samples' NDVI. However, its influence on the burned samples is much less. We observe that for three years (2013-2015) the explanation power of moisture deficit for burned samples were much lower than unburned ones, but became relatively similar in the following two years. This not only reconfirms fire's positive impact on water use efficiency, but also demonstrates such effect is gradually fading away and almost non-existent after three years. Fire enhanced the positive relationship between productivity and climate variables (precipitation and temperature). Though precipitation and temperature can explain 50% to 70% of variance for both burned and unburned samples. Yet burned samples' NDVI can be better explained by precipitation and temperature. This may be due to fire caused

secondary succession which facilitated establishment of live component that correlates well with temperature and precipitation. Fire enhanced grasslands resilience. The explanation power of precipitation and temperature for burned samples in 2015 decreased significantly, even less than that of the unburned. This drop in explanation power can only be attributed to the fire's presence, implying the fact that burned samples' productivity were not impacted significantly during water stress as found for unburned samples. This again has validated the previous finding about fire's enhancement on grasslands resilience.

6.2 Contributions

This research has two major contributions. First, detailed field survey data were conducted for five years (excluding the pre-fire historic field survey) to study the recovery pattern of the grassland ecosystem from the wildfire. Field data were analyzed to evaluate the grassland recovery in a longer temporal not found in the study area. Meanwhile, the research devised fire-sensitive biophysical parameters that not only improve the quality of field dataset, but carry information that are suitable for measuring grassland post-fire recovery. Moreover, driving factors are considered using a diverse of explanatory variables that can provide insight for future grassland fire studies in this area. Second, this research successfully evaluated the feasibility of satellite RS approaches in grassland fire study, both from the theoretical as well as practical perspectives. The validation of the popular Landsat product, especially NDVI, opens up exciting opportunities to investigate grassland fire for a much longer temporal scale suitable for studying fire regimes, and also to trace the historic fire events with similar satellite product. RS approaches used in this research were never intended as complete, let alone definitive, but merely serving as an example to pave the way for new sophisticated approaches in the area of grassland wildfire research.

The study investigated the potential of remote sensing product in studying post-fire vegetation

recovery both from theoretical as well as applications using popular Landsat product. However, more work is required to quantify the vegetation productivity trajectory with comprehensive driving factors that involve major disturbances like grazing and drought. This is because grasslands have evolved and shaped by these constant processes ever since its distant past. Moreover, vegetation recovery not only takes place at the dimension of productivity, but also in biodiversity to ensure the ecological integrity of the ecosystem's health. All these challenges can be potentially addressed using remote sensing techniques. The paper demonstrated the effectiveness of NDVI in quantifying vegetation recovery. Long-term time series analysis can be conducted by accessing historical remote sensing archives to study fire ecology in a proper historical perspective. Meanwhile, by incorporation radar imagery, we are able to get more reliable soil properties and also the vegetation texture information that help answer recovery in biodiversity.

6.3 Challenges & Future Work

Though it is certain that methods proposed in this research can and will be improved upon due to the fast advance of related fields, it is the quality of data that determines the final outcome of the analysis result and findings. If not enough attention is paid on the input data quality, "garbage in, garbage out"[1] will ensue. In fact, this becomes most relevant especially for RS based approaches due to their direct dependence on usually large imagery inventory, stored in either flat file system or database. Computer algorithms are and will continue to solve challenges from the massive load of dataset. However, their effectiveness can be significantly hampered by the unpredicted data quality issues, as demonstrated in this study.

Quality of this research heavily relies on its two major data sources: field survey and RS im-

[1] "Garbage in, garbage out" is a computer science terminology describing the situation when flawed data input generates nonsensical output "garbage".

agery. Both data sources pose their unique challenges that cannot be resolved easily at this moment and may remain a barrier for future grassland post-fire study. Major data related issues are discussed in this section, together with potential approaches to mitigate their impact.

6.3.1 Quality of Field Data

Field data underpins the quality of RS based researches such as this study, as it establishes the ground reference, if not "ground truth", for developing, calibrating and validating appropriate RS based solutions. In fact, most RS approaches aims to provide cost-effect solutions to find proxies of in situ measurement from the ground — ultimately being interpreted in the "currency" of ground level parameters, instead of their "face value" without the context of ground reference. Therefore, quality of field data governs the reliability of RS based approaches.

In this study, field data were used to establish the ground truth of vegetation post-fire recovery dynamics and also to develop and validate RS based approaches. There are numerous challenges present in the field data. Some are not feasible to resolve due to both cost restrictions (extensive samplings at various intervals for several years to capture long-term changes) and the unpredictability of fire's natural occurrence (comprehensive pre-fire field survey as well as timing, location, season, duration, intensity of the fire) (Wakimoto et al., 2005). These cannot be addressed in the observational study such as this. As a result, fine-controlled experimental study is called for that can to some extent answer this challenge. Meanwhile, there are some challenges in the field data that can be addressed effectively to improve the result of this study, including various sources of errors. This section discusses major challenges rising from different sources of errors identified in the field dataset. Meanwhile, possible solutions are provided for future related research effort.

6.3.1.1 Limited Sample Size

The most prominent challenge comes from insufficient sample size to support robust statistical analysis as demonstrated in chapter 2 (on page 63). This can be also confirmed by other researchers of the northern mixed prairie (Wakimoto et al., 2005, pp. 44, 56, 69, 116, 134, 142-156). Furthermore, field designs in the first several years were not specifically tailored to this research, causing considerably limited sample sizes; whereas in theory a factorial field design (presence of burning, presence of grazing, three levels of vegetation cover, i.e., with the minimum total sample size of $2 \times 2 \times 3 = 12$) was expected to allow reliable statistical analysis. As a result, some proposed analysis could not be implemented in this research. This also undermined the explanation power of some statistical analysis.

6.3.1.2 Inconsistencies in Field Data

Moreover, quality of field samples can be significantly affected from various sources of errors. This research shows that in general, major sources of errors are introduced from inconsistent field seasons and field measurement.

6.3.1.2.1 Field Season The semi-arid grassland is sensitive to its physical environment, including long term climate pattern, short term weather condition, as well as extreme weather events. As a result, its phenology pattern varies accordingly. Maximum growing season is usually selected as the favoured window for field surveys due to its preferable timing when the vegetation reaches its maximum developing stage, thusly allowing satellites to capture the strong signal from the vegetation on the ground. However, such timing is always a post priori fact and impossible to be determined beforehand. This makes it challenging to quantitatively compare vegetation dynamics across different growing seasons.

6.3.1.2.2 Field Measurement Each Landsat satellite orbits the earth every 99 minutes. This feat cannot be achieved with in situ ground measurement. As a result, differences in timing of the field measurement produce inconsistent datasets, introducing errors into subsequent data analysis. Strictly established instrument operation procedures help mitigate such problem. A prime example is the ASD measurement used in this research. Due to the significance of the dataset as well as its sensitivity to local weather conditions, operation protocols were always supposed to be followed to ensure its data quality. In fact, this research shows that ASD measurement proved to be the most robust dataset among all the field dataset. However, operation protocols still can be disrupted by the ephemeral weather conditions in the field, as well as improper instrument operation from less experienced field crew. Such error can be demonstrated by the ASD data from 2012 in this research. It was so severely affected (chapter 5 on page 76) that the whole dataset could not be included into the proposed analysis. Another dataset prone to such error is soil property measurement. As a "land of living skies", the prairie displays fast changing weather patterns with rainfall concentrated in the summer. The window of usually one week field survey causes considerable variations in soil property (especially soil moisture), making such dataset less suitable for rigorous data analysis as demonstrated in chapter 5 on page 73.

6.3.1.2.3 Human Errors Moreover, inconsistency also arises from human-introduced errors of different field crews across years. In the study, there are a few examples of such errors. Vegetation cover is an important biophysical parameter used here. However, field data compilation has revealed several problems regarding this parameter: *(a)* recording error when data entries were either assigned to incorrect plots or incorrectly determined; *(b)* changes in protocols when vegetation covers were estimated considering vegetation's vertical structures in some years yet not being followed in other years; *(c)* discrepancy in estimation when the total vegetation cover could not

sum up to 100%. Such errors can only be mitigated through improved field design and measurement protocols. Two solutions can effectively address the issue presented in the latter case. First, more crew members should be assigned to measure important field parameters. For example, vegetation cover estimation was conducted by two members in 2017's field data collection. Each data entry was determined by the average of the two observers. Also in this way, several other errors previously identified was also avoided. Alternatively, certain parameters can be measured using computer algorithms to ensure its robustness. In terms of vegetation cover, photographs can be taken in the field from which relevant parameters can be derived either in situ or in the laboratory using image classification or machine vision algorithms.

Some field data related problems found in this research can be potentially solved by employing new technologies. Two platforms are especially ready to answer such challenges. One is from the dataloggers and data acquisition systems that can be deployed in the field. These systems are able to collect, store and even transmit data at fine temporal resolutions to support robust data analysis and modelling. With more open-source hardware platforms available, custom solutions can be built in a fast and cost-effective fashion to suit specific needs of diverse researches. However, deployment and maintenance of such systems bring new challenges, especially when the study area is under strict preservation with minimum disruption permitted such as GNP in this study. In this case, unmanned aerial vehicle (UAV) comes as the rescue with its versatile and cost-effective RS capabilities.

6.3.2 Quality of RS Data

RS based solutions undoubtedly demonstrated its great potential in grassland fire studies demonstrated in this research. However, it has its own challenges. This research shows that the most significant challenge comes from the quality of RS product itself, mainly accuracy of quality as-

sessment (QA) band and detector stripping.

6.3.2.1 Quality of QA Band

Quality of QA band has direct impact on the outcome of the grassland fire study. One of the most painstaking process in this research is selecting suitable imagery to *(a)* pair up with the field survey data for validating the RS based solution; and *(b)* to build a time series of imagery for long-term grassland recovery investigation. The desirable scenes are those least affected by clouds and shadows. However, cloud-free scenes were often insufficient to support intended analysis due to their limited number available within the investigated timeframe and study area. As a result, also included in the study were the scenes polluted with clouds and shadows on condition that they would not severely affect the final data analysis result. Therefore, there is a trade-off between the investigated timeframe and image quality. The longer time series of imagery included in the study, the more challenging it is to find cloud-free pixels usable for data analysis. Though the temporal resolution of Landsat satellite is 16 days, with 8-day repeat coverage of any Landsat scene area and coverage sidelap of adjacent orbits (7.3% to 84% of the scene) (NASA, 2018) provide additional data to this research, impact of clouds and shadows still poses as the culprit of degraded RS analysis result.

QA band is prepared by USGS and contained as part of the original Landsat product package. Each pixel in the QA band records the quality of a given pixel. QA band plays a vital role in RS fire study as they determines whether certain pixels can be included in the data analysis. Several types of QA bands have been published during the time frame of this research by USGS and their quality has been tested in this research with mixed performance. There are in total three types of QA bands available to this study: `cmask`, `sr_cloud` and `qa` bands. Figure 6.1 shows examples for the former two products. Some QA bands are riddled with problems that put their effectiveness

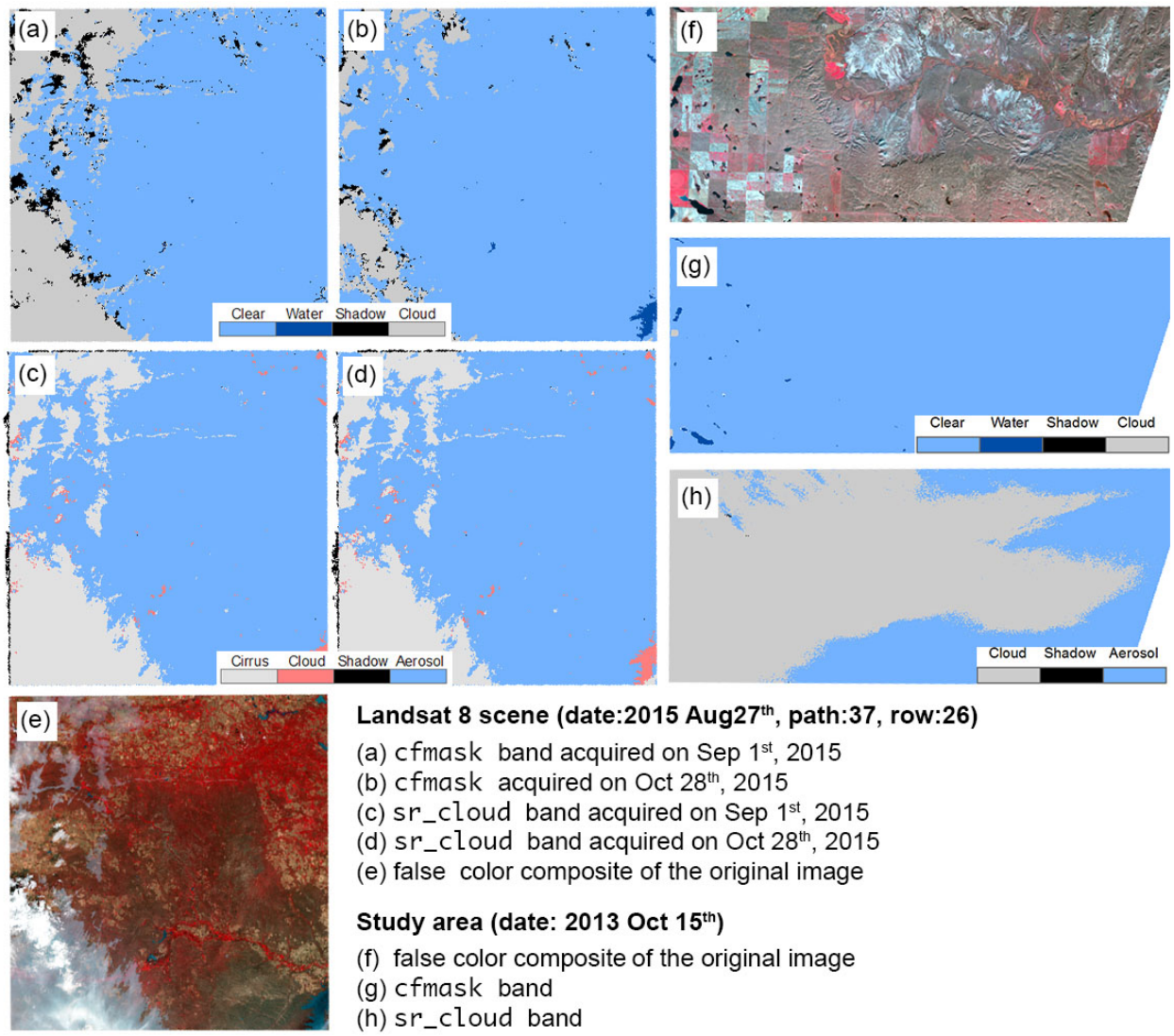

Figure 6.1: Inconsistent quality of cloud masks derived from various Landsat product.

under question:

1. Different QA bands disagree with one other, as indicated by the different results of `cfmask` e.g. Figure 6.1(b) versus `sr_mask` e.g. Figure 6.1(d) for the exact same scene. This is probably because that different QA bands are designed to suit various purposes. `cfmask` contains four classes to show the general imaging conditions with less focus on clouds. Whereas `sr_cloud` band is more focused on detecting clouds as it is built to distinguish different types of clouds and the shadow. Result indicates that this band is able to detect cirrus clouds, which will be

regarded by `cfmask` as "clear" when the confidential level is $\leq 12.5\%$. However, result from this study area, i.e. Figure 6.1(h), disapproves the effectiveness of `sr_band`.

2. `cfmask` bands downloaded at different times from the same data provider show inconsistent results, which implies that the underlying algorithm of `cfmask` band produced different outputs (QA bands) from the same single input (original Landsat surface reflectance bands). The author has tested certain other scenes repeatedly and this issue persisted. Due to limited resources, the problematic scenes were only tested at two different dates. However, it is sufficient to confirm the flaws in the QA band. This inconsistency can be indicated by the different cloud and shadow coverages between Figure 6.1(a) and (b), dated September 1st, 2015 and October 28th, 2015 respectively — about two months apart. This flaw is in fact documented by USGS (2017c). Even though the algorithm has been validated for cloud detection (Foga et al., 2017), it still remains a challenge to capture certain cloud and shadow conditions.
3. `qa` band was later released as the only QA band shipped with Landsat product, probably intended to supersede the previous `cfmask` and `sr_mask` bands. It contains 16 flags to mark seven possible scenarios (USGS, 2017b). It is designed to distinguish different types of clouds, shadow and also water — information originally contained in the aforementioned two QA bands. Its quality was checked against the original Landsat scene visually for the study area and showed satisfactory result. However, there is no control over the confidential levels previously shipped with `cf_mask` band (technically sperate band called "`cfmask_conf`").

In this study, when qa band was not available and only `cfmask` and `sr_cloud` were present, `cfmask` was used with its confidence level set at $\leq 12.5\%$. This is because `cfmask` showed better overall performance at capturing cloud shadows, and detecting water bodies which is significant due to the presence of Frenchman River in the study area; though it sometimes demonstrated in-

consistent result as discussed previously.

6.3.2.2 Detector stripping

Several artifacts directly impacts quality of RS data. Of which, the issue of data stripping proves to cause the main source of error in this research. It is a major problem of Landsat 7 product due to the failure of its scan line corrector. However, data stripping is also present in a few Landsat 8 scenes in this study. Stripping occurs when individual RS detectors appear lighter or darker than their neighbouring detectors, or signal loss during the transmission of Landsat instruments (USGS, 2017a). Since data stripping in most cases cannot be corrected, it can cause severely impact on intended data analysis.

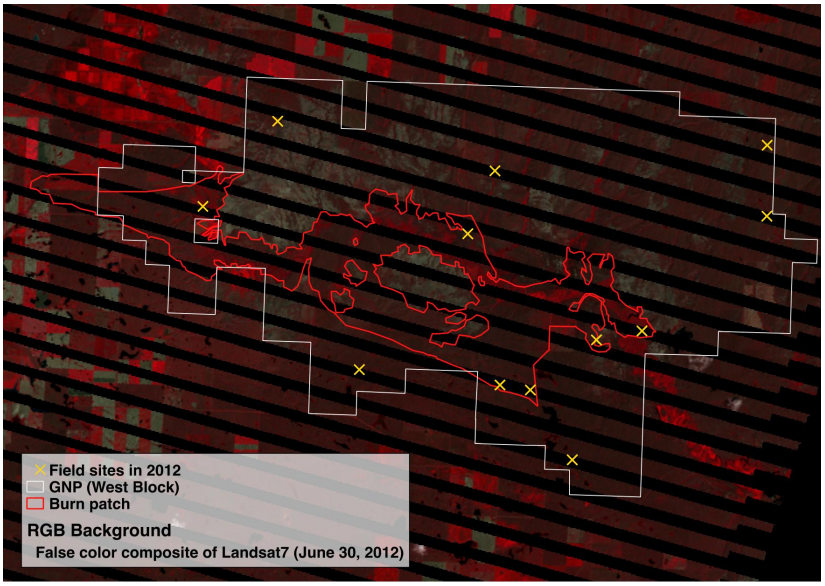

Figure 6.2: Data stripping of Landsat 7 ETM+ product directly impacts data analysis. Notice that most field sites conducted in 2012 unfortunately fall on the stripes that makes them impossible to be included in subsequent data analysis.

In this research, the baseline year is 2012 when only Landsat 7 imagery were available. Due to the stripping issue, it was very challenging to collect enough samples for data analysis (Figure 6.2). This severely impaired the robustness of the RS approaches in this study. Meanwhile, data stripping was present in some scenes from Landsat 8 product, howbeit its impact to this research was not as prominent as in the former case.

Data striping issue is very difficult to overcome in RS studies. Mathematical models such as

principle component analysis or filtering can produce a non-stripped scene with a lower resolution. However, most RS studies such as grassland post-fire recovery demands accurate quantitative information. As a result, image smoothing algorithm is more of an art than a science; hencefore not a viable solution. We may instead want to find alternative RS data sources such as Landsat 5 or SPOT, to name a few. Multi-source RS product itself may pose other challenges such as different (spatial and/or temporal) resolutions and spectral response functions, making it difficult to process and integrate them; nevertheless the fundamental data related problems can be circumvented, such as data striping discussed here.

References

Albini, F. A. (1976). Estimating wildfire behavior and effects. *USDA For. Serv.*, *4235*(789273912), 44 ST – Guidelines and sample protocol for sampli. Retrieved from http://adsabs.harvard.edu/abs/2003AGUFMGC52A..06G{%}5Cnhttp://www.firemodels.org/downloads/behaveplus/publications/Albini{_}INT-30{_}1976.pdf doi: USDAForestServiceGeneralTechnicalReportINT-30

Anderson, K. L., Smith, E. F., & Owensby, C. E. (1970). Burning Bluestem Range. *Journal of Range Management*, *23*(2), 81–92.

Anderson, R. C. (2006). Evolution and origin of the central grassland of North America : climate, fire, and mammalian grazers. *Journal of the Torrey Botanical Society*, *133*(4), 626–647. doi: 10.3159/1095-5674(2006)133[626:eaootc]2.0.co;2

Andrews, P. L. (1986). *BEHAVE: Fire Behavior Prediction and Fuel Modeling System/Burn Subsystem, Part I* (Tech. Rep.). Ogden, UT: USDA Forest Service Intermountain Research Station.

Archibold, O. W., & Wilson, M. R. (1980). The natural vegetation of Saskatchewan prior to agricultural settlement. *Canadian Journal of Botany*, *58*(19), 2031–2042.

Asner, G. P. (1998). Biophysical and biochemical sources of variability in canopy reflectance. *Remote Sensing of Environment*, *64*(3), 234–253. doi: 10.1016/S0034-4257(98)00014-5

Augustine, D. J., Derner, J. D., & Milchunas, D. G. (2010, may). Prescribed Fire, Grazing, and Herbaceous Plant Production in Shortgrass Steppe. *Rangeland Ecology & Management*, *63*(3), 317–323. Retrieved from http://www.bioone.org/doi/abs/10.2111/REM-D-09-00044.1 doi: 10.2111/REM-D-09-00044.1

Bailey, R. G. (1980). *Description of the ecoregions of the United States. Misc. Publ. 1391*. Washington, DC: U.S. Department of Agriculture, Forest Service.

Banerjee, S., He, Y., Xulin, & Si, B. C. (2011). Spatial relationships between leaf area index and topographic factors in a semiarid grassland: Joint multifractal analysis. *Australian Journal of Crop Science*, *5*(6), 756–763.

Barker, W. T., & Whitman, W. C. (1988). Northern great plains. *Rangelands*, *10*(6), 266–272.

Barrett, S. W., & Arno, S. F. (2010). *Indian Fires in the Northern Rockies - Ethnohistory and Ecology* (R. Boyd, Ed.). Corvallis, Oregon: Oregon State University Press.

Barsi, J. A., Lee, K., Kvaran, G., Markham, B. L., & Pedelty, J. A. (2014). The Spectral Response of the Landsat-8 Operational Land Imager. *Remote Sensing*(6), 10232–10251. doi: 10.3390/rs61010232

Benning, T. L., & Bragg, T. B. (1993). Response of Big Bluestem (Andropogon gerardii Vitman) to Timing of Spring Burning. *The American Midland Naturalist*, *130*, 127–132.

Blair, J. M. (1997). Fire , N Availability , and Plant Response in Grasslands : A Test of the Transient Maxima Hypothesis. *Ecology*, *78*(8), 2359–2368.

Bond, W. J., & Keeley, J. E. (2005, jul). Fire as a global 'herbivore': the ecology and evolution of flammable ecosystems. *Trends in ecology & evolution*, *20*(7), 387–94. Retrieved from http://www.ncbi.nlm.nih.gov/pubmed/16701401 doi: 10.1016/j.tree.2005.04.025

Briske, D. D. (1991). Developmental morphology and physiology of grasses. In R. K. Heitschmidt & J. W. Stuth (Eds.), *Grazing management: An ecological perspective* (pp. 85–108). Portland, OR: Timber Press.

Brockway, D. G., Gatewood, R. G., & Paris, R. B. (2002). Restoring fire and an ecological process in shortgrass prairie ecosystems: initial effects of prescribed burning during the dormant and growing seasons. *Journal of Environmental Management*, *65*, 135–152.

Brunsdon, C., & Singleton, A. (2015). The Future of Applied Geocomputation. In C. Brunsdon & A. Singleton (Eds.), *Geocomputation – a practical primer* (pp. 320–322). Thousand Oaks, California: SAGE Publications Ltd.

Cain, M. L., Bowman, W. D., & Hacker, S. D. (2011). Alternative Stable States. In *Ecology* (Second Edi ed., pp. 357–362). Sunderland, MA, USA: Sinauer Associates, Inc.

Cao, X., Chen, J., Matsushita, B., & Imura, H. (2010). Developing a MODIS-based index to discriminate dead fuel from photosynthetic vegetation and soil background in the Asian steppe area. *International Journal of Remote Sensing*, *31*(6), 1589–1604. doi: 10.1080/01431160903475274

Chapman, H. H. (1936). Effects of fire in propagation of seedbed for longleaf pine seedlings. *Journal of Forestry*(34), 852–854.

Chuvieco, E., Martín, M. P., & Palacios, A. (2002). Assessment of different spectral indices in the red-near-infrared spectral domain for burned land discrimination. *International Journal of Remote Sensing*, *23*(23), 5103–5110. doi: 10.1080/01431160210153129

Chuvieco, E., Ventura, G., & Martín, M. P. (2005). AVHRR multitemporal compositing techniques for burned land mapping. *International Journal of Remote Sensing*, *26*(5), 1013–1018. doi: 10.1080/01431160412331299235

Coghlan, A. (2017). *A Little Book of R For Time Series.* Retrieved 2018-02-13, from https://media.readthedocs.org/pdf/a-little-book-of-r-for-time-series/latest/a-little-book-of-r-for-time-series.pdf

Collins, S. L. (1987). Interaction of disturbances in tallgrass prairie: a field experiment. *Ecology*(68), 1243–1250.

Collins, S. L., & Wallace, L. L. (1990). *Fire in North American Tallgrass Prairies* (S. L. Collins & L. L. Wallace, Eds.). Norman, OK: University of Oklahoma Press. Retrieved from http://books.google.com/books?hl=en{&}lr={&}id=GS5k9EAuNr0C{&}pgis=1

Courtwright, J. (2007). "When We First Come Here It All Looked like Prairie Land Almost ": Prairie Fire and Plains Settlement. *The Western History Quarterly*, *38*(2), 157–179.

Csillag, F., Kertész, M., Davidson, A., & Mitchell, S. (2001). On the measurement of diversity-productivity relationships in a northern mixed grass prairie (Grasslands National Park, Saskatchewan, Canada). *Community Ecology*, *2*(2), 145–159. Retrieved from http://www.zpok.hu/img{_}upload/cb39111eba7a31c9c0e48686fa8e3c87/csillag.pdf

Cunfer, G. (2005). *On the great plains: Agriculture and Environment* (D. L. Flores, Ed.). College Station, TX: Texas A&M University Press.

Daughtry, C. S., Hunt, E. R., & McMurtrey, J. E. (2004). Assessing crop residue cover using shortwave infrared reflectance. *Remote Sensing of Environment*, *90*(1), 126–134. doi: 10.1016/j.rse.2003.10.023

Dubinin, M., Potapov, P., Lushchekina, A., & Radeloff, V. C. (2010, aug). Reconstructing long time series of burned areas in arid grasslands of southern Russia by satellite remote sensing. *Remote Sensing of Environment*, *114*(8), 1638–1648. Retrieved from http://linkinghub.elsevier.com/retrieve/pii/S0034425710000696 doi: 10.1016/j.rse.2010.02.010

Dwyer, D. D., & Pieper, R. D. (1967). Fire effects of blue grama-pinyon-juniper rangeland in New Mexico. *Journal of Range Management*(20), 359–362.

Environment Canada. (2017). *Historical Data (Home > Environment and natural resources > Weather, Climate and Hazard > Past weather and climate).* Retrieved 2017-12-11, from http://climate.weather.gc.ca/historical{_}data/search{_}historic{_}data{_}e.html

Farmwest. (2017). *Evapotranspiration Dataset.* Retrieved 2017-12-11, from http://www.farmwest.com/

Foga, S., Scaramuzza, P. L., Guo, S., Zhu, Z., Dilley, R. D., Beckmann, T., … Laue, B. (2017). Cloud detection algorithm comparison and validation for operational Landsat data products. *Remote Sensing of Environment*, *194*, 379–390. Retrieved from http://dx.doi.org/10.1016/j.rse.2017.03.026 doi: 10.1016/j.rse.2017.03.026

Ford, P. L. (1999). Response of Buffalograss (Buchloe dactyloides) and Blue Grama (Bouteloua gracilis) to Fire. *Great Plains Research*, *9*(Fall 1999), 261–276. Retrieved from http://digitalcommons.unl.edu/cgi/viewcontent.cgi?article=1453{&}context=greatplainsresearch

Ford, P. L., & Johnson, G. V. (2006, oct). Effects of dormant- vs. growing-season fire in shortgrass steppe: Biological soil crust and perennial grass responses. *Journal of Arid Environments*, *67*(1), 1–14. Retrieved from http://linkinghub.elsevier.com/retrieve/pii/S0140196306000498 doi: 10.1016/j.jaridenv.2006.01.020

Ford, P. L., & McPerson, G. R. (1998). econatres.napc15.pford.pdf. In C. Warwick (Ed.), *Proceedings of the fifteenth north american prairie conference* (pp. 71–76). Bend, Oregon: Natural Areas Association.

Ford, P. L., & McPherson, G. R. (1996). Ecology of fire in shortgrass prairie of the southern Great Plains. In D. M. Finch (Ed.), *Ecosystem disturbance & wildlife conservation in western grasslands: A symposium proceedings* (pp. 20–39). Darby, Pennsylvania: Diane Publishing Co.

Fourty, T. (1997). Vegetation Water and Dry Matter Contents Estimated from Top-of-the-Atmosphere Reflectance Data : A Simulation Study. *Remote Sensing of Environment*, *61*(1), 34–45.

Franklin, J. F., Bledsoe, C. S., & Callahan, J. T. (1990). Contributions of the Long-Term Ecological Research Program: An expanded network of scientists, sites, and programs can provide crucial comparative analyses. *BioScience*, *40*(7), 509–523. doi: 10.2307/1311319

Fuhlendorf, S. D., Engle, D. M., Kerby, J., & Hamilton, R. (2009, jun). Pyric herbivory: rewilding landscapes through the recoupling of fire and grazing. *Conservation biology : the journal of the Society for Conservation Biology*, *23*(3), 588–98. Retrieved from http://www.ncbi.nlm.nih.gov/pubmed/19183203 doi: 10.1111/j.1523-1739.2008.01139.x

Gao, B. C., & Goetz, A. F. H. (1994). Extraction of dry leaf spectral features from reflectance spectra of green vegetation. *Remote Sensing of Environment*, *47*(3), 369–374. doi: 10.1016/0034-4257(94)90104-X

Gates, E. A. (2016). *The Effects of Fire and Grazing in the Nothern Mixed-Grass Prairie: Implications from the Pautre Wildfire* (Master of Science, Montana State University). Retrieved from https://scholarworks.montana.edu/xmlui/bitstream/handle/1/9773/GatesE0516.pdf?sequence=1

Gates, E. A., Vermeire, L. T., Marlow, C. B., & Waterman, R. C. (2017). Reconsidering rest following fire: Northern mixed-grass prairie is resilient to grazing following spring wildfire. *Agriculture, Ecosystems and Environment*, *237*, 258–264. Retrieved from http://dx.doi.org/10.1016/j.agee.2017.01.001 doi: 10.1016/j.agee.2017.01.001

Gibson, D. J. (1989). Effects of Animal Disturbance on Tallgrass Prairie Vegetation. *American Midland Naturalist*, *121*(1), 144–154.

Gibson, D. J. (2009). *Grasses & Grassland Ecology*. New York, USA: Oxford University Press Inc.

Gibson, D. J., & Hulbert, L. C. (1987). Effects of fire, topography and year-to-year climatic variation on species composition in tallgrass prairie. *Vegetatio*, *72*, 175–185.

Gill, A. M. (1975). Fire and the Australian flora: a review. *Australian Forestry*(38), 4–25.

Glitzenstein, J. S., Platt, W. J., & Streng, D. R. (1995). Effects of Fire Regime and Habitat on Tree Dynamics in North Florida Longleaf Pine Savannas. *Ecological Monographs*, *65*(4), 441–476.

GNP. (2017a). *2010 Grasslands National Park of Canada Management Plan.* Retrieved 2017-01-20, from http://www.pc.gc.ca/eng/pn-np/sk/grasslands/plan/plan6.aspx

GNP. (2017b). *Fact sheet of GNP.* Retrieved 2017-12-08, from http://parkscanadahistory.com/publications/fact-sheets/eng/grasslands.pdf

Grover, H. D., & Musick, H. B. (1990). Shrubland encroachment in southern New Mexico, U.S.A.: an analysis of desertification processes in the American Southwest. *Climatic Change*(17), 305–330.

Guo, X. (2002). Discrimination of Saskatchewan prairie ecoregions using multitemporal 10-day composite NDVI data. *Prairie Perspectives: Geographical Essays*, *5*, 176–188.

Guo, X. (2004). Canadian prairie drought assessment through MODIS vegetation indices. *Proceedings of SPIE*, *5544*, 149–158. Retrieved from http://link.aip.org/link/?PSI/5544/149/1{&}Agg=doi doi: 10.1117/12.559581

Guo, X., Price, K. P., & Stiles, J. M. (2000). Biophysical and Spectral Characteristics of Cool- and Warm-Season Grasslands under Three Land Management Practices in Eastern Kansas. *Natural Resources Research*, *9*(4), 321–331.

Guo, X., Zhang, C., Wilmshurst, J. F., & Sissons, R. (2005). Monitoring Grassland Health with Remote Sensrn Approaches. *Prairie Perspectives*(8), 11–22.

He, Y., Guo, X., Dixon, P., & Wilmshurst, J. F. (2008). *Satellite Monitoring of Northern Ecosystems Using Multi-sensors* (Tech. Rep.). Winnipeg, Manitoba: Parks Canada.

He, Y., Guo, X., & Wilmshurst, J. F. (2006). Studying mixed grassland ecosystems I: Suitable hyperspectral vegetation indices. *Canadian Journal of Remote Sensing*, *32*(2), 98–107. doi: 10.5589/m06-009

Heirman, A. L., & Wright, H. A. (1973). Fire in medium fuels of west Texas. *Journal of Range Management*(26), 331–335.

Heyward, F. (1937). The effect of frequent fires on profile development of longleaf pine forest soils. *Journal of Forestry*(35), 23–27.

Holechek, J. L., Pieper, R. D., & Herbel, C. H. (1998). *Range Management: Principles and Practices*. New Jersey: Prentice Hail.

Hopkins, H., Albertson, F. W., & Riegel, A. (1948). Some effects of burning upon a prairie in west-central Kansas. *Transactions of the Kansas Academy of Science*(51), 131–141.

Howe, H. F. (1994). Managing Species Diversity in Tallgrass Prairie: Assumptions and Implications. *Conservation Biology*, *8*(3), 691–704. doi: 10.1046/j.1523-1739.1994.08030691.x

Jayaweera, K., & Ahlnas, K. (1974). Detection of Thunderstorms from Satellite Imagery for Forest Fire Control. *Journal of Forestry*, *72*(12), 768–770.

Jensen, J. R. (2005). *Introductory Digital Image Processing: A Remote Sensing Perspective* (3rd ed.; K. C. Clarke, Ed.). Upper Saddle River, NJ: Pearson Education, Inc.

Johnson, L. C., & Matchett, J. R. (2001). Fire and Grazing Regulate Belowground Processes in Tallgrass Prairie. *Ecology*, *82*(12), 3377–3389.

Kansas Natural Heritage Inventory. (2007). *Native prairie hay meadows: a landowner's management guide*. Lawrence, KS: University of Kansas.

Key, C. H., & Benson, N. C. (2006). Remote Sensing Measure of Severity, the Normalized Burn Ratio. In D. C. Lutes (Ed.), *Firemon: Fire effects monitoring and inventory system* (pp. LA–26). Fort Collins, CO, USA: Rocky Mountains Research Station, USDA Forest Service. doi: 10.2737/RMRS-GTR-164

Knapp, A. K. (1984). Post-burn differences in solar radiation, leaf temperature, and water stress influencing production in a lowland prairie. *American Journal of Botany*, *71*(2), 220–227.

Knapp, A. K., Briggs, J. M., Hartnett, D. C., & Collins, S. L. (1998). *Grassland dynamics : long-term ecological research in tallgrass prairie*. New York: Oxford University Press.

Knapp, A. K., Fahnestock, J. T., Hamburg, S. P., Statland, L. B., Seastedt, T. R., & Schimel, D. S. (1993). Landscape Patterns in Soil-Plant Water Relations and Primary Production in Tallgrass Prairie. *Ecology*, *74*(2), 549–560.

Knapp, E. E., Estes, B. L., & Skinner, C. N. (2009). *Ecological Effects of Prescribed Fire Season : A Literature Review and Synthesis for Managers* (Tech. Rep. No. September). Albany, CA: U.S. Department of Agriculture, Forest Service, Pacific Southwest Research Station.

Kruger, S. (2001). *Effects of fire on range plant species in the northern mixed grass prairie* (MSc Thesis, The University of Montana). Retrieved from https://scholarworks.umt.edu/cgi/viewcontent.cgi?article=7977{&}context=etd

Kucera, C. L. (1981). Grasslands and Fire. In *Fire regimes and ecosystem properties* (pp. 90–111). Honolulu, HI: USDA Forest Service. Retrieved from https://ia801400.us.archive.org/30/items/CAT83781017/CAT83781017.pdf

La Pierre, K. J., Yuan, S., Chang, C. C., Avolio, M. L., Hallett, L. M., Schreck, T., & Smith, M. D. (2011). Explaining temporal variation in above-ground productivity in a mesic grassland: The role of climate and flowering. *Journal of Ecology*, *99*(5), 1250–1262. doi: 10.1111/j.1365-2745.2011.01844.x

Launchbaugh, J. L. (1964). Effects of early spring burning on yields of native vegetation. *Journal of Range Management*(17), 5–6.

Leach, M. K., & Givnish, T. J. (1996). Ecological determinants of species loss in remnant prairies. *Science*(273), 1555–1558.

Li, M., & Guo, X. (2014). Long Term Effect of Major Disturbances on the Northern Mixed Grassland Ecosystem—A Review. *Open Journal of Ecology*, *04*(04), 214–233. Retrieved from http://file.scirp.org/pdf/OJE{_}2014032814161559.pdf doi: 10.4236/oje.2014.44021

Li, Z., & Guo, X. (2015). Remote sensing of terrestrial non-photosynthetic vegetation using hyperspectral, multispectral, SAR, and LiDAR data. *Progress in Physical Geography*, *40*(2), 276–304. doi: 10.1177/0309133315582005

Lu, B., He, Y., & Tong, A. (2016). Evaluation of spectral indices for estimating burn severity in semiarid grasslands. *International Journal of Wildland Fire*, *25*(2), 147–157. doi: 10.1071/WF15098

Madden, E. M., Hansen, A. J., & Murphy, R. K. (1999). Influence of prescribed fire history on habitat and abundance of passerine birds in Northern Mixed-Grass Prairie. *The Canadian Field Natrualist*, *113*(4), 627–640.

Missoula Fire Sciences Laboratory. (2012). *Information from LANDFIRE on fire regimes of mixed-grass prairie communities.* U.S. Department of Agriculture. Retrieved 2018-03-01, from https://www.fs.fed.us/database/feis/fire{_}regimes/Mixed{_}grass{_}prairie/all.html

NASA. (2018). *The Worldwide Reference System*. Retrieved 2018-02-13, from https://landsat.gsfc.nasa.gov/the-worldwide-reference-system/

Nau, R. (2015). *Statistics forecasting: notes on regression and time series analysis*. Retrieved 2015-11-07, from http://people.duke.edu/{~}rnau/411home.htm

Oesterheld, M., Loreti, J., Semmartin, M., & Paruelo, J. M. (1999). Grazing, fire, and climate effects on primary productivity of grasslands and savanna. In W. L. R. (Ed.), *Ecosystems of the world 16 ecosystems of disturbed ground* (pp. 287–306). New York: Elsevier.

Parks Canada. (2013). *Grasslands National Park What' s New*. Retrieved 2014-09-19, from http://www.pc.gc.ca/eng/pn-np/sk/grasslands/ne.aspx

Parton, W. J., Scurlock, J. M. O., Ojima, D. S., Schimel, D. S., & Hall, D. O. (1995). Impact of Climate Change on Grassland Production and Soil Carbon Worldwide. *Global Change Biology*(1), 13–22.

Peet, M., Anderson, R. C., & Adams, M. S. (1975). Effect of fire on big bluestem production. *American Midland Naturalist*, *94*(1), 15–26. doi: 10.2307/2424534

Peterson, D. W., & Reich, P. B. (2001). Prescribed Fire in Oak Savanna: Fire Frequency Effects on Stand Structure and Dynamics. *Ecological Applications*, *11*(3), 914–927.

Petropoulos, G. P., Kontoes, C., & Keramitsoglou, I. (2011). Burnt area delineation from a uni-temporal perspective based on landsat TM imagery classification using Support Vector Machines. *International Journal of Applied Earth Observation and Geoinformation*, *13*(1), 70–80. Retrieved from http://dx.doi.org/10.1016/j.jag.2010.06.008 doi: 10.1016/j.jag.2010.06.008

Pickett, S. T. A., Kolasa, J., Armesto, J. J., & Collins, S. L. (1989). The Ecological Concept of Disturbance and Its Expression at Various Hierarchical Levels. *Oikos*, *54*, 129–136. Retrieved from http://www.jstor.org/stable/3565258?origin=crossref doi: 10.2307/3565258

Powell, J., Martin, B., Dreitz, V. J., & Allred, B. W. (2018). Grazing Preferences and Vegetation Feedbacks of the Fire-Grazing Interaction in the Northern Great Plains. *Rangeland Ecology and Management*, *71*(1), 45–52. Retrieved from https://doi.org/10.1016/j.rama.2017.09.003 doi: 10.1016/j.rama.2017.09.003

Pyne, S. J. (1982). *Fire in America: A Cultural History of Wildland and Rural Fire*. Princeton, New Jersey: Princeton University Press.

Pyne, S. J. (2001). *Fire: A brief history*. Seattle: University of Washington Press.

Rannie, W. F. (2001). "Awful Splendour": Historical Accounts of Prairie Fire in Southern Manitoba Prior to 1870. *Prairie forum*, *26*(1), 17–46.

Rauste, Y., Herland, E., Frelander, H., Soini, K., Kuoremaki, T., & Ruokari, A. (1997). Satellite-based forest fire detection for fire control in boreal forests. *International Journal of Remote Sensing*, *18*(12), 2641–2656. doi: 10.1080/014311697217512

Redmann, R. (1978). Plant and Soil Water Potentials following Fire in a Northern Mixed Grassland. *Journal of Range Management*, *31*(6), 443–445. doi: 10.2307/3897203

Rollins, M. G. (2009). LANDFIRE: A nationally consistent vegetation, wildland fire, and fuel assessment. *International Journal of Wildland Fire*, *18*(3), 235–249. doi: 10.1071/WF08088

Rothermal, R. C. (1983). *How to Predict the Spread and Intensity of Forest and Range Fires* (Tech. Rep.). Ogden, UT: USDA Forest Service Intermountain Research Station General Technical Report.

Sala, O. E., Chapin, F. S. I., Armesto, J. J., Berlow, E., Bloomfield, J., Dirzo, R., … Wall, D. H. (2000, mar). Global Biodiversity Scenarios for the Year 2100. *Science*, *287*(5459), 1770–1774. Retrieved from http://www.sciencemag.org/cgi/doi/10.1126/science.287.5459.1770 doi: 10.1126/science.287.5459.1770

Sala, O. E., van Vuuren, D., & Pereira, H. (2005). Biodiversity across scenarios. In S. R. Carpenter, P. L. Pingali, E. M. Bennett, & M. Zurek (Eds.), *Ecosystems and human well-being: Scenarios* (pp. 375–408). Washington DC: Island Press.

Sauer, C. (1950). Grassland Climax , Fire , and Man. *Journal of Range Management*, *3*(1), 16–21.

Savage, C. (2011). *Prairie - A natural history* (N. Flight, Ed.). Vancouver: D&M Publishers Inc.

Scasta, J. D., Duchardt, C., Engle, D. M., Miller, J. R., Debinski, D. M., & Harr, R. N. (2016). Constraints to restoring fire and grazing ecological processes to optimize grassland vegetation structural diversity. *Ecological Engineering*, *95*, 865–875. Retrieved from http://dx.doi.org/10.1016/j.ecoleng.2016.06.096 doi: 10.1016/j.ecoleng.2016.06.096

Scasta, J. D., Engle, D. M., Talley, J. L., Weir, J. R., Stansberry, J. C., Fuhlendorf, S. D., & Harr, R. N. (2012, sep). Pyric-Herbivory to Manage Horn Flies (Diptera: Muscidae) on Cattle. *Southwestern Entomologist*, *37*(3), 325–334. Retrieved from http://www.bioone.org/doi/abs/10.3958/059.037.0308 doi: 10.3958/059.037.0308

Schepers, L., Haest, B., Veraverbeke, S., Spanhove, T., Borre, J. V., & Goossens, R. (2014). Burned Area Detection and Burn Severity Assessment of a Heathland Fire in Belgium Using Airborne Imaging Spectroscopy (APEX). *Remote Sensing*(6), 1803–1826. doi: 10.3390/rs6031803

Scholes, R. J., & Archer, S. R. (1997). Tree-grass interactions in savannas. *Annual Review of Ecology, Evolution, and Systematics*(28), 517–544.

Schröder, B. (2006). Pattern, process, and function in landscape ecology and catchment hydrology – how can quantitative landscape ecology support predictions in ungauged basins? *Hydrology and Earth System Sciences Discussions*, *3*(3), 1185–1214. doi: 10.5194/hessd-3-1185-2006

Shantz, H. L. (1954). The Place of Grasslands in the Earth ' s Cover of Vegetation. *Ecology*, *35*(2), 143–145. Retrieved from http://www.jstor.org/pss/1931110

Shay, J., Whelan-Enns, G., Appleby, A., Usher, R., Kavanagh, K., Sims, M., … Dinerstein, E. (2013). *Northern mixed grasslands.* Retrieved 2013-11-21, from http://worldwildlife.org/ecoregions/na0810

Steuter, A. A., & McPherson, G. R. (1995). Fire as a Physical Stress. In D. J. Bedunah & R. E. Sosebee (Eds.), *Wildland plants: Physiological ecology and developmental morphology* (pp. 550–579). Denver, CO: Society for Range Management.

Sui, D. (2014). Opportunities and impediments for open GIS. *Transactions in GIS*, *18*(1), 1–24. doi: 10.1111/tgis.12075

Umbanhowar, C. E. (1996). Recent fire history of the northern Great Plains. *American Midland Naturalist*(135), 115–121.

USDA. (2018). *Fire Effects Information System: Syntheses about fire ecology and fire regimes in the United States.* Retrieved 2018-03-04, from https://www.feis-crs.org/feis/

USGS. (2017a). *Detector Striping.* Retrieved 2018-02-13, from https://landsat.usgs.gov/detector-striping

USGS. (2017b). *Landsat 8 Pre-Collection Quality Assessment Band.* Retrieved 2018-02-13, from https://landsat.usgs.gov/qualityband

USGS. (2017c). *What is the C Function of Mask (CFMask) algorithm?* Retrieved 2018-02-14, from https://landsat.usgs.gov/what-cfmask

Uys, R. (2004). The effects of different fire regimes on plant diversity in southern African grasslands. *Biological Conservation*(118), 489–499.

van Wagtendonk, J. W., Root, R. R., & Key, C. H. (2004). Comparison of AVIRIS and Landsat ETM+ detection capabilities for burn severity. *Remote Sensing of Environment*, *92*(3), 397–408. doi: 10.1016/j.rse.2003.12.015

Vermeire, L. T., Crowder, J. L., & Wester, D. B. (2011). Plant community and soil environment response to summer fire in the Northern Great Plains. *Rangeland Ecology and Management*, *64*(1), 37–46. doi: 10.2111/REM-D-10-00049.1

Vitousek, P. M., & Hooper, D. U. (1993). Biological diversity and terrestrial ecosystem biogeochemistry. In E. D. Schulze & H. A. Mooney (Eds.), *Biodiversity and ecosystem function* (pp. 3–140). Berlin: Springer.

Vogl, R. J. (1979). Some Basic Principles of Grassland Fire Management. *Environmental Management*, *3*(1), 51–57. doi: 10.1007/BF01867068

Wakimoto, R. H., Willard, E. E., Hedrich, M., & Reid, B. (2005). *Historic Fire Regimes and Change Since European Settlement on the Northern Mixed Prairie: Effect on Ecosystem Function and Fire Behavior* (Tech. Rep.). Missoula, MT: University of Montana. Retrieved from https://www.firescience.gov/projects/98-1-5-04/project/98-1-5-04{_}final{_}report.pdf

White, P. S. (1979, jul). Pattern, process, and natural disturbance in vegetation. *The Botanical Review*, *45*(3), 229–299. Retrieved from http://link.springer.com/10.1007/BF02860857 doi: 10.1007/BF02860857

White, P. S., & Pickett, S. T. A. (1985). Natural disturbance and patch dynamics: an introduction. In *The ecology of natural disturbance and patch dynamics* (pp. 3–16). Orlando, FL: Academic Press.

White, R. S., & Currie, P. O. (1983). Prescribed burning in the northern Great Plains: yield and cover responses of 3 forage species in the mixed grass prairie. *Journal of Range Management*(36), 179–183.

Willmes, C., Kürner, D., & Bareth, G. (2014). Building research data management infrastructure using open source software. *Transactions in GIS*, *18*(4), 496–509. doi: 10.1111/tgis.12060

Wright, H. A., & Bailey, A. W. (1982). *Fire ecology - United States and Southern Canada*. New York: John Wiley and Sons.

WWF Global. (2009). *Northern Great Plains.* Retrieved 2013-11-21, from http://wwf.panda.org/?uProjectID=CA0059

Yang, X., Kovach, E., & Guo, X. (2013, apr). Biophysical and spectral responses to various burn treatments in the northern mixed-grass prairie. *Canadian Journal of Remote Sensing*, *39*(02), 175–184. Retrieved from http://pubs.casi.ca/doi/abs/10.5589/m13-023 doi: 10.5589/m13-023

Appendix A

Sample Field Form

Field Work in GNP, 2017 Summer

Site:					**Date:**			**Recorder:**			
Weather: *Sunny, Windy, Raining, Cloudy, partly cloudy*					**Grazed:** Y N			**Grassland Type :** Disturbed / Upland / Sloped / Valley			
X/Lng:			**Y/Lat:**			**Error:**			**Elev:**		
Quad	Grass	Forb	Shrub	S.D.	Litter	Lichen	Moss	Rock	B.Soil	Height	Species
N1											
N2											
N3											
N4											
N5											
E1											
E2											
E3											
E4											
E5											
S1											
S2											
S3											
S4											
S5											
W1											
W2											
W3											
W4											
W5											

Notes:

Appendix B

R Code for r^2 Curve Computation

In summary, the R script performs the following tasks:

1. load raw biophysical data for a specific year
2. calculate derived biophysical parameters
3. compute variance of biophysical parameters — the response variable of R^2 analysis
4. load asd data
5. calculate the mean curve of unburned reflectance
6. compute the variance of burned reflectance — the explanatory variable of R^2 analysis
7. loop through each wavelength
   (a) perform linear regression
   (b) get r^2 result of the fitted linear model
8. create a plot with the following information
   (a) Landsat 7 and 8 band configuration
   (b) r^2 curve
   (c) mean reflectance curve of burned samples
   (d) mean reflectance curve of unburned samples

Code of the script:

```
################################################################
# TODO: This R script is intended to fulfill Objective 2.1
# this is a sample script to calucate r2 curve for parameter
# `live%/dead%` for year 2013.
################################################################

# load dependant libraries
require(ggplot2)

# prepare a clean workspace
rm(list = ls())
setwd('~/Matthew/PhD/MSc/B.ASDTheory/asd_bio/live_div_dead')

########################
# Define params
########################

# names of burned sites and unburned sites
# they will be used to load biophysical data and asd data
```

```r
sites.unburned <- c("sg1", "u1", "sg13", "u4", "u0")
sites.burned <- c("vg2", "vg1", "sg2", "sg9", "dc1")

# the target year
year = 2013

# load biophysical data
bio.df <- read.csv(paste('../../../A.FieldAnalysis/data/', as.character(year),
  '/field_', year, '_data.csv', sep = ''))

# separate burned and unburned samples
bio.df.unburned <- bio.df[bio.df[['is_burned']] == 0, ]
bio.df.burned   <- bio.df[bio.df[['is_burned']] == 1, ]

# release memory
remove(bio.df)

# for burned sites, flag 'good' samples (with no NA or 0s for interested
# biophysical parameters)
site_burned_no_na <- bio.df.burned[
  !is.na(bio.df.burned$grass_perc)  &
  !is.na(bio.df.burned$forb_perc)   &
  !is.na(bio.df.burned$shrub_perc)  &
  !is.na(bio.df.burned$s_dead_perc) &
  !is.na(bio.df.burned$litter_perc) &
  (bio.df.burned$s_dead_perc + bio.df.burned$litter_perc != 0)
  , ]

# calculate interested parameters for burned sites
live.burned <-
  ( site_burned_no_na$grass_perc +
    site_burned_no_na$forb_perc  +
    site_burned_no_na$shrub_perc
  ) /
  ( site_burned_no_na$s_dead_per +
    site_burned_no_na$litter_per
  )

# aggregate burned samples from quadrat level to site level
live.burned <- aggregate(
  x   = live.burned,
  by  = list(site = site_burned_no_na$site),
  FUN = "mean" # use MEAN function for the aggregation
)

```

```r
# for unburned sites, flag 'good' samples (with no NA or 0s for interested
# biophysical parameters)
site_unburned_no_na <- bio.df.unburned[
    !is.na(bio.df.unburned$grass_perc)  &
    !is.na(bio.df.unburned$forb_perc)   &
    !is.na(bio.df.unburned$shrub_perc)  &
    !is.na(bio.df.unburned$s_dead_perc) &
    !is.na(bio.df.unburned$litter_perc) &
    (bio.df.unburned$s_dead_perc + bio.df.unburned$litter_perc != 0)
  , ]

# calculate interested parameters for unburned sites
live.unburned <-
  ( site_unburned_no_na$grass_perc +
    site_unburned_no_na$forb_perc  +
    site_unburned_no_na$shrub_perc
  ) /
  ( site_unburned_no_na$s_dead_perc +
    site_unburned_no_na$litter_perc
  )

# aggregate unburned samples from quadrat level to site level
live.unburned <- aggregate(
  x   = live.unburned,
  by  = list(site =  site_unburned_no_na$site),
  FUN = "mean"
)

# release memory
remove(site_burned_no_na, site_unburned_no_na, bio.df.burned, bio.df.unburned)

# calculate current baseline biophysical parameter
local.baseline.bio <- mean(live.unburned$x)

# global baseline is not implemented in this research, set as 0
global.baseline.bio <- 0

# prepare the response variable
response <- data.frame(
  site = tolower(live.burned$site),
  data = live.burned$x - local.baseline.bio - global.baseline.bio
)

# release memory
remove(live.burned, live.unburned)
```

```r

# preapre the explanatory variable
explanatory <- list()

# define wavelengths
my.wavelengths <- c(350 : 1350, 1410 : 1800, 1950 : 2400)

# load reflectances for burned and unburned samples
ref.df.unburned <- list()
ref.df.burned   <- list()

for(i in seq_along(sites.unburned)){

  # load unburned reflectance (csv files) from disk
  ref.df.unburned[[i]] <- read.csv(
    paste('../../raw_reflectance/', as.character(year),'/data/',
      sites.unburned[i], '_ref.csv', sep = '')
  )

  # change col names to lower case for the sake of automation across years
  colnames(ref.df.unburned[[i]]) <- tolower(colnames(ref.df.unburned[[i]]))

  # get only desired wavelengths
  ref.df.unburned[[i]] <- subset(ref.df.unburned[[i]],
    wavelength %in% my.wavelengths)
}

for(i in seq_along(sites.burned)){

  # load burned reflectance (csv files) from disk
  ref.df.burned[[i]] <- read.csv(
    paste('../../raw_reflectance/', as.character(year),'/data/',
      sites.burned[i],'_ref.csv', sep = '')
  )

  # change col names to lower case for the sake of automation across years
  colnames(ref.df.burned[[i]]) <- tolower(colnames(ref.df.burned[[i]]))

  # get only desired wavelengths
  ref.df.burned[[i]] <- subset(ref.df.burned[[i]],
    wavelength %in% my.wavelengths)
}

# utility function to collect site's ids
find_site_on_colnames <- function (my.lst, my.site){
```

```
  for(i in (1:length(my.lst))){
    if (startsWith(colnames(my.lst[[i]])[2], my.site)){
      return (my.lst[[i]])
    }
  }
  return (NA)
}

# utility function to return site based on the name
find_site_on_row <- function (my.lst, my.site){
  for(i in (1:length(my.lst))){
    if (startsWith(as.character(my.lst[[i]][1, ]$site), my.site)){
      return (my.lst[[i]])
    }
  }
  return (NA)
}

### start - calculate mean value for unburned reflectance
print('calc unburned mean ref...')
temp.ref.unburned.sum <- 0
temp.ref.unburned.n <- 0
for(i in 1:length(ref.df.unburned)){
  temp.ref.unburned.sum = temp.ref.unburned.sum +
    apply(ref.df.unburned[[i]][-1], 1, function(x) { sum(x) })
  temp.ref.unburned.n = temp.ref.unburned.sum +
    apply(ref.df.unburned[[i]][-1], 1, function(x) { length(x) })
}

# summary
ref.unburned.mean <- temp.ref.unburned.sum / temp.ref.unburned.n

# realse memory
remove(temp.ref.unburned.sum, temp.ref.unburned.n)

### end - calculate mean value for unburned reflectance

### start - calculate variance for burned reflectance
for(i in seq_along(sites.burned)){
  site.id = sites.burned[i]
  print(paste('processing', site.id))
  ref.site = find_site_on_colnames(ref.df.burned, site.id)

  # calculate this site's mean reflectance
  explanatory[[i]] <- data.frame(site = site.id,
```

```
    data = apply(ref.site[-1], 1, function(x) { mean(x, na.rm = TRUE) })
  )

  # calculate delta reflectance by subtracting local unburned baseline
  # Note: global baseline is not implemented in this research (`0`)
  global.baseline.ref <- 0
  explanatory[[i]]$data = explanatory[[i]]$data - ref.unburned.mean
    - global.baseline.ref
}

# release memory
remove(ref.site)

#########################################################################
# Regression to compute the r2 curve
# - loop through each wavelength and perform lm(response ~ explanatory)
# - response:  response <- data.frame(site, data)
# - explanatory: explanatory <- list(data.frame(site, data<350~2400>))
#########################################################################

# initilize 2 arrays to hold result for r2 and p-value
r2 <- vector()
p.value <- vector() # init p-value

# loop through each wavelength, i
for(i in 1 : length(my.wavelengths)){
  wv = my.wavelengths[i]
  cat("\rlambda =",wv, "nm")

  # initialize response and explanatory variables
  resp = vector()
  expl = vector()

  # loop through all biosites, j
  for(j in 1 : length(sites.burned)){
    site = as.character(response[j, ]$site)
    bio  = response[j, ]$data
    resp = c(resp, bio)

    # find reflectance for biosites.j, wavelength.i
    ref.site = find_site_on_row(explanatory, site)
    expl = c(expl, ref.site[i, ]$data)
  } # end j for sites

  # run regression and gather r2 and p statistics
```

```r
    val_r2 = summary.lm(lm(resp ~ expl))$r.squared
    val_p  = summary.lm(lm(resp ~ expl))$coefficients[ , 4][1]

    # concatenate current r2 and p values to respective arrays
    r2 = c(r2, val_r2)
    p.value = c(p.value, val_p)

} # end i for my.wavelengths

#########################################################################
# Visualizaiton of the result
#   - r2 curve from computation (thick black curve)
#   - p-value curve (thin black curve)
#   - Mean reflectance curve of unburned sites (thin green curve)
#   - Mean reflectance curve of burned sites (thin red curve)
#   - Band configuration of Landsat 7 and 8 (translucent bands)
#########################################################################

# calculate the averaged reflectance curve for unburned samples
unburned_ref <- vector()
for(i in 1:length(sites.unburned)){
  if(length(unburned_ref) == 0){
    unburned_ref <- ref.df.unburned[[i]][-1]
  } else {
    unburned_ref <- cbind(unburned_ref, ref.df.unburned[[i]][-1])
  }
}
unburned_mean <- apply(unburned_ref, 1, function(x) { mean(x, na.rm = TRUE) })

# calculate the averaged reflectance curve for burned samples
burned_ref <- vector()
for(i in 1:length(sites.burned)){
  if(length(burned_ref) == 0){
    burned_ref <- ref.df.burned[[i]][-1]
  } else {
    burned_ref <- cbind(burned_ref, ref.df.burned[[i]][-1])
  }
}
burned_mean <- apply(burned_ref, 1, function(x) { mean(x, na.rm = TRUE) })

# release memory
remove(expl, explanatory, i, j, ref.df.burned, ref.df.unburned, site, site.id,
  ref.unburned.mean, wv, val_r2, ref.site, response, resp, local.baseline.bio,
  bio, find_site_on_colnames, find_site_on_row, burned_ref, unburned_ref)

```

```r
# band configuration for Landsat 7 and 8 sensors, for more info refer to
# https://landsat.usgs.gov/what-are-band-designations-landsat-satellites
my.sensors <- list(
  tm = list( # TM and ETM+ sensors for Landsat 4, 5, 7
    blue  = c(450, 520),
    green = c(520, 600),
    red   = c(630, 690),
    nir   = c(770, 900),
    sswir = c(1550, 1750),
    lswir = c(2090, 2350)
  ),
  oli = list( # OLI sensor for Landsat 8
    blue  = c(450, 510),
    green = c(530, 590),
    red   = c(640, 670),
    nir   = c(850, 880),
    sswir = c(1570, 1650),
    lswir = c(2110, 2290)
  )
)

# define colors for the 2 sensors, numbers in the labels are to
# ensure the correct order for items in the list
my.sensors.colors <- c(
  ”1.blue”  = '#0000ff',
  ”2.green” = ”#1a9641”,
  ”3.red”   = ”#d7191c”,
  ”4.nir”   = ”#FC7E8A”,
  ”5.sswir” = ”#fec44f”,
  ”6.lswir” = '#d95f0e'
)

# define colors for 4 curves (r2, p, burned/unburned average reflectance)
my.colors <- c(
  ”1.Unburned” = '#1a9641',  # dark green
  ”2.Burned”   = '#d7191c',  # dark red
  ”3.R2”       = '#000000',  # black
  ”4.p.value”  =  '#000000'  # black
)

# define line styles for 4 curves
my.lines <- c(
  ”1.Unburned” = 'dashed',
  ”2.Burned”   = 'dashed',
  ”3.R2”       = 'solid',
```

```
  "4.p.value"  = 'solid'
)

# define line withs for 4 curves
my.lines.width <- c(
  "1.Unburned" = 0.5,  # moderate
  "2.Burned"   = 0.5,  # moderate
  "3.R2"       = 1,    # thick
  "4.p.value"  = 0.25  # thin
)

# styling lengend entries for the 4 curves
my.legend.label = expression(
  lambda[unburned], # unburned curve
  lambda[burned],   # burned curve
  r^2,              # r2 curve
  paste(            # p-value curve
    italic("p"),
    "-value"
));

# write the output in pdf format
pdf("r2_2013.pdf", width = 8, height = 6)

gg <- ggplot() +

  # labels for x-axis and major y-axis
  labs(x = expression(lambda * (nm)), y = expression(r^2)) +

  # plot's title
  ggtitle(
    bquote(Delta["live%/dead%"] * "~" * Delta[lambda] * " in " * 2013 *
      " (n = " * .(length(sites.burned)) * ")"
    )) +

  # apply colours to dataset
  scale_colour_manual(
    name   = NULL,
    values = my.colors,
    labels = my.legend.label
  ) +

  # apply line-types to dataset
  scale_linetype_manual(
    name   = NULL,
```

```
    values = my.lines,
    labels = my.legend.label
  ) +

  # formatting major and minor y-axes
  scale_y_continuous(

    # formatting major y-axis
    breaks = seq(0, 1, by = 0.10), # y axis from 0 to 1, with 0.1 increment
    labels = sprintf("%.2f", seq(0,1,by = 0.10)), # format y labels (2 decimal)
    expand = c(0, 0), # force x and y axes intersecting at (0, 0)

    # setting up minor y-axis
      sec.axis = sec_axis(~ . * 1.0,
      name = expression(paste(italic("p"), "-value"))
  )) +

  # use correct line types/width in legend
  # because R's default treatment is not desirablebug bs
  guides(
    color = guide_legend(
    override.aes = list(
      linetype = my.lines,
      lwd      = my.lines.width
  ))) +

  # use black-white theme and place/style the legend properly
  theme_bw() +
  theme(
    legend.text.align     = 0,
    plot.title            = element_text(hjust = 0.5),
    legend.justification  = "top",
    legend.box.background = element_rect(colour = "grey50")
  )

# loop through each sensors
for (i in 1 : length(my.sensors)) {

  # loop through each sensor's band-color configuration
  for (j in 1 : length(my.sensors.colors)) {
    delta.sensor = 1/length(my.sensors)

    # draw a translucent rectangle for each band
    gg <- gg + geom_rect(aes_string(

```

```
      # band's nominal wavelengths (lower and upper bounds)
      xmin  = my.sensors[[i]][[j]][1],
      xmax  = my.sensors[[i]][[j]][2],

      ymin  = (i-1) * delta.sensor,
      ymax  = i * delta.sensor),
      fill  = as.character(my.sensors.colors[j]),
      alpha = 0.3) +

      # draw arrows and text to discriminate different sensor products
      geom_segment( # arrow for lower bound
        aes_string(
          x    = 2400,
          y    = (i-1) * delta.sensor,
          xend = 2400,
          yend = i * delta.sensor
        ),
        arrow = arrow(
          angle  = 30,
          length = unit(0.2, "cm")
        ),
        size = 0.2,
        color = "#575757"
      ) + # end geom_segment
      geom_segment( # arrow for upper bound
        aes_string(
          x    = 2400,
          y    = i * delta.sensor,
          xend = 2400,
          yend = (i-1) * delta.sensor
        ),
       arrow = arrow(
         angle  = 30,
         length = unit(0.2, "cm")),
         size   = 0.2,
         color  = "#575757"
       ) + # end geom_segment
      annotate( # sensor's label
        "text",
        x = 2400,
        y = (i - 0.67) * delta.sensor, # snudge the label to avoid overlapping
        label = toupper(
          names(my.sensors)[i]),
          col = "#575757"
      ) # end annotate
```

```
  } # end for j
} # end for i

# draw the 4 curves: r2, p-value burned/unburned reflectance
gg +
  geom_line( # p-value curve
    aes(
      x        = my.wavelengths,
      y        = p.value,
      color    = "4.p.value",
      linetype = "4.p.value"
    ),
    size = my.lines.width["4.p.value"]
  ) + # end geom_line
  geom_line( # r2 curve
    aes(
      x        = my.wavelengths,
      y        = r2,
      color    = "3.R2",
      linetype = "3.R2"
    ),
    size = my.lines.width["3.R2"]
  ) + # end geom_line
  geom_line( # averaged reflectance for burned samples
    aes(
      x        = my.wavelengths,
      y        = burned_mean,
      color    = "2.Burned",
      linetype = "2.Burned"
    ),
    size = my.lines.width["2.Burned"]
  ) + # end geom_line
  geom_line( # averaged reflectance for unburned samples
    aes(
      x        = my.wavelengths,
      y        = unburned_mean,
      color    = "1.Unburned",
      linetype = "1.Unburned"
    ),
    size = my.lines.width["1.Unburned"]
  ) # end geom_line

# close the (pdf) file
dev.off()
```

Appendix C

Python Code for Automating NDVI Calculation

In summary, the Python script performs the following tasks:

1. Scan a folder where all Landsat scenes are saved (and unzipped),
2. Loop through each scene and calculate NDVI
   (a) use QA band info to mask polluted (cloud/shadow) pixels
   (b) calculate NDVI for non-polluted pixels
   (c) attach coordinate system to calculated NDVI scene
   (d) build raster pyramids to the NDVI scene
   (e) clip the NDVI scene with the boundary of study area
   (f) save result to hard drive

Code of the script:

```
#!/usr/local/bin/python

############################################################
# TODO: This Python script is intended to fulfill Objective
# 2.3. This is a sample script to calucate NDVI values from
# a collection of Landsat 8 imagery extracted and saved in a
# directory. NDVI rasters will be cliped with the study area.
############################################################

# import dependant libraries
from osgeo import gdal # GDAL is used for reading/writing rasters
import numpy as np # NumPy is used to perform raster calculations
from numpy import *
import os,sys,glob # For searching/filtering for certain files
import subprocess # This is required for clipping with gdalwarp

# define a function to calculate NDVI for a single scene
# - basename: Landsat imagery's individual band has its filename
#     in the format of 'LC80370262015191LGN00_sr_band5.tif', to
#     automate the calculation process, `basename` is devised and
#     in the shown example gets 'LC80370262015191LGN00_'. Later
#     in the script different bands will be referenced by appending
#     appropriate sufixes such as 'sr_band5.tif' or 'sr_band4.tif'.
# - outputdir: the directory to store output NDVI rasters.
# - clip_shpfile: shapefile of the study area's boundary
```

```
def calcNdvi(basename, outputdir, clip_shpfile):

    ######################
    # Config path names
    ######################

    # Red/NIR Channel of Landsat 8 product
    red_tif = basename + 'sr_band4.tif'
    nir_tif = basename + 'sr_band5.tif'

    # QA channel or cloud & shadow mask layer,
    # alternatively 'cfmask.tif' can be used here
    cfmask = basename + 'pixel_qa.tif'

    # The output name for the ndvi scene
    ndvi_tif = os.path.join(outputdir, os.path.basename(basename) + 'ndvi.tif')

    # The output name for clipped ndvi for the study area
    ndvi_tif_wgnp = os.path.join(outputdir, os.path.basename(basename) \
    + 'ndvi_wgnp.tif')

    # get absolute paths for ndvi scene, clipped ndvi,
    # and the shapefile boundary
    ndvi_tif = os.path.abspath(ndvi_tif)
    ndvi_tif_wgnp = os.path.abspath(ndvi_tif_wgnp)
    clip_shpfile = os.path.abspath(clip_shpfile)

    ######################
    # Load data
    ######################

    # load Red Channel's data
    g = gdal.Open(red_tif)
    red = g.ReadAsArray()

    # get NoData value, we will honor this value in the output
    nodata = g.GetRasterBand(1).GetNoDataValue()

    # load NIR Channel's data
    g = gdal.Open(nir_tif)
    nir = g.ReadAsArray()

    # load QA Channel's data
    g = gdal.Open(cfmask)

```

```
    # check if pixel is non-polluted (cloud-free, shadow-free). Note that this
    # algorithm is for 'pixel_qa.tif'. 'cfmask.tif' will be a different case.
    qa = g.ReadAsArray()
    check = np.logical_and(np.logical_and(red > 0, nir > 0), qa & 40 == 0)
    # 40 is a mask defined to indicate polluted (cloud, shadow) pixels.
    #
    # 40 (Decimal) is the binary representation of `101000`, wherein value of
    # `1` indicates presence of a certain condition and `0` if otherwise.
    # Values of this mask are read from right to left.
    #
    # Conditions are defined with the metadata in the downloaded package and
    # also shown down below. Fore more info about QA band usage,
    # please refer to https://landsat.usgs.gov/qualityband.
    #
    # Here in the NDVI calculation, only 'cloud shadow' (4th bit) and 'cloud'
    # (6th bit) are considered after studying the QA bands for the whole study
    # area across different years.
    #
    # `bitmap_description` definition in the associated metadata (xml file)
    # <bit num="0">fill</bit>
    # <bit num="1">clear</bit>
    # <bit num="2">water</bit>
    # <bit num="3">cloud shadow</bit>
    # <bit num="4">snow</bit>
    # <bit num="5">cloud</bit>
    # <bit num="6">cloud confidence</bit>
    # <bit num="7">cloud confidence</bit>
    # <bit num="8">cirrus confidence</bit>
    # <bit num="9">cirrus confidence</bit>

    # coerce reflectance from int to float to yield float NDVI values
    red = array(red, dtype = float)
    nir = array(nir, dtype = float)

    # calculate NDVI values for only non-polluted pixels.
    ndvi = np.where ( check,  (nir - red ) / ( nir + red ), nodata )

    ######################
    # save NDVI to disk
    ######################
    geo = g.GetGeoTransform()
    proj = g.GetProjection()
    shape = red.shape
    driver = gdal.GetDriverByName("GTiff")
    dst_ds = driver.Create(ndvi_tif, shape[1], shape[0], 1, gdal.GDT_Float32)
```

```
    band = dst_ds.GetRasterBand(1)

    # write ndvi data to memory & flush data to disk
    band.WriteArray(ndvi)
    band.FlushCache()

    # set the NoData value
    band.SetNoDataValue(nodata)

    # calculate stats
    stats = band.GetStatistics(0, 1)

    # georeference the image and set the projection
    dst_ds.SetGeoTransform(geo)
    dst_ds.SetProjection(proj)

    # build pyramids
    dst_ds.BuildOverviews(overviewlist=[2, 4, 8, 16 , 32, 64, 128])

    # save, close
    dst_ds = None

    # clip ndvi scene with shapefile boundary
    cmd = ['gdalwarp', '-cutline', clip_shpfile, '-crop_to_cutline', '-dstalpha',\
    ndvi_tif, ndvi_tif_wgnp]
    proc = subprocess.Popen(cmd, stdout = subprocess.PIPE, stderr = subprocess.PIPE)
    stdout,stderr=proc.communicate()
    exit_code=proc.wait()

    if exit_code: #Oops, something went wrong!
        raise RuntimeError(stderr)

################################################
# Config input data and call calcNdvi function
################################################

# the shapefile used for clipping ndvi scenes
clip_shpfile = "../../boundary/fire_env.shp"

# the output folder where ndvi results will be saved
output_folder = "../ndvi_landsat8_py"

input_dir = "../imagery/extracted_landsat8"
os.chdir(input_dir)

```

```
# grab all scenes based on their qa bands as identifier
files = glob.glob("*pixel_qa.tif")
files_n = len(files)
files_i = 0

# loop through all scenes and calculate ndvi
for file in files:
    parts = file.split("_")
    files_i += 1
    calcNdvi(parts[0] + "_", output_folder, clip_shpfile)

    # report progress
    print("progress " + str(round(files_i * 100.0 / files_n, 1)) + "%")

# exit the program upon completion of NDVI calculation
sys.exit(0);
```